AD_____

Award Number: DAMD17-99-1-9441

TITLE: Extracellular Matrix Regulations of Membrane Type 1-Matrix Metalloproteinase (MT1-MMP) and Matrix Metalloproteinase-2(MMP-2) in Human Breast Fibroblasts

PRINCIPAL INVESTIGATOR: Sonia Hernandez-Barrantes, Ph.D.
Dr. Rafael Fridman

CONTRACTING ORGANIZATION: Wayne State University
Detroit, Michigan 48202

REPORT DATE: August 2002

TYPE OF REPORT: Annual Summary

PREPARED FOR: U.S. Army Medical Research and Materiel Command
Fort Detrick, Maryland 21702-5012

REPORT DOCUMENTATION PAGE

Form Approved
OMB No. 074-0188

1. AGENCY USE ONLY (Leave blank)	2. REPORT DATE	3. REPORT TYPE AND DATES COVERED
	August 2002	Annual Summary (1 Jul 99 - 1 Jul 02)

4. TITLE AND SUBTITLE
Extracellular Matrix Regulations of Membrane Type 1-Matrix Metalloproteinase (MT1-MMP) and Matrix Metalloproteinase-2(MMP-2) in Human Breast Fibroblasts

5. FUNDING NUMBERS
DAMD17-99-1-9441

6. AUTHOR(S)
Sonia Hernandez-Barrantes, Ph.D.
Dr. Rafael Fridman

7. PERFORMING ORGANIZATION NAME(S) AND ADDRESS(ES)
Wayne State University
Detroit, Michigan 48202

E-Mail: crsonia@yahoo.com

8. PERFORMING ORGANIZATION REPORT NUMBER

9. SPONSORING / MONITORING AGENCY NAME(S) AND ADDRESS(ES)
U.S. Army Medical Research and Materiel Command
Fort Detrick, Maryland 21702-5012

10. SPONSORING / MONITORING AGENCY REPORT NUMBER

11. SUPPLEMENTARY NOTES

12a. DISTRIBUTION / AVAILABILITY STATEMENT
Approved for Public Release; Distribution Unlimited.

12b. DISTRIBUTION CODE

13. ABSTRACT *(Maximum 200 Words)*

The tissue inhibitors of metalloproteinases (TIMPs) are specific inhibitors of MMP activity. However, TIMP-2 acts as a positive regulator by promoting pro-MMP-2 activation by MT1-MMP. We showed that binding of either TIMP-2 or TIMP-4 to active MT1-MMP inhibits the autocatalytic turnover of MT1-MMP on the cell surface. In spite of TIMP-4's ability to bind pro-MMP-2 we demonstrated that TIMP-4, unlike TIMP-2, does not promote pro-MMP-2 activation by MT1-MMP. When co-expressed with TIMP-2, TIMP-4 competitively reduced pro-MMP-2 activation by MT1-MMP. Recent evidence indicates that MT1-MMP undergoes ectodomain shedding. We analyzed the released MT1-MMP forms and found a complex pattern of shedding involving two major fragments of 50 and 18 kDa. Inhibition studies using TIMP-2 and TIMP-4 demonstrated both autocatalytic (18kDa) and non-catalytic (50kDa) shedding mechanisms. Our studies suggest that autocatalytic shedding evolved as a specific mechanism to terminate MT1-MMP activity on the cell surface by disrupting enzyme integrity at a vital structural site. In contrast, functional data suggest that the non-autocatalytic shedding generates soluble active MT1-MMP species capable of binding TIMP-2. In addition to a balance between TIMP-2 and TIMP-4, a balance between shedded MT1-MMP species may be critical factors in determining the pericellular and extracellular activity of this enzyme.

14. SUBJECT TERMS
Tissue Inhibitors of Metalloproteinases, Matrix Metalloproteinases

15. NUMBER OF PAGES
43

16. PRICE CODE

17. SECURITY CLASSIFICATION OF REPORT	18. SECURITY CLASSIFICATION OF THIS PAGE	19. SECURITY CLASSIFICATION OF ABSTRACT	20. LIMITATION OF ABSTRACT
Unclassified	Unclassified	Unclassified	Unlimited

Table of Contents

Introduction:

For this research, I investigated the regulation of two members of the Matrix Metalloproteinase (MMPs) family, MMP-2 and MT1-MMP and the role of their natural inhibitors, namely, Tissue Inhibitor of Matrix Metalloproteinases (TIMPs), a family currently comprising four members. Since these enzymes are produced by fibroblasts, I tried to study their regulation in fibroblasts isolated from breast tissue. However, the manipulation of the fibroblasts turned to be very elusive. This difficulty let us to choose a vaccinia expression system to study the regulation of these matrix metalloproteinases in an eukaryotic system, which provides us with a more controllable system. We also modified **Task 1** on the proposal that states: "Parallel studies to determine the processing of MT1-MMP and the role of TIMP-2 in MMP-2 activation will be performed in a vaccinia expression system in which mammalian cells are infected and transfected with full length human MT1-MMP cDNA" to extend our studies not only on the role of TIMP-2 but on yet another inhibitor, TIMP-4, which functionally is similar to TIMP-2.

My project dealt with a key aspect of breast cancer metastasis and involved the use of a variety of techniques including cell biology and biochemistry in a relevant experimental model.

Body:

Turnover of extracellular matrix (ECM) is a fundamental process of many physiological and pathological conditions. A major group of enzymes responsible for ECM degradation is the matrix metalloproteinases (MMPs). All MMPs are produced in a latent form (pro-MMP) requiring activation for catalytic activity, a process that is usually accomplished by proteolytic removal of the propeptide domain. Once activated, all MMPs are specifically inhibited by a group of tissue inhibitors of metalloproteinases (TIMPs) that bind to the active site inhibiting catalysis (1). Over the last five years, the MMP family has been expanded to include a new subfamily of membrane-tethered MMPs known as membrane-type MMPs (MT-MMPs). MT1-MMP (MMP-14) was the first member of the MT-MMP family to be discovered and was identified as the first physiological activator of pro-MMP-2 (gelatinase A) (2,3). The role of MT1-MMP in pericellular proteolysis is not restricted to pro-MMP-2 activation as MT1-MMP is a functional enzyme that can also degrade a number of ECM components (4) and hence can play a direct role in ECM turnover. MT1-MMP has also been shown to be a key enzyme in tumor metastasis and angiogenesis (5).

Perhaps the most interesting aspect of MT1-MMP is the nature of its interactions with TIMP-2 and the role they play in pro-MMP-2 activation. To facilitate the association of the prodomain of pro-MMP-2 with the active site of MT1-MMP, pro-MMP-2 must be positioned in close association with MT1-MMP. To achieve this, TIMP-2 acts as a molecular link between pro-MMP-2 and MT1-MMP (3). It has been shown that the NH_2-terminal region of TIMP-2 binds to the active site of an active MT1-MMP on the cell surface generating a pro-MMP-2 "receptor" (6). In turn, the COOH-terminal region of TIMP-2 binds to the COOH-terminal domain of pro-MMP-2, also known as the hemopexin-like domain (HLD) (3,6). This trimeric MT1-MMP/TIMP-2/pro-MMP-2 complex permits the association of pro-MMP-2 to the cell surface, which eventually facilitates its activation by a neighboring TIMP-2-free MT1-MMP. However, this model of pro-MMP-2 activation had not been established in a living cell system due to the difficulty in modulating the level of TIMP-2 expression. In addition, there were conflicting results regarding the MT1-MMP form(s) responsible for the formation of the MT1-MMP/TIMP-2 complex (7).

Emerging evidence indicates that MT1-MMP is regulated by a process of ectodomain shedding (8,9)

Through this process soluble MT1-MMP fragments are generated which may posses important functional consequences for pericellular proteolysis in normal and malignant processes.

Results form our studies on the role of TIMP-2 on proMMP-2 activation by MT1-MMP showed that in addition to its ability to form the pro-MMP-2 "receptor", TIMP-2 can also regulate the nature of MT1-MMP forms present in the cells by its ability to inhibit MT1-MMP activity. This effect is due to the TIMP-2 inhibition of the autocatalytic turnover of MT1-MMP on the cell surface. In turn, we expect that this event will also regulate ectodomain shedding.

TIMP-2 belongs to a family of four TIMP inhibitors, which presently includes TIMP-1, TIMP-2, TIMP-3 and TIMP-4 (10). Studies on TIMP-MMP interactions have shown that TIMP-4, like TIMP-2 is also capable of forming a complex with pro-MMP-2, which is mediated by binding of the inhibitor to the HLD of the enzyme (11). Thus, functionally, TIMP-4 is similar to TIMP-2. In addition, sequence analyses revealed a 70% identity between TIMP-2 and TIMP-4 (10,12). Based on these observations, we asked whether TIMP-4, like TIMP-2, could also promote pro-MMP-2 activation by MT1-MMP. To study the interactions of TIMP-2 and TIMP-4 with MT1-MMP and their effects in its processing, ectodomain shedding and pro-MMP-2 activation, we expressed human TIMP-2 and/or TIMP-4 in a vaccinia expression system (13,14).

Purpose: The goal of this study was to study the regulation of MT1-MMP and MMP-2 and the role of TIMP-2 and TIMP-4 in this process. Since these matrix metalloproteinases are over-expressed in many cancers, including breast cancer, it is relevant to study the role of TIMPs in the processing of MT1-MMP and MMP-2 activation. I hypothesized that TIMP-2 and TIMP-4 will affect the processing of MT1-MMP and its activation of pro-MMP-2. The purpose of these studies is to examine in detail the regulatory mechanisms underlying the processing and ectodomain shedding of MT1-MMP and its activation of pro-MMP-2 to understand how these processes contribute to the degradation of ECM during cancer metastasis.

Objective: To investigate the effect of TIMP-2 and TIMP-4 on the processing, ectodomain shedding of MT1-MMP and pro-MMP-2 activation.

Key Research Accomplishments:

- A cellular approach designed to express MT1-MMP in the absence or presence of TIMP-2/TIMP-4 facilitated the characterization of the four major MT1-MMP species and revealed a unique interaction between MT1-MMP and these inhibitors.
- We showed that TIMP-2 and TIMP-4 regulate the amount of active MT1-MMP (57 kDa) on the cell surface.
- In the absence of TIMP-2 or TIMP-4, MT1-MMP undergoes autocatalysis to a 44-kDa form, which displays an N-terminus starting at G^{285} and hence lacks the entire catalytic domain.
- Neither pro-MT1-MMP (N terminus S^{24}) nor the 44-kDa form bound TIMP-2. In contrast, active MT1-MMP (N-terminus Y^{112}) formed a complex with TIMP-2 suggesting that regulation of MT1-MMP processing is mediated by a complex of TIMP-2 with the active enzyme.

- TIMP-2 enhanced the activation of pro-MMP-2 by MT1-MMP.
- Our data suggest that the 57-kDa species of MT1-MMP is the major pro-MMP-2 activator. This species is the active enzyme form, as determined by N-terminal sequencing, and its appearance correlated with enhanced pro-MMP-2 activation.
- TIMP-4 failed to promote activation of pro-MMP-2 by MT1-MMP.
- MT1-MMP is susceptible to autocatalytic (18kDa fragment) and non-autocatalytic (56, 50 and 31-35 kDa) shedding mechanisms.
- The 18 kDa fragment showed no catalytic activity and did not bind TIMP-2.

List of Reportable Outcomes:

- The results of this research were published in:
  Journal of Biological Chemistry (JBC) Vol **275**, No.16, Issue of April 21, pp.12080-12089, 2000
  Biochemical and Biophysical Research Communications **281**, 126-130, 2001
  Journal of Biological Chemistry (JBC) Vol **277**, No.29, Issue of July 19, pp.26340-26350, 2002
  Semin. Cancer Biol **12**, 131-138 , 2002
  (Reprints Attached).

- Presentation of a poster in the Molecular Aspects of Metastasis Meeting held in Snowmass, Colorado in September, 1999.
  Role Of Timp-2 In MT1-MMP Processing And Pro-MMP-2 Activation
  Sonia Hernandez-Barrantes, Marta Toth, Margarida Bernardo, David Gervasi and Rafael Fridman
  Department of Pathology, Wayne State University and Karmanos Cancer Institute, Detroit, MI 48201.

- Presentation of a poster in the VIIIth International Conference of the Metastasis Research Society held in London, England in September, 2000.
  Co-expression of TIMP-4 with MT1-MMP cannot promote pro-MMP-2 activation. Differential roles of TIMPs in regulation of pericellular proteolysis.
  *Sonia Hernandez-Barrantes[1], Yoichiro Shimura[1], Paul D. Soloway[2] and Rafael Fridman[1].
  [1]Department of Pathology, Wayne State University, Detroit, MI, USA, and [2]Department of Molecular and Cellular Biology, Roswell Park Cancer Institute, Buffalo, NY, USA.

- Presentation of a poster discussion session in the 92nd American Association for Cancer Research (AACR) held in New Orleans, Louisiana in March, 2001. This worked was honored with an AACR-AstraZeneca Scholar-in-Training Award .
  Differential roles of TIMP-2 and TIMP-4 in pro-MMP-2 Activation by MT1-MMP. Potential implication for Pericellular Proteolysis in Malignant Processes.

- Ph.D degree obtained was supported by this award.

Conclusions:

Our results demonstrated that the concentration of active MT1-MMP (57 kDa) on the cell surface was directly and positively regulated by TIMP-2.

Absence of inhibitor, on the other hand, resulted in a significant decrease in the amount of active enzyme on the cell surface leading to the generation of a membrane-bound inactive 44-kDa species, which was further processed to lower molecular weight forms. Based on the results in the vaccinia system, which allowed modulation of the level of TIMP-2 expression in the cells, we can conclude that the accumulation of the 57-kDa species of MT1-MMP and the reduction in the amount of the 44-kDa forms is a sole consequence of the presence of TIMP-2. The data obtained with this study show for the first time in a living cellular system that pro-MMP-2 activation by wild-type MT1-MMP is tightly regulated by the level of TIMP-2 expression in the cells.

Binding of TIMP-2 to activated MT1-MMP (57 kDa) inhibited autocatalysis and consequently, active enzyme accumulated on the cell surface as cells produced more MT1-MMP. This suggested that, under conditions of low levels of TIMP-2 expression relative to MT1-MMP, TIMP-2 may act as a positive regulator of MT1-MMP activity and therefore may enhance pericellular proteolysis including pro-MMP-2 activation and ECM degradation. Excess TIMP-2 will eventually block all active MT1-MMP inhibiting proteolysis. This model reflects the dynamic and unique interactions between MT1-MMP and TIMP-2 in living cells that tightly regulate MT1-MMP pericellular activity.

Furthermore, these studies established that like TIMP-2, TIMP-4 binds to MT1-MMP and inhibits MT1-MMP autocatalytic turnover. In addition, we showed the inability of TIMP-4 to promote pro-MMP-2 activation by MT1-MMP and demonstrated that this effect can only be mediated by TIMP-2 in spite of the ability of both inhibitors to form a non-covalent complex with pro-MMP-2 through its hemopexin-like domain. These results suggest that the lack of pro-MMP-2 activation in the presence of TIMP-4 is due to the inability of this inhibitor to generate a ternary complex with MT1-MMP and pro-MMP-2. Thus, while TIMP-4 binds to active MT1-MMP, the TIMP-4/MT1-MMP complex cannot act as a receptor for pro-MMP-2 and therefore activation does not ensue. Furthermore, our studies suggested that TIMP-4 competes for the binding of TIMP-2 to MT1-MMP and prevents its ability to support pro-MMP-2 activation. These observations and the fact that the expression of TIMP-4 has been shown to overlap with that of TIMP-2 in various instances suggest that a balance of these inhibitors may alter the net activity of MMP-2 with TIMP-2, under certain conditions, promoting MMP-2 and MT1-MMP-dependent proteolysis and TIMP-4 acting as a general MMP inhibitor. The results of this study demonstrate a differential role for members of the TIMP family in the inhibition of MT1-MMP activity and in MT1-MMP-dependent pro-MMP-2 activation.

Moreover, our data on ectodomain shedding suggest that autocatalytic shedding evolved as a specific mechanism to terminate MT1-MMP activity on the cell surface by disrupting enzyme integrity at a vital site. In contrast, functional data suggest that the non-autocatalytic shedding generates soluble active MT1-MMP species capable of binding TIMP-2. These studies suggest that ectodomain shedding is yet another regulatory mechanism to regulate pericellular and extracellular activities of MT1-MMP through a delicate balance of active and inactive enzyme-soluble fragments.

References:

1.Murphy, G., and Willenbrock, F. (1995) *Methods Enzymol.* **248**, 496-510

2.Sato, H., Takino, T., Okada, Y., Cao, J., Shinagawa, A., Yamamoto, E., and Seiki, M. A. (1994) *Nature* **370**, 61-65

3.Strongin, A.Y., Collier, I., Bannikov, G., Marmer, B.L., Grant, G.A., and Goldberg, G.I. (1995) *J.Biol.Chem.* **270**, 5331-5338

4.d'Ortho, M.P., Will, H., Atkinson, S., Butler, G., Messent, A., Gavrilovic, J., Smith, B., Timpl, R., Zardi, L., and Murphy, G. (1997) *Eur. J. Biochem.* **250**, 751-757

5.Hiraoka, N., Allen, E., Apel, I.J., Gyetko, M.R., and Weiss, S.J. (1998) Cell **95**, 365-377

6.Butler, G.S., Butler, M.J., Atkinson, S.J., Will, H., Tamura, T., van Westrum, S.S., Crabbe,T., Clements, J., d'Ortho, M.P., and Murphy, G. (1998) *J. Biol. Chem.* **273**, 871-880

7.Caterina, J.J., Yamada, S., Caterina, N.C., Longenecker, G., Holmback, K., Shi, J., Yermovsky,A.E., Engler, J.A., and Birkedal-Hansen, H. (2000) *J. Biol. Chem.* **275**, 26416-26422

8.Seiki, M (1999) APMIS **107**, 137-143

9.Imai, K., Ohuchi, E., Aoki, T., Nomura, H., Fujii, Y., Sato, H., Seiki, M., and Okada, Y. (1996) Cancer Res. **56**, 2707-2710

10.Brew, K., Dinakarpandian, D., and Nagase, H. (2000) *Biochim. Biophys. Acta* **1477**, 267-283

11.Bigg, H,F., Shi, Y.E., Liu, Y.E., Steffensen, B., and Overall, C.M. (1997) *J. Biol. Chem.* **272**, 15496-15500

12.Greene, J., Wang, M., Liu, Y.E., Raymond, L.A, Rosen, C., and Shi, Y.E. (1996) *J. Biol. Chem.* **271**, 30375-30380

13.Fridman, R., Fuerst, T.R., Bird, R.E., Hoyhtya, M., Oelkuct, M., Kraus, S., Komarek, D., Liotta, L.A., Berman, M.L., and Stetler-Stevenson, W.G. (1992) *J. Biol. Chem.* **267**, 15398-15405

14. Fuerst, T.R., Earl, P.L., and Moss, B. (1987) *Mol. Cell. Biol.* **7**, 2538-2544

Appendices:

- Reprints Attached:
  Journal of Biological Chemistry (JBC) Vol **275**, No.16, Issue of April 21, pp.12080-12089, 2000
  Biochemical and Biophysical Research Communications **281**, 126-130, 2001
  Journal of Biological Chemistry (JBC) Vol **277**, No.29, Issue of July 19, pp.26340-26350, 2002
  Semin. Cancer Biol **12**, 131-138 , 2002

THE JOURNAL OF BIOLOGICAL CHEMISTRY

Vol. 275, No. 16, Issue of April 21, pp. 12080–12089, 2000
Printed in U.S.A.

Binding of Active (57 kDa) Membrane Type 1-Matrix Metalloproteinase (MT1-MMP) to Tissue Inhibitor of Metalloproteinase (TIMP)-2 Regulates MT1-MMP Processing and Pro-MMP-2 Activation*

(Received for publication, July 13, 1999, and in revised form, January 21, 2000)

Sonia Hernandez-Barrantes‡, Marta Toth‡, M. Margarida Bernardo, Maria Yurkova, David C. Gervasi, Yuval Raz, QingXiang Amy Sang§, and Rafael Fridman¶

From the Department of Pathology and Karmanos Cancer Institute, Wayne State University, Detroit, Michigan 48201 and the §Department of Chemistry, Biochemistry Division, Florida State University, Tallahassee, Florida 32306-4390

Previous studies have shown that membrane type 1-matrix metalloproteinase (MT1-MMP) (MMP-14) initiates pro-MMP-2 activation in a process that is tightly regulated by the level of tissue inhibitor of metalloproteinase (TIMP)-2. However, given the difficulty in modulating TIMP-2 levels, the direct effect of TIMP-2 on MT1-MMP processing and on pro-MMP-2 activation in a cellular system could not be established. Here, recombinant vaccinia viruses encoding full-length MT1-MMP or TIMP-2 were used to express MT1-MMP alone or in combination with various levels of TIMP-2 in mammalian cells. We show that TIMP-2 regulates the amount of active MT1-MMP (57 kDa) on the cell surface whereas in the absence of TIMP-2 MT1-MMP undergoes autocatalysis to a 44-kDa form, which displays a N terminus starting at Gly^{285} and hence lacks the entire catalytic domain. Neither pro-MT1-MMP (N terminus Ser^{24}) nor the 44-kDa form bound TIMP-2. In contrast, active MT1-MMP (N terminus Tyr^{112}) formed a complex with TIMP-2 suggesting that regulation of MT1-MMP processing is mediated by a complex of TIMP-2 with the active enzyme. Consistently, TIMP-2 enhanced the activation of pro-MMP-2 by MT1-MMP. Thus, under controlled conditions, TIMP-2 may act as a positive regulator of MT1-MMP activity by promoting the availability of active MT1-MMP on the cell surface and consequently, may support pericellular proteolysis.

Turnover of extracellular matrix (ECM)[1] is a fundamental process of many normal and pathological conditions. A major group of enzymes responsible for ECM degradation is the matrix metalloproteinases (MMPs). The MMPs are multidomain zinc-dependent endopeptidases that, with few exceptions, share a basic structural organization comprising a propeptide, catalytic, hinge, and C-terminal (hemopexin-like) domains (1, 2). All MMPs are produced in a latent form (pro-MMP) requiring activation for catalytic activity, a process that is usually accomplished by proteolytic removal of the propeptide domain. Once activated, all MMPs are specifically inhibited by a group of tissue inhibitors of metalloproteinases (TIMPs) (3).

Over the last five years, the MMP family has been expanded to include a new subfamily of membrane-tethered MMPs known as membrane-type MMPs (MT-MMPs), which as of today includes five enzymes: MT1-, MT2-, MT3-, MT4-, and MT5-MMP (4–8). The MT-MMPs, with the exception of MT4-MMP (9), are unique because they are anchored to the plasma membrane (PM) by means of a hydrophobic stretch of approximately 20 amino acids leaving the catalytic domain exposed to the extracellular space. MT1-MMP (MMP-14) was the first member of the MT-MMP family to be discovered and was identified as the first physiological activator of pro-MMP-2 (gelatinase A) (4, 10). The role of MT1-MMP in pericellular proteolysis is not restricted to pro-MMP-2 activation as MT1-MMP is a functional enzyme that can also degrade a number of ECM components (11–14) and hence can play a direct role in ECM turnover. MT1-MMP has been recently shown to be the first member of the MMP family indispensable for normal growth and development since mice deficient in MT1-MMP exhibit a variety of connective tissue pathologies and a short life span (15). MT1-MMP has also been shown to be a key enzyme in tumor metastasis and angiogenesis (16, 17).

Perhaps the most interesting aspect of MT1-MMP is the nature of its interactions with TIMP-2 and the role they play in pro-MMP-2 activation. Studies using PM extracts containing MT1-MMP (10) or a transmembrane-deleted form of MT1-MMP (18) have shown that, at low concentrations, TIMP-2 stimulates pro-MMP-2 activation whereas at high concentrations it inhibits activation. In addition, cross-linking experiments using PM preparations demonstrated the binding of TIMP-2 to MT1-MMP and to the hemopexin-like domain of pro-MMP-2 (10). Based on these observations, a model for the activation of pro-MMP-2 has been proposed in which the catalytic domain of MT1-MMP binds to the N-terminal portion of TIMP-2, leaving the negatively charged C-terminal region of TIMP-2 available for the binding of the hemopexin-like domain of pro-MMP-2 (10, 19). This ternary complex has been suggested to cluster pro-MMP-2 at the cell surface near a TIMP-2-free active MT1-MMP molecule, which is thought to initiate activation of the bound pro-MMP-2. Pro-MMP-2 activation would occur only at low TIMP-2 concentrations relative to

* This work was supported by National Institutes of Health Grant CA-61986 and Department of Defense Grant DAMD17-99-1-9440 (to R. F.), National Insititues of Health Grant CA-78646 (to Q-X. S.), and Department of Defense Predoctoral Fellowship DAMD17-99-1-9441 (to S. H-B.). The costs of publication of this article were defrayed in part by the payment of page charges. This article must therefore be hereby marked "*advertisement*" in accordance with 18 U.S.C. Section 1734 solely to indicate this fact.

‡ Contributed equally to the results of this work.

¶ To whom all correspondence should be addressed: Dept. of Pathology, Wayne State University, 540 E. Canfield Ave., Detroit, MI 48201. Tel.: 313-577-1218; Fax: 313-577-8180; E-mail: rfridman@med.wayne.edu.

[1] The abbreviations used are: ECM, extracellular matrix; MMP, matrix metalloproteinase; TIMP, tissue inhibitor of metalloproteinase; PAGE, polyacrylamide gel electrophoresis; PBS, phosphate-buffered saline; mAb, monoclonal antibody; pAb, polyclonal antibody; pfu, plaque-forming units; FBS, fetal bovine serum; ECL, enhanced chemiluminescence; PM, plasma membrane; MT, membrane-type.

MT1-MMP, which would permit availability of active MT1-MMP to activate the pro-MMP-2 bound in the ternary complex. Thus, under restricted conditions, TIMP-2 is thought to promote the activation process by acting as a molecular link between MT1-MMP and pro-MMP-2. Kinetic studies with PM containing MT1-MMP (19) and studies with the catalytic domain of MT1-MMP immobilized on agarose beads (18) have supported this model. However, this model of pro-MMP-2 activation has not been established in a living cell system due to the difficulty in modulating the level of TIMP-2 expression.

Conflicting results have been reported regarding the MT1-MMP form(s) responsible for the formation of the MT1-MMP·TIMP-2 complex (10, 19–22). In fact, only a few studies examined the direct binding of TIMP-2 to full-length MT1-MMP. Strongin *et al.* (10) reported the binding of MT1-MMP from phorbol ester-treated HT-1080 PM to TIMP-2 bound to an MMP-2-C-terminal domain-affinity column. The bound MT1-MMP turned out to be the active enzyme starting at Tyr^{112}. Using radiolabeled TIMP-2 and PM extracts derived from COS-1 cells transfected with the full-length MT1-MMP cDNA, Zucker *et al.* (20) showed the formation of a ~80-kDa cross-linking product. However, the nature of the cross-linked MT1-MMP form(s) was not determined. Other studies showed the cross-linking of radiolabeled TIMP-2 with a purified autoactivated recombinant MT1-MMP lacking the transmembrane domain (13). However, binding of TIMP-2 to pro-MT1-MMP has not been examined. Finally, a 56-kDa form of MT1-MMP lacking the prodomain, found in the culture media of breast cancer cells, co-purified with TIMP-2 (23). Although various sources of MT1-MMP were used, these results were consistent with the active form of MT1-MMP being responsible for the binding of TIMP-2. Nonetheless, conflicting results were recently reported by Cao *et al.* (22), who proposed that the prodomain of MT1-MMP is essential for the binding of TIMP-2 to MT1-MMP and that pro-MT1-MMP can activate pro-MMP-2.

A major limitation in the study of MT1-MMP-TIMP-2 interactions has been the source of MT1-MMP, which included truncated enzymes and enzymes expressed in bacteria (18, 24). Furthermore, PM extracts (10, 19) and mammalian cells transfected with the MT1-MMP cDNA (4, 22, 25) contain endogenous TIMPs and/or MMPs. Thus, the direct contribution of TIMP-2 to pro-MMP-2 activation and its effect on MT1-MMP processing could not be clearly assessed. Here, a vaccinia virus expression system in mammalian cells (26–28), which allowed control of the level of TIMP-2 expression in the cells, was used to investigate the effect of various TIMP-2 levels on MT1-MMP processing and pro-MMP-2 activation and to identify the nature of the major MT1-MMP species detected.

EXPERIMENTAL PROCEDURES

Buffers—The following buffers were used: collagenase buffer (50 mM Tris-HCl, pH 7.5, 5 mM $CaCl_2$, 150 mM NaCl, and 0.02% Brij-35), lysis buffer (25 mM Tris-HCl, pH 7.5, 1% IGEPAL CA-630: a non-ionic detergent from Sigma, 100 mM NaCl, 10 μg/ml aprotinin, 1 μg/ml leupeptin, 2 mM benzamidine, and 1 mM phenylmethylsulfonyl fluoride), HNTG buffer (50 mM Tris, pH 7.5, 150 mM NaCl, 0.1% IGEPAL, and 10% glycerol), harvest buffer (60 mM Tris-HCl, pH 7.5, 0.55% SDS, and 2 mM EDTA), and buffer R (50 mM HEPES, pH 7.5, 150 mM NaCl, 5 mM $CaCl_2$, 0.01% Brij-35, and 1% (v/v) dimethyl sulfoxide).

Recombinant Vaccinia Viruses and Cell Culture—The production of the recombinant vaccinia virus (vTF7-3) expressing bacteriophage T7 RNA polymerase has been described by Fuerst *et al.* (28). Recombinant vaccinia viruses, expressing either human TIMP-2 (vSC59-T2) or TIMP-1 (vT7-T1) were obtained by homologous recombination, as described previously (28, 29). To construct the recombinant vaccinia virus expressing human MT1-MMP, the full-length MT1-MMP cDNA (a generous gift from Dr. G. Goldberg, Washington University, St. Louis, MO) was amplified by polymerase chain reaction and then cloned into the pTF7EMCV-1 expression vector, under control of the T7 promoter (30). After sequence verification of the insert in both directions, the resulting pTF7EMCV-1-MT1 plasmid was used to generate a recombinant vaccinia virus containing the full-length human MT1-MMP cDNA (vT7-MT1) by homologous recombination with wild type vaccinia virus, as described previously (26, 28). Non-malignant monkey kidney epithelial BS-C-1 (CCL-26) and human fibrosarcoma HT-1080 (CCL-121) cells were obtained from the American Type Culture Collection (ATCC, Rockville, MD) and cultured in Dulbecco's modified Eagle's medium supplemented with 10% fetal bovine serum (FBS) and antibiotics. HeLa S3 cells were obtained from ATCC (CCL-2.2) and grown in suspension in minimal essential Spinner medium (Quality Biologicals, Inc., Gaithersburg, MD) supplemented with 5% horse serum. All other tissue culture reagents were purchased from Life Technologies, Inc. (Grand Island, NY).

Recombinant Proteins and Antibodies—Human pro-MMP-2, TIMP-2, and TIMP-1 were expressed in HeLa S3 cells infected with the appropriate recombinant vaccinia viruses and purified to homogeneity, as described previously (26, 27, 31). The anti-TIMP-2 mAb CA101 (32) and a rabbit pAb to MT1-MMP (here referred to as pAb 437) (33) have been previously described. The rabbit pAb 160 and pAb 36 to MT1-MMP were generated and characterized, as described previously (34).

Infection-Transfection and Pulse-Chase Analysis of MT1-MMP—BS-C-1 cells in 6-well plates were infected with 30 plaque forming units (pfu)/cell of vTF7-3 for 45 min in Dulbecco's modified Eagle's medium containing 2.5% FBS. The media were then removed and the infected cells were transfected with 2 μg/ml of the pTF7EMCV-1-MT1 plasmid in Opti-MEM (Life Technologies, Inc.) (1 ml/well) using LipofectAMINE (Life Technologies, Inc.), as described by the manufacturer. After an incubation of 3.5 h, the medium was aspirated and replaced with 1 ml/well of Dulbecco's modified Eagle's medium without methionine supplemented with L-glutamine, 25 mM HEPES, pH 7.5, 0.1% dialyzed FBS, and 500 μCi/ml [^{35}S]methionine (NEN Life Science Products Inc., Wilmington, DE). After a 15-min pulse, the plates were placed on ice, the medium was aspirated and the cells received 1 ml/well of chase media (Opti-MEM with 0.1% dialyzed FBS, 25 mM HEPES, pH 7.5, and 4.8 mM methionine). At the end of the chase period (0–120 min at 37 °C), the medium was aspirated and the cells were lysed with 100 μl/well of harvest buffer. The lysates were then subjected to five cycles of boiling and freezing followed by a brief centrifugation. The supernatants were collected into clean tubes with the addition of 5 mM iodoacetamide, 2.5% Triton X-100, and 20 μg/ml aprotinin (final concentrations). For immunoprecipitations, lysates were incubated (16 h, 4 °C) with 5 μg of the pAb 437 to MT1-MMP followed by addition of 30 μl of protein G-Sepharose beads for an additional overnight incubation at 4 °C. After recovering the beads by brief centrifugation, the supernatants were discarded and the beads were washed five times with cold HTNG buffer. The immunoprecipitates were recovered from the beads with 4× Laemmli sample buffer (35), boiled, and resolved by SDS-PAGE under reducing conditions followed by autoradiography.

Expression of MT1-MMP and TIMP-2 by Infection—To express MT1-MMP, BS-C-1 cells (10^6 cells/35-mm well) in 6-well plates were co-infected with 5 pfu/cell each of vTF7-3 and vT7-MT1 for 45 min in 0.5 ml/well of Dulbecco's modified Eagle's medium containing 2.5% FBS (infection medium) at 37 °C. In some experiments, the pfu/cell of the vT7-MT1 virus was varied (0–10 pfu/cell) to modulate the level of MT1-MMP expression. To co-express MT1-MMP with TIMP-2, and to modulate the level of inhibitor expression, BS-C-1 cells were co-infected with 5 pfu/cell each of vTF7-3 and vT7-MT1 and increasing amounts (0–10 pfu/cell) of vSC59-T2 for 45 min in 0.5 ml/well of infection medium at 37 °C. To co-express MT1-MMP and TIMP-1, the vSC59-T2 virus was replaced with vT7-T1. As a control, BS-C-1 cells were infected with the vTF7-3 virus alone at 5 pfu/cell. After the infection, the virus containing-medium was aspirated and each well received 2-ml of fresh infection medium without viruses. The infected cells were then incubated for a minimum of 6 h at 37 °C, before any further experimentation.

Activation of Pro-MMP-2—At the indicated times following infection, the medium was aspirated and replaced with 1 ml/well of Opti-MEM media (Life Technologies, Inc.) containing 2 nM recombinant pro-MMP-2. The cells were then incubated for various times at 37 °C. The medium was collected and clarified by a brief centrifugation (2,000 × *g*, 5 min) and the cells were solubilized in 100 μl/well of cold lysis buffer and centrifuged (13,000 × *g*) for 15 min at 4 °C. Samples of the medium (5 μl) and lysates (5 μl) were mixed with 4× Laemmli sample buffer (35) without reducing agents and without heating and subjected to gelatin zymography, as described previously (36).

Immunoblot Analysis—Infected BS-C-1 cells in 6-well plates, as described above, were lysed in cold lysis buffer (100 μl/well). The lysates (20 μl from each sample) were mixed with 4× Laemmli sample buffer

with β-mercaptoethanol and then resolved by reducing SDS-PAGE followed by immunoblot analysis using the appropriate antibodies. The immune complexes were detected using the ECL system (Pierce, Rockford, IL), according to the manufacturer's instructions.

Surface Biotinylation—Twenty-four hours post-infection, BS-C-1 cells in 150-mm tissue culture dishes were surface-biotinylated with 0.5 mg/ml of the water-soluble, cell impermeable, biotin analog sulfo-NHS-biotin (Pierce) for 30 min at 4 °C in PBS containing 0.1 mM $CaCl_2$ and 1 mM $MgCl_2$ (PBS-CM). The biotinylation reaction was quenched (10 min at 4 °C) with a freshly prepared solution of 50 mM NH_4Cl in PBS-CM. After two washes with cold PBS-CM, the biotinylated cells were solubilized in harvest buffer (2 ml/150-mm dish), as described above. The lysates were then boiled (5 min), centrifuged (13,000 × *g*, 5 min) and the supernatants were supplemented with 2.5% Triton X-100 (final concentration). The lysates (500 μl) were immunoprecipitated with the appropriate antibody and protein G-Sepharose beads. The immunoprecipitates were resolved by reducing SDS-PAGE followed by blotting to a nitrocellulose membrane. The biotinylated proteins were detected with streptavidin-horseradish peroxidase and ECL.

Isolation of PM—BS-C-1 cells were infected with vaccinia viruses to express MT1-MMP alone or MT1-MMP with TIMP-2, as described above. The next day, the medium was aspirated and the cells were scraped into cold 25 mM Tris-HCl, 50 mM NaCl, pH 7.4. The samples were centrifuged (800 × *g*, 5 min) twice at 4 °C. The pellets were resuspended in the same buffer containing 8.5% sucrose, 10 μg/ml aprotinin, 2 μg/ml leupeptin, 1 mM phenylmethylsulfonyl fluoride, 4 mM benzamidine, and 10 mM *N*-ethylmaleimide. After sonication, the solutions were centrifuged at 19,000 × *g* at 4 °C for 30 min. The supernatants were collected and centrifuged at 100,000 × *g* at 4 °C for 1.25 h. The pellets were resuspended in the same buffer containing protease inhibitors and no sucrose. The PM fractions of HT-1080 cells treated (12 h, 37 °C) with 100 nM phorbol ester were prepared as described previously (36, 37).

Activation of Pro-MMP-2 by PM of BS-C-1 Cells Co-expressing MT1-MMP and TIMP-2—Pro-MMP-2 (55 nM) was incubated at 37 °C with each PM fraction (0.15 μg/μl) in a total volume of 200 μl of collagenase buffer. At varying times, 20 μl of the reaction mixture were added to acrylic cuvettes containing 2 ml of a 7 μM solution of the fluorescence quenched substrate $MOCAcPLGLA_2pr(Dnp)$-AR-NH_2 (Peptides International, Louisville, KY) (38) in buffer R, at 25 °C (31). Substrate hydrolysis was monitored with a Photon Technology International spectrofluorometer interfaced to a Pentium computer, equipped with the RatioMaster™ and FeliX™ hardware and software, respectively. The cuvette compartment was maintained at 25 °C. Fluorescence measurements were carried out at excitation and emission wavelengths of 328 and 393 nm and excitation and emission band passes of 1 and 3 nm, respectively. Less than 10% hydrolysis of the fluorogenic peptide substrate was monitored, as described by Knight (39). At the PM concentrations used, hydrolysis of this substrate by MT1-MMP was insignificant when compared with the hydrolysis by MMP-2.

Coupling of TIMP-2 to Affi-Gel 10 Matrix—Purified recombinant TIMP-2 (200 μg) in PBS was allowed to bind to 200 μl of Affi-Gel 10 (Bio-Rad) for 1 h at 22 °C with rotation. To block any active esters, 20 μl of 1 M ethanolamine-HCl, pH 8, were added to the reaction mixture followed by a 1-h incubation at 22 °C. The matrix (Affi-Gel 10-TIMP-2) was allowed to settle and the supernatant was subjected to reducing 12% SDS-PAGE to determine the amount of uncoupled TIMP-2. The Affi-Gel 10-TIMP-2 matrix was washed four times with PBS and equilibrated in collagenase buffer. The immobilized TIMP-2 maintained its capability to bind pro-MMP-2, as determined by SDS-PAGE analysis of the bound enzyme.

Binding of MT1-MMP to Immobilized TIMP-2—BS-C-1 cells in 150-mm dishes were infected to express MT1-MMP alone as described above. The cells were solubilized in lysis buffer (2 ml/dish) and the lysates (500 μl) were incubated (12 h, 4 °C) with a 50-μl suspension of either Affi-Gel 10-TIMP-2 matrix or Affi-Gel 10 matrix. The samples were centrifuged (13,000 × *g*, 5 min) and the supernatant (unbound fraction) and the matrix (bound fraction) were collected. The matrix beads were washed (5 times) with HNTG buffer. The beads and the unbound fraction (20 μl) were mixed with 20 μl of 4× Laemmli sample buffer with β-mercaptoethanol. The samples were then resolved by 12% SDS-PAGE followed by immunoblot analysis with the pAb 437, as described above.

Co-immunoprecipitation of MT1-MMP with TIMP-2—A pulse-chase experiment of MT1-MMP biosynthesis was carried out as described above except that the BS-C-1 cells were lysed in lysis buffer after the chase. Aliquots (20 μl) of the ^{35}S-lysates were then incubated with or without unlabeled TIMP-2 (150 nM) for 2 h at 4 °C followed by immunoprecipitation with anti-TIMP-2 mAb CA101 and protein G-Sepharose beads, as described above. In parallel, another aliquot (20 μl) of the lysates received 10× harvest buffer followed by immunoprecipitation with the pAb 437 to anti-MT1-MMP, as described above. The immunoprecipitates were resolved by reducing SDS-PAGE followed by autoradiography.

Immunoaffinity Purification and N-terminal Sequencing of MT1-MMP Species—ImmunoPure Immobilized Protein A beads (Pierce) (1 ml) were incubated (1 h, 22 °C) with 2 ml of the pAb 437 serum in binding buffer (0.01 M sodium phosphate, pH 7.5–8.0, containing 150 mM NaCl). The beads were washed with 0.2 M sodium borate, pH 9.0, followed by coupling of the antibodies with 20 mM dimethyl pimelimidate hydrochloride in the same buffer for 30 min at 22 °C. The beads were then centrifuged (5 min, 2000 × *g*) and the supernatant was aspirated. The beads were resuspended in a solution of 0.2 M ethanolamine, pH 8.0, followed by a 2-h incubation with gentle rocking at room temperature. The pAb 437/Protein A beads were washed with binding buffer. BS-C-1 cells in eight 150-mm dishes infected to co-express MT1-MMP and TIMP-2 were lysed in harvest buffer. The lysate was supplemented with 2.5% Triton X-100 (final concentration) and incubated (12 h, 4 °C) with the pAb 437/Protein A beads. After a brief centrifugation, the beads were collected and washed three times with harvest buffer supplemented with 2.5% Triton X-100. The bound proteins were eluted with sample buffer, boiled, and subjected to reducing 10% SDS-PAGE in 1.5-mm wide gel cassettes and transferred to a polyvinylidene difluoride membrane (Bio-Rad). The transferred proteins were stained with 0.1% Coomassie Blue Brilliant R-250 in 1% acetic acid, 40% methanol. An aliquot of the eluted proteins was also subjected to immunoblot analysis using the pAb 437. After identification, the corresponding bands were cut out from the polyvinylidene difluoride membrane and sent for microsequencing to ProSeq (Boxford, MA).

RESULTS

Biosynthesis of Recombinant MT1-MMP and Activation of Pro-MMP-2—To examine the expression and biosynthesis of MT1-MMP, BS-C-1 cells were infected with the vTF7-3 vaccinia virus and then transiently transfected with the pTF7EMCV-1-MT1 plasmid. After the infection-transfection procedure, the processing of MT1-MMP was examined by pulse-chase analysis followed by immunoprecipitation with the pAb 437. As shown in Fig. 1*A*, MT1-MMP was synthesized as a ~60-kDa protein that was sequentially processed to a major 57-kDa form and to a heterogeneous species of 44–40 kDa. Cleavage to the 57-kDa form was clearly detected after a 30-min chase period. After 45 min, the 44–40-kDa forms were detected. After 90 min, a ~35-kDa product was also immunoprecipitated by the pAb 437. In vTF7-3-infected but non-transfected BS-C-1 cells (Fig. 1*A*, *NT*), endogenous MT1-MMP was not detected demonstrating the lack of expression of endogenous enzyme in BS-C-1-infected cells.

The pTF7EMCV-1-MT1 plasmid was used to construct a recombinant vaccinia virus expressing full-length human MT1-MMP (vT7-MT1) by homologous recombination, as described previously (26, 28). BS-C-1 cells were co-infected with vTF7-3 and increasing pfu/cell of vT7-MT1 and then examined for their ability to activate exogenous pro-MMP-2. Generation of active MMP-2 in the media and the lysates was monitored by gelatin zymography. As shown in Fig. 1*B*, co-infection of BS-C-1 cells with vTF7-3 and vT7-MT1 resulted in pro-MMP-2 processing to the ~64-kDa intermediate form and the 62-kDa active species (14) in both the media and cell lysates. In contrast, BS-C-1 cells infected with the vTF7-3 virus alone failed to initiate pro-MMP-2 activation despite a small amount of autocatalytically generated MMP-2 present in the pro-MMP-2 stock solution. A very weak ~57-kDa gelatinolytic band was also detected in the lysates of cells co-infected with the two viruses but not with vTF7-3 alone. The 57-kDa form is derived from MT1-MMP, as will be discussed below. In the absence of exogenous pro-MMP-2, infected BS-C-1 cells showed no detectable levels of endogenous pro-MMP-2 (data not shown), as previously reported (26, 27).

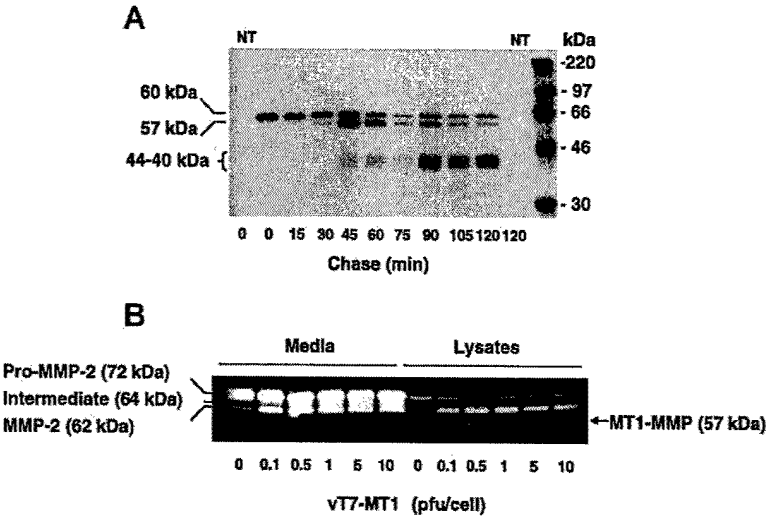

FIG. 1. **Processing and activity of MT1-MMP.** *A*, BS-C-1 cells were infected (45 min) with 30-pfu/cell of vTF7-3 and then transfected with 2 μg/well of the pTF7EMCV-1-MT1 expression vector. At 3.5 h post-infection transfection, the cells were pulse-labeled with [^{35}S]methionine for 15 min and then chased for 0–120 min. At the indicated times, the cells were lysed in harvest buffer and the lysates were immunoprecipitated with the pAb 437 and protein G-Sepharose beads. The immunoprecipitates were resolved by 10% SDS-PAGE under reducing conditions followed by autoradiography. *NT*, BS-C-1 cells infected with the vTF7-3 virus but not transfected and processed at 0 and 120 min. *B*, BS-C-1 cells were infected with 5 pfu/cell of vTF7-3 or co-infected with 5 pfu/cell of vTF7-3 and increasing pfu/cell (0.1–10) of vT7-MT1 to express MT1-MMP. At 12 h post-infection, the cells were incubated with 2 nM exogenous pro-MMP-2 for an additional 7 h at 37 °C. The medium (5 μl) and lysates (5 μl) were then harvested and analyzed by gelatin zymography.

Effects of TIMP-2 on Pro-MMP-2 Activation and MT1-MMP Processing—Previous *in vitro* studies demonstrated a role for TIMP-2 in pro-MMP-2 activation by MT1-MMP (10, 18, 19). However, the role of TIMP-2 in pro-MMP-2 activation has not been established in a cell-based assay. To investigate the role of TIMP-2 in MT1-MMP-dependent activation of pro-MMP-2, we used the vaccinia system to co-express MT1-MMP with TIMP-2 in BS-C-1 cells using the appropriate recombinant vaccinia viruses. To vary the level of inhibitor in the system, BS-C-1 cells were co-infected with various amounts (pfu/cell) of vSC59-T2, the TIMP-2-expressing vaccinia virus, while keeping constant the amount of vT7-MT1, thus varying the MT1-MMP/TIMP-2 ratio. It should be noted that all cells were infected with the polymerase-expressing virus (vTF7-3). After infection, the cells were incubated with exogenous pro-MMP-2. The lysates were then analyzed for MT1-MMP and TIMP-2 expression by immunoblot analysis (Fig. 2*A*) and pro-MMP-2 activation was monitored by gelatin zymography of the media and the lysates (Fig. 2*B*). As shown in the immunoblot of Fig. 2*A*, the level of TIMP-2 expression was dependent on the amounts (pfu/cell) of vSC59-T2 virus used to infect the cells. Under the same conditions, BS-C-1 cells infected to express MT1-MMP alone showed no detectable expression of endogenous TIMP-2 by immunoblot analysis (Fig. 2*A*) and by ELISA determination (data not shown), in agreement with our previous studies in vaccinia-infected cells (26, 27, 31).

Immunoblot analysis of the same lysates with the anti-MT1-MMP pAb 437 showed a profile of MT1-MMP forms that varied with the level of TIMP-2 expression. In the absence of TIMP-2, the lysates exhibited the 60- and 44–40-kDa species of MT1-MMP with the latter being the major species. Increased expression of TIMP-2 correlated with the accumulation of the 57-kDa species of MT1-MMP, which was concomitant with a gradual decrease in the 44–40-kDa forms. The 57-kDa species of MT1-MMP detected in the co-infected cells co-migrated with the MT1-MMP form present in the PM of phorbol ester-treated HT-1080 cells (Fig. 2*A*, *lane c*). Lack of a direct correlation between the intensity of the bands corresponding to the 44–40-kDa species and the intensity of the bands corresponding to the 60- and 57-kDa forms may be due to a differential solubilization of these forms from the cells when using Nonidet P-40 (IGEPAL) as detergent. Indeed, extraction with SDS (harvest buffer) significantly improved the yield and detection of the 60-kDa species of MT1-MMP (data not shown).

Zymographic analysis (Fig. 2*B*) showed that the activation of pro-MMP-2 by MT1-MMP, as determined by the appearance of the 62-kDa species of MMP-2, was dependent on the level of TIMP-2 expression. Low levels of TIMP-2 expression correlated with an enhanced activation of pro-MMP-2 when compared with cells expressing MT1-MMP alone in both the media and the cell lysates. On the other hand, high levels of TIMP-2 expression were associated with lower amounts of active MMP-2 (62 kDa). In the lysates of cells co-expressing MT1-MMP and TIMP-2, we also detected a weak ~57-kDa-gelatinolytic band (Fig. 2*B*), which was identified as MT1-MMP (see Fig. 3). Time course analysis (Fig. 2*C*) of the activation process by MT1-MMP co-expressed with TIMP-2, revealed the presence of active MMP-2 (62 kDa) in the lysates as early as 30 min after addition of pro-MMP-2. At the same time, the enzyme in the medium remained mostly in the latent form. With time, the 62-kDa species was also detected in the medium suggesting that after surface activation the 62-kDa form dissociates from the cell surface and it is released into the medium (Fig. 2*C*).

TIMP-2 but Not TIMP-1 Induces the Accumulation of the 57-kDa Form of MT1-MMP—As shown above (Fig. 2), co-expression of MT1-MMP and TIMP-2 induced the accumulation of the 57-kDa species of MT1-MMP, which exhibited gelatinolytic activity. To further investigate the effects of TIMP-2 on the accumulation of the 57-kDa species and to compare its effect with that of TIMP-1, BS-C-1 cells were infected to express MT1-MMP alone or MT1-MMP with increasing amounts of either TIMP-2 or TIMP-1. These experiments were carried out in the absence of exogenous pro-MMP-2. Generation of the 57-kDa species was monitored by gelatin zymography and immunoblot analysis. As shown in Fig. 3*A*, the intensity of the 57-kDa gelatinolytic species increased as a function of the amount (pfu/cell) of the vSC59-T2 virus (Fig. 3*A*, *lanes 4–6*). On the other hand, lysates of cells expressing MT1-MMP alone (Fig. 3*A*, *lane 3*) showed little or no detectable gelatinolytic bands. Co-expression of MT1-MMP with TIMP-1 had no effect

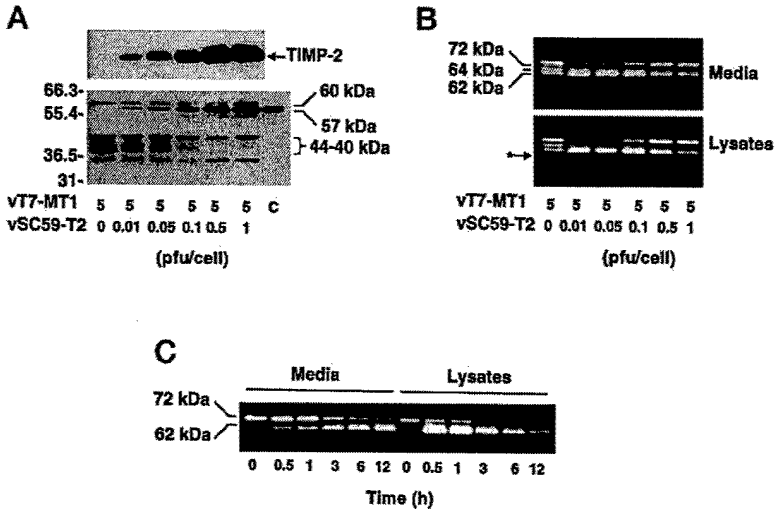

FIG. 2. **TIMP-2 enhances the activation of pro-MMP-2 by MT1-MMP and induces the accumulation of the 57-kDa species of MT1-MMP.** *A* and *B*, BS-C-1 cells were co-infected with 5 pfu/cell each of vTF7-3 and vT7-MT1 and increasing amounts of vSC59-T2 (0–1 pfu/cell) to co-express MT1-MMP and TIMP-2. At 6 h post-infection, the cells were incubated with 2 nM exogenous pro-MMP-2 for an additional 12 h at 37 °C followed by solubilization of the cell monolayer with lysis buffer. In *A*, lysates (20 μl) were subjected to reducing 12% SDS-PAGE followed by immunoblot analysis using the anti-TIMP-2 mAb (CA101) (*upper panel*) and the anti-MT1-MMP pAb 437 (*lower panel*). Detection of the antigens was performed using ECL (Pierce). As control (*lane C*), PM fractions (16 μg) of phorbol ester-treated HT-1080 cells were similarly analyzed. In *B*, the media and lysates (5 μl each) were subjected to gelatin zymography. *Asterisk* shows the 57-kDa MT1-MMP enzyme. *C*, BS-C-1 cells were co-infected with 5 pfu/cell each of vTF7-3 and vT7-MT1 and 0.01 pfu/cell of vSC59-T2. At 6 h post-infection, the cells were incubated with 2 nM exogenous pro-MMP-2 for various times (0–12 h). At each time, the medium and lysates were harvested and analyzed by gelatin zymography. These experiments were repeated at least three times with similar results.

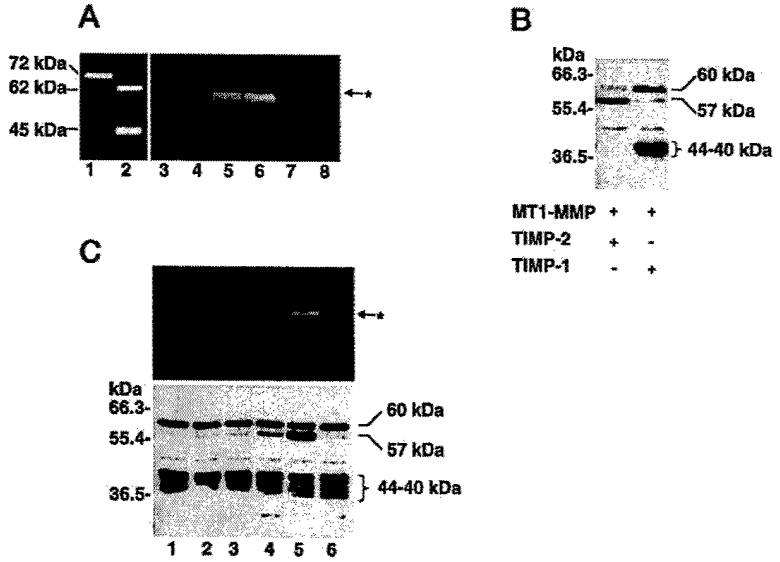

FIG. 3. **Effect of TIMP-2 and TIMP-1 on the profile of MT1-MMP forms.** *A*, BS-C-1 were co-infected with 5 pfu/cell each of vTF7-3 and vT7-MT1 (*lanes 3–8*) and increasing amounts of vSC59-T2 (*lane 4*, 0.01 pfu/cell; *lane 5*, 0.1 pfu/cell; *lane 6*, 1 pfu/cell) or vT7-T1 (*lane 7*, 0.01 pfu/cell; *lane 8*, 1 pfu/cell). At 12 h post-infection, the cells were harvested in 100 μl of lysis buffer and the lysates (20 μl) were analyzed by gelatin zymography. *Lane 1* shows purified pro-MMP-2 (5 ng) and *lane 2* shows active MMP-2 (62 and 45 kDa) (5 ng), as references. *B*, BS-C-1 cells were co-infected with 5 pfu/cell each of vTF7-3 and vT7-MT1 and either vSC59-T2 (5 pfu/cell) to co-express TIMP-2 or vT7-T1 (5 pfu/cell) to co-express TIMP-1. The lysates were resolved by reducing 12% SDS-PAGE followed by immunoblot analysis using the pAb 437 and detection by ECL. *C*, BS-C-1 cells were co-infected with 5 pfu/cell each of vTF7-3 and vT7-MT1. After infection, the cells were incubated (12 h, 37 °C) without (*lane 1*) or with increasing amounts of either exogenous TIMP-2 (*lane 2*, 1 ng/ml; *lane 3*, 10 ng/ml; *lane 4*, 100 ng/ml; *lane 5*, 500 ng/ml) or TIMP-1 (*lane 6*, 500 ng/ml). The lysates were harvested and analyzed by gelatin zymography and immunoblot analysis with the pAb 437 to MT1-MMP. *Asterisks* in *A* and *C* show the 57-kDa MT1-MMP gelatinolytic enzyme.

on the gelatinolytic activity (Fig. 3*A*, *lanes 7* and *8*) and on the profile of the MT1-MMP forms (Fig. 3*B*) when compared with cells co-expressing MT1-MMP and TIMP-2 (Fig. 3*B*) or MT1-MMP alone (shown in Fig. 3*C*, *lane 1*).

The accumulation of the 57-kDa species was also observed after addition of exogenous TIMP-2 to cells expressing MT1-MMP. As shown in Fig. 3*C*, 500 ng of TIMP-2 (Fig. 3*C*, *lane 5*) clearly induced the appearance of the 57-kDa gelatinolytic form when compared with cells that did not receive the inhibitor (Fig. 3*C*, *lane 1*). Consistently, immunoblot analysis of the same lysates showed a dose-dependent accumulation of the 57-kDa species after addition of exogenous TIMP-2 (Fig. 3*C*, *lanes 4* and *5*). Under these conditions, reduction in the relative amounts of the 44–40-kDa species of MT1-MMP was not evident. This suggests that exogenous TIMP-2, as opposed to inhibitor co-expressed with MT1-MMP (Fig. 3*B*), is less effi-

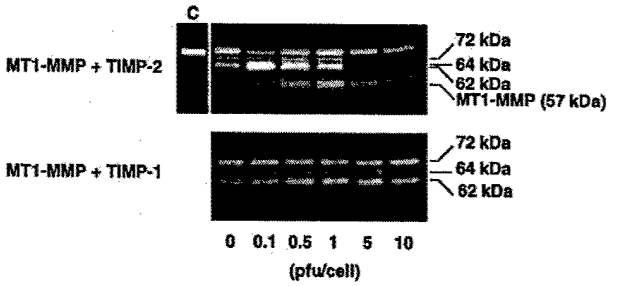

FIG. 4. **TIMP-2 but not TIMP-1 regulates the MT1-MMP-dependent activation of pro-MMP-2.** BS-C-1 cells were co-infected with 5 pfu/cell each of vTF7-3 and vT7-MT1 and increasing amounts (0–10 pfu/cell) of either vSC59-T2 (MT1-MMP + TIMP-2) or vT7-T1 (MT1-MMP + TIMP-1). At 6 h post-infection, the cells were incubated with 2 nM exogenous pro-MMP-2 for an additional 10 h at 37 °C. The lysates were then harvested and analyzed by gelatin zymography. *Lane c* shows pro-MMP-2 incubated with BS-C-1 cells infected with 5 pfu/cell of vTF7-3 alone. These experiments were repeated at least three times with similar results.

cient in preventing the generation of the 44–40-kDa forms. Addition of exogenous TIMP-1 (500 ng) had no effect on the appearance of the 57-kDa gelatinolytic species and did not alter the profile of MT1-MMP forms, as determined by zymography and immunoblot analysis, respectively (Fig. 3*C, lane 6*).

We then compared the effects of TIMP-2 and TIMP-1 on the ability of MT1-MMP to initiate pro-MMP-2 activation. To this end, BS-C-1 cells were infected to express MT1-MMP with either TIMP-2 or TIMP-1 using the appropriate vaccinia viruses as described under "Experimental Procedures." After infection, the cells were examined for their ability to initiate pro-MMP-2 activation by gelatin zymography. As shown in Fig. 4, TIMP-2 enhanced the MT1-MMP-dependent activation of pro-MMP-2 at low inhibitor concentrations when compared with MT1-MMP alone. At high inhibitor concentrations (5–10 pfu/cell of vSC59-T2), a significant inhibition of pro-MMP-2 activation was observed. In addition, the presence of TIMP-2 correlated with the appearance of the 57-kDa species of MT1-MMP. In contrast to TIMP-2, co-expression of MT1-MMP with TIMP-1 had little or no effect on the rate of pro-MMP-2 activation (Fig. 4) and the 57-kDa form was not detected in the lysates.

Effect of TIMP-2 on the Cellular Distribution of MT1-MMP Forms—We investigated the effect of TIMP-2 on the nature of the MT1-MMP forms expressed on PM isolated from co-infected BS-C-1 cells. As shown in Fig. 5*A*, the PM of BS-C-1 cells expressing only MT1-MMP contained the 60- and 44–40-kDa forms, as determined by immunoblot analysis using the pAb 437 (Fig. 5*A, lane 3*). Co-expression of MT1-MMP and TIMP-2 correlated with the detection of both the 60- and 57-kDa forms in the PM whereas the amount of the 44–40-kDa species was significantly reduced (Fig. 5*A, lane 4*). PM of control cells (infected with vTF7-3 alone) showed neither MT1-MMP forms (Fig. 5*A, lane 2*), as expected. PM of phorbol ester-treated HT-1080 cells were analyzed in parallel and found to contain the 57-kDa form of MT1-MMP, as a major enzyme species (Fig. 5*A, lane 1*). The PM fractions were also examined for the presence of TIMP-2 (Fig. 5*B*). As expected, TIMP-2 was only detected in the PM of BS-C-1 cells co-expressing MT1-MMP and TIMP-2 (Fig. 5*B, lane 4*) and in the PM of HT-1080 cells (Fig. 5*B, lane 1*).

The surface association of MT1-MMP and TIMP-2 in BS-C-1 cells expressing MT1-MMP with or without TIMP-2 was examined by surface biotinylation followed by immunoprecipitation with the appropriate antibodies. The 60- and 44–40-kDa forms of MT1-MMP were the major surface-biotinylated species immunoprecipitated from cells expressing MT1-MMP alone (Fig. 5*C, lane 1*), in agreement with the results obtained with the PM fractions. As expected, no biotinylated endogenous TIMP-2 was immunoprecipitated from the same sample (Fig. 5*C, lane 3*). In the cells co-infected to express MT1-MMP and TIMP-2, the 57-kDa form of MT1-MMP was also surface-biotinylated, in addition to the 60- and 44–40-kDa forms (Fig. 5*C, lane 4*). TIMP-2 was also detected on the cell surface (Fig. 5*C, lane 6*) suggesting its association with MT1-MMP. The specificity of these procedures was demonstrated by the lack of signal in the absence of antibodies (Fig. 5*C, lanes 2* and *5*). A similar profile of MT1-MMP forms was previously reported by Lehti *et al.* (25) on the surface of phorbol ester-treated HT-1080 cells, which are known to express TIMP-2 (10, 19). These results also demonstrate that the processing and cellular localization of MT1-MMP forms in the vaccinia-infected cells is similar to that found in cells naturally expressing MT1-MMP.

We next examined the ability of the PM fractions derived from cells expressing MT1-MMP alone (containing the 60- and 44–40-kDa species) or MT1-MMP with TIMP-2 (containing the 60- and 57-kDa species) (shown in Fig. 5*A*) to initiate pro-MMP-2 activation as described under "Experimental Procedures." As shown in Fig. 5*D*, the PM fraction of cells expressing MT1-MMP alone was unable to initiate pro-MMP-2 activation over a 5-h period, as determined by the background activity measured with a fluorescence quenched substrate (38). In contrast, pro-MMP-2 incubation with PM derived from cells co-expressing MT1-MMP and TIMP-2 resulted in a 12-fold enhancement of MMP-2 activity over that measured with PM of cells expressing MT1-MMP alone. It should be mentioned that the PM fraction capable of activating pro-MMP-2 was derived from cells infected to express MT1-MMP with relatively low amounts of TIMP-2 (0.1 pfu/cell of vSC59-T2) since high levels of TIMP-2 expression resulted in PM fractions unable to generate MMP-2 activity (data not shown). Taken together, these results suggest that the 57-kDa species of MT1-MMP is required for pro-MMP-2 activation.

The 57-kDa Species of MT1-MMP Binds TIMP-2—Previous studies demonstrated that MT1-MMP could form a complex with TIMP-2 on the cell surface (10). Our studies indicated that three major forms of MT1-MMP (60-, 57-, and 44–40 kDa) were present on the surface of cells with the amount of the 57-kDa species increasing in the presence of TIMP-2. In addition, our studies with BS-C-1 cells co-infected to express MT1-MMP and TIMP-2 showed that these cells exhibited surface expression of TIMP-2 suggesting that the inhibitor was interacting with MT1-MMP. Therefore, we asked which of the MT1-MMP forms could bind TIMP-2. To this end, samples of various time points of a pulse-chase experiment were incubated with or without exogenous unlabeled TIMP-2 and then subjected to immunoprecipitation with anti-TIMP-2. As shown in Fig. 6*A*, the samples from the 0, 45-, and 90-min chase periods contained the 60-, 57-, and/or the 44–40-kDa forms of MT1-MMP, as demonstrated after immunoprecipitation with the pAb 437. Addition of unlabeled TIMP-2 and the anti-TIMP-2 mAb to each of these samples revealed that, under these conditions, only the ^{35}S-labeled 57-kDa form of MT1-MMP co-precipitated with the inhibitor (Fig. 6*A*). In the absence of TIMP-2, no signal was detected with the anti-TIMP-2 antibody (data not shown).

To further examine the nature of the MT1-MMP species capable of binding TIMP-2, we used an Affi-Gel 10-TIMP-2-affinity matrix. To this end, lysates were prepared from BS-C-1 cells expressing MT1-MMP alone since co-expression with TIMP-2 would have affected binding to the affinity matrix. As shown in Fig. 6*B*, the 57-kDa species bound to the TIMP-2-affinity matrix (Fig. 6*B, lane 1*) whereas the 60- and 44–40-

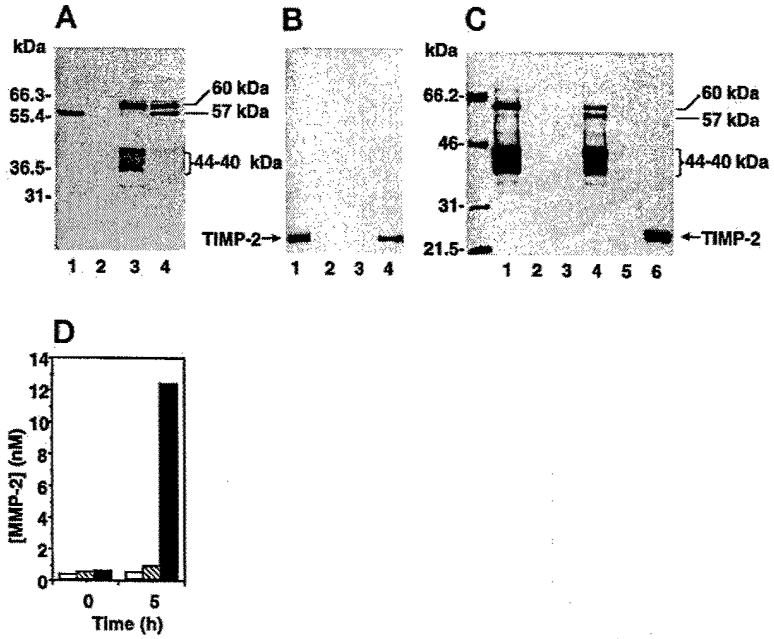

FIG. 5. **Effect of TIMP-2 on the PM localization and surface association of MT1-MMP forms.** *A* and *B*, immunoblot analysis of MT1-MMP and TIMP-2 in PM fractions. PM (12 μg/lane) isolated from BS-C-1 cells infected with 5 pfu/cell each of vTF7-3 and vT7-MT1 to express MT1-MMP (*lane 3*) or co-infected with vT7-MT1 (5 pfu/cell) and vSC59-T2 (0.1 pfu/cell) to co-express MT1-MMP and TIMP-2 (*lane 4*) were subjected to reducing 10% SDS-PAGE followed by immunoblot analysis with pAb 437 to MT1-MMP (*A*) or with a mAb to TIMP-2 (*B*). As controls, PM isolated from BS-C-1 cells infected with the vTF7-3 virus alone (*lane 2*) and of phorbol ester-treated HT-1080 cells (16 μg) (*lane 1*) were analyzed in parallel. *C*, biotinylation of MT1-MMP forms in BS-C-1 cells co-infected to express MT1-MMP alone (*lanes 1–3*) or MT1-MMP and TIMP-2 (*lanes 4–6*) as described above. The lysates (500 μl) were immunoprecipitated with either the pAb 437 to MT1-MMP (*lanes 1* and *4*) or the mAb CA101 to TIMP-2 (*lanes 3* and *6*) and protein G-Sepharose beads. As controls, the lysates received protein G-Sepharose beads without antibody (*lanes 2* and *5*). The immunoprecipitates were resolved by reducing 12% SDS-PAGE followed by blotting to a nitrocellulose membrane and detection by streptavidin-horseradish peroxidase and ECL. The biotinylated molecular weight markers shown are from Bio-Rad. *D*, activation of pro-MMP-2 by PM. Pro-MMP-2 (55 nM), in collagenase buffer, was incubated at 37 °C in the absence (*open bar*) and presence of PM (0.15 μg/μl) isolated from BS-C-1 cells infected to express MT1-MMP (*hatched bar*) or co-express MT1-MMP and TIMP-2 (*black bar*), as described above (*A*). MMP-2 activity was measured at 0 and 5 h incubation as described under "Experimental Procedures." Similar results were obtained in two independent experiments.

kDa forms of MT1-MMP did not (Fig. 6*B*, *lane 3*) in agreement with the co-immunoprecipitation experiment. These results also show that although cells expressing MT1-MMP alone contain low levels of the 57-kDa species of MT1-MMP, this form can be enriched by the affinity step. The 57-kDa species failed to bind to the TIMP-2 affinity column in the presence of 5 mM EDTA (data not shown). No binding of MT1-MMP species was detected to the affinity matrix without TIMP-2 (Fig. 6*B*, *lane 2*). PM fractions isolated from phorbol ester-treated HT-1080 cells containing only the 57-kDa species were used as positive control (Fig. 6*B*, *lane 4*).

N Termini of the MT1-MMP Species—To define the nature of the MT1-MMP species including the TIMP-2-binding 57-kDa form, a lysate of BS-C-1 cells infected to co-express MT1-MMP and TIMP-2 to induce accumulation of the 57-kDa species was subjected to immunoaffinity purification as described under "Experimental Procedures." The 60-, 57-, and 44-kDa (upper band) MT1-MMP species were isolated from the lysates and subjected to N-terminal sequencing. As shown in Fig. 7, the isolated 57-kDa form of MT1-MMP displays a N terminus starting at Tyr^{112} and therefore is identical to the active species of MT1-MMP previously reported (10, 25). The N terminus of the 60-kDa species starts at Ser^{24} demonstrating that this species is the latent form (pro-MT1-MMP) (1). The 44-kDa form starts at Gly^{285}, which is at the beginning of the hinge region (1, 8), and therefore lacks the complete catalytic domain. In agreement with the N-terminal sequencing data, a pAb to the propeptide domain of pro-MT1-MMP (pAb 36) (34) failed to recognize both the 57- and 44-kDa species (data not shown).

DISCUSSION

A cellular approach designed to express MT1-MMP in the absence or presence of TIMP-2 facilitated the characterization of the three major MT1-MMP species and revealed a unique interaction between MT1-MMP and TIMP-2 by which the inhibitor regulates the nature of MT1-MMP enzymes on the cell surface. The results presented here demonstrate that the concentration of active MT1-MMP (57 kDa) on the cell surface was directly and positively regulated by TIMP-2. Absence of inhibitor, on the other hand, resulted in a significant decrease in the amount of active enzyme on the cell surface leading to the generation of a membrane-bound inactive 44-kDa species, which was further processed to lower molecular weight forms. N-terminal sequencing of the 44-kDa species revealed that this form starts at Gly^{285} and hence lacks the entire catalytic domain but maintains the hemopexin-like domain and the hinge region (1). A previous study reported a N-terminal sequence of a 43-kDa species of MT1-MMP starting at Ile^{256} in the catalytic domain (25). This species was isolated from the media of HT-1080 cells transfected to overexpress a soluble transmembrane-deleted MT1-MMP and therefore the enzyme and/or mechanism responsible for MT1-MMP cleavage in solution could not be established. Although both the previously reported 43-kDa form (25) and the 44-kDa species identified in the present study are functionally inactive, our sequencing data were obtained with wild type MT1-MMP and therefore the N terminus of the 44-kDa species is likely to represent a true cleavage site.

Previous studies implicated MMP-2 in the processing of active MT1-MMP to the 44-kDa species (40, 41). However, our results clearly show that this process is MMP-2 independent

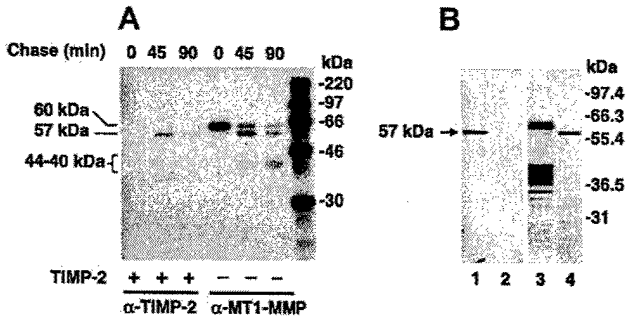

FIG. 6. **The 57-kDa form of MT1-MMP binds TIMP-2.** *A*, BS-C-1 cells were infected-transfected to express MT1-MMP as described in the legend to Fig. 1*A*. Three and half hours post-infection, the cells were pulse-labeled with [^{35}S]methionine for 15 min and chased for 90 min. At various times (0, 45, and 90 min), the cells were harvested in lysis buffer. A fraction of the lysates (20 μl) was incubated (2 h, 4 °C) with 150 nM unlabeled TIMP-2 (+) and then immunoprecipitated with the mAb to TIMP-2 (α-TIMP-2). In parallel, another fraction of the lysates (20 μl), which did not receive unlabeled TIMP-2 (−), was supplemented with harvest buffer to immunoprecipitate MT1-MMP with the pAb 437 (α-MT1-MMP), as described under "Experimental Procedures." The immunoprecipitates were resolved by 10% SDS-PAGE under reducing conditions followed by autoradiography. *B*, BS-C-1 cells were infected to express MT1-MMP. The next day, the cells were lysed in lysis buffer. The lysates (500 μl each) were incubated (12 h, 4 °C) with either Affi-Gel 10-TIMP-2 matrix (*lanes 1* and *3*) or Affi-Gel 10 matrix without immobilized TIMP-2 (*lane 2*) (50 μl suspension each). The bound fraction was eluted with 20 μl of Laemmli sample buffer with β-mercaptoethanol. The samples (bound and unbound) were resolved by 12% SDS-PAGE followed by immunoblot analysis with the pAb 437 to MT1-MMP. *Lane 1*, fraction bound to Affi-Gel 10-TIMP-2 matrix; *lane 2*, fraction bound to Affi-Gel 10 matrix; *lane 3*, unbound fraction from Affi-Gel 10-TIMP-2 matrix; and *lane 4*, PM of phorbol ester-treated HT-1080 cells, as control.

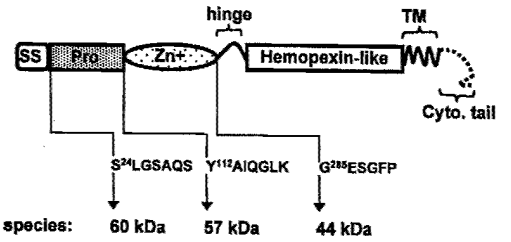

FIG. 7. **N-terminal sequence of MT1-MMP forms.** Diagram of the location and sequence of the MT1-MMP forms isolated. *SS*, signal sequence; *pro*, propeptide domain; *Zn*$^+$, catalytic domain; *TM*, transmembrane region; *Cyto. tail*, cytoplasmic tail.

since vaccinia-infected BS-C-1 cells do not produce detectable pro-MMP-2 (26, 27). Cleavage at the Gly-Gly^{285} peptide bond and consequent generation of the 44-kDa species was significantly inhibited by TIMP-2, as shown in cells co-expressing MT1-MMP and TIMP-2. Ellebroeck *et al.* (40) reported a reduction of the 44-kDa species in concanavalin A-treated ovarian carcinoma cells receiving exogenous TIMP-2. However, the effects of TIMP-2 on the profile of the MT1-MMP forms could not be differentiated from the pleiotrophic effects of concanavalin A, which may include effects on TIMP-2 and/or MT1-MMP expression as well as effects on cellular organization and plasma membrane structure. A recent study indicated that TIMP-2 modulates MT1-MMP activity in melanoma cells. However, a direct correlation between TIMP-2 expression and MT1-MMP processing could not be established (42). Based on the results in the vaccinia system, which allowed modulation of the level of TIMP-2 expression in the cells, we can conclude that the accumulation of the 57-kDa species of MT1-MMP and the reduction in the amount of the 44-kDa forms is a sole consequence of the presence of TIMP-2. The fact that TIMP-2, but not TIMP-1, inhibited the generation of the 44-kDa species further demonstrates that MT1-MMP processing is an autocatalytic event. The lack of effect of TIMP-1 is consistent with the weak inhibitory activity of TIMP-1 for MT1-MMP, as previously reported (12, 43). However, the inhibitory effect of TIMP-2 can be mimicked by general synthetic MMP inhibitors (40, 41) or by exposure of cells to concanavalin A or phorbol ester, which may induce TIMP-2 expression.

Due to the difficulty in modulating the level of MT1-MMP and TIMP-2 expression in cells the direct contribution of TIMP-2 to the activation of pro-MMP-2 could not be established in a cell-based system. The data presented here show for the first time in a living cellular system that pro-MMP-2 activation by wild type MT1-MMP is tightly regulated by the level of TIMP-2 expression in the cells. These results are consistent with the biphasic role of TIMP-2 in pro-MMP-2 activation as first proposed by Strongin *et al.* (10) *in vitro*. The stimulatory effect of TIMP-2 on pro-MMP-2 activation has been attributed to the formation of a ternary complex between MT1-MMP, TIMP-2, and pro-MMP-2 (10, 18, 19). However, our data show that BS-C-1 cells expressing MT1-MMP alone were able to initiate pro-MMP-2 activation suggesting that TIMP-2, and hence ternary complex formation, may not be an absolute requirement for pro-MMP-2 activation. Consistently, a C-terminal truncated TIMP-2, unable to form a complex with pro-MMP-2, and marimastat, a synthetic MMP inhibitor, can promote, at relatively low concentrations, the accumulation of active MT1-MMP and consequently the activation of pro-MMP-2.[2] Under these conditions, the surface association of pro-MMP-2 is likely to be mediated by other factors, which may include stable structural elements and/or nonspecific adsorption. Previous studies have shown that the association of pro-MMP-2 with the cell surface can be mediated by a variety of factors including ECM components (44, 45), heparin (19), and/or the integrin $\alpha_v\beta_3$ (46).

Our findings suggest that the effects of TIMP-2 on pro-MMP-2 activation may also be related to its ability to control the amount of active MT1-MMP in the cells by preventing the autocatalytic processing of active MT1-MMP on the cell surface. This is based on the observation that co-expression of MT1-MMP with increasing levels of TIMP-2 produced a gradual accumulation of the 57-kDa species that correlated, at the lowest level of inhibitor, with enhanced pro-MMP-2 activation when compared with cells expressing MT1-MMP alone. Thus, by binding and inhibiting a fraction of active MT1-MMP, TIMP-2 reduces the extent of autocatalytic processing of free 57-kDa species and therefore promotes its accumulation on the cell surface, which in turn enhances pro-MMP-2 activation. However, the ratio between free and TIMP-2-bound (inhibited) active (57 kDa) MT1-MMP has yet to be determined. At high inhibitor concentrations, activation of pro-MMP-2 was significantly diminished despite the higher amounts of 57-kDa MT1-MMP detected under those conditions. A plausible explanation for this apparent inconsistency may be the titration of all active MT1-MMP species by TIMP-2, which results in inhibition of pro-MMP-2 activation as previously proposed (18, 19). Furthermore, the maximum pro-MMP-2 activation observed at the lowest level of the 57-kDa species detected in the cells may reflect the high catalytic efficiency of active and TIMP-2-free MT1-MMP toward pro-MMP-2. This may also be the case in cells infected to express only MT1-MMP. Our data suggest that the 57-kDa species of MT1-MMP is the major pro-MMP-2 activator. This species is the active enzyme form, as determined by N-terminal sequencing, and its appearance correlated with

[2] M. Toth, D. Gervasi, Y. A. De Clerck, and R. Fridman, unpublished results.

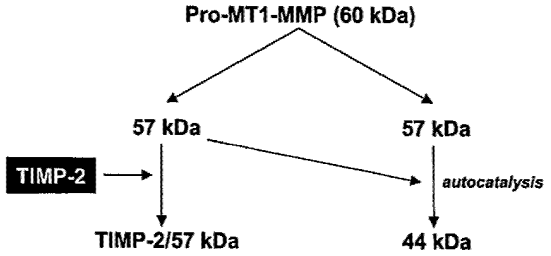

FIG. 8. **Diagram of MT1-MMP processing and interactions with TIMP-2.**

enhanced pro-MMP-2 activation. In addition, we have shown that only PM fractions containing the 57-kDa species (derived from cells co-expressing MT1-MMP and TIMP-2) were able to initiate pro-MMP-2 activation whereas PM fractions lacking the 57-kDa species had no activity toward pro-MMP-2. Finally, the 57-kDa species co-migrated with the 57-kDa species of MT1-MMP detected in PM fractions of phorbol ester-treated HT-1080 cells, which were shown to activate pro-MMP-2 (10, 37, 47) and to contain mostly active MT1-MMP (10, 19).

The nature of the MT1-MMP species responsible for TIMP-2 binding remains controversial. Both latent (21, 22) and active species (10) of MT1-MMP have been implicated in binding to the inhibitor. The data presented here are consistent with the 57-kDa species of MT1-MMP being the major TIMP-2 binding form. Co-immunoprecipitation and TIMP-2 affinity experiments demonstrated that the 57-kDa species of MT1-MMP bound to TIMP-2, whereas pro-MT1-MMP and the 44-kDa form showed no binding under the same conditions suggesting that the latter forms exhibit a reduced affinity for TIMP-2. Considering that the 57-kDa species starts at Tyr^{112} and that pro-MT1-MMP showed no significant TIMP-2 binding, it is reasonable to assume that TIMP-2 interacts with the active site of MT1-MMP (48). Furthermore, the binding of TIMP-2 to the 57-kDa species was abolished in the presence of EDTA, suggesting that the catalytic Zn^{2+} ion is required for TIMP-2 binding. These results are not consistent with the propeptide domain of pro-MT1-MMP being required for TIMP-2 binding (22).

Fig. 8 depicts a model of MT1-MMP processing and its regulation by TIMP-2. Cells produce pro-MT1-MMP that is activated by a pro-convertase-dependent mechanism (14, 49). Activation may occur in the trans-Golgi network and/or at the cell surface, as furin is also targeted to the PM and to the extracellular space (50, 51). Surface-anchored active MT1-MMP (57 kDa) is a fully functional enzyme capable of pericellular proteolysis. However, in the absence of TIMP-2, the 57-kDa species undergoes autocatalytic conversion to a 44-kDa inactive membrane-tethered form by cleavage at the hinge region (Gly^{285}), which diminishes the surface availability of active MT1-MMP. The 44-kDa form is further processed to a series of lower molecular weight degradation products. Under these conditions, the extent of MT1-MMP-dependent proteolysis would be determined by a balance between pro-MT1-MMP expression and activation, the rate of autocatalytic processing and enzyme internalization. Binding of TIMP-2 to activated MT1-MMP (57 kDa) inhibits autocatalysis and consequently, active enzyme accumulates on the cell surface as cells produce more MT1-MMP. This suggests that, under conditions of low levels of TIMP-2 expression relative to MT1-MMP, TIMP-2 may act as a positive regulator of MT1-MMP activity and therefore may enhance pericellular proteolysis including pro-MMP-2 activation and ECM degradation. The 57-kDa·TIMP-2 complex also favors the localization of pro-MMP-2 (by ternary complex formation) on the cell surface thereby promoting pro-MMP-2 activation (10, 19). However, other pro-MMP-2-cell surface interaction could play a role (19, 44, 46). Excess TIMP-2, relative to MT1-MMP, will eventually block all active MT1-MMP inhibiting proteolysis. This model reflects the dynamic and unique interactions between MT1-MMP and TIMP-2 in living cells that tightly regulate MT1-MMP pericellular activity.

REFERENCES

1. Massova, I., Kotra, L. P., Fridman, R., and Mobashery, S. (1998) *FASEB J.* **12,** 1075–1095
2. Birkedal-Hansen, H., Moore, W. G., Bodden, M. K., Windsor, L. J., Birkedal-Hansen, B., DeCarlo, A., and Engler, J. A. (1993) *Crit. Rev. Oral Biol. Med.* **4,** 197–250
3. Murphy, G., and Willenbrock, F. (1995) *Methods Enzymol.* **248,** 496–510
4. Sato, H., Takino, T., Okada, Y., Cao, J., Shinagawa, A., Yamamoto, E., and Seiki, M. (1994) *Nature* **370,** 61–65
5. Takino, T., Sato, H., Shinagawa, A., and Seiki, M. (1995) *J. Biol. Chem.* **270,** 23013–23020
6. Will, H., and Hinzmann, B. (1995) *Eur. J. Biochem.* **231,** 602–608
7. Puente, X. S., Pendas, A. M., Llano, E., Velasco, G., and Lopez-Otin, C. (1996) *Cancer Res.* **56,** 944–949
8. Pei, D. (1999) *J. Biol. Chem.* **274,** 8925–8932
9. Itoh, Y., Kajita, M., Kinoh, H., Mori, H., Okada, A., and Seiki, M. (1999) *J. Biol. Chem.* **274,** 34260–34266
10. Strongin, A. Y., Collier, I., Bannikov, G., Marmer, B. L., Grant, G. A., and Goldberg, G. I. (1995) *J. Biol. Chem.* **270,** 5331–5338
11. d'Ortho, M. P., Will, H., Atkinson, S., Butler, G., Messent, A., Gavrilovic, J., Smith, B., Timpl, R., Zardi, L., and Murphy, G. (1997) *Eur. J. Biochem.* **250,** 751–757
12. d'Ortho, M. P., Stanton, H., Butler, M., Atkinson, S. J., Murphy, G., and Hembry, R. M. (1998) *FEBS Lett.* **421,** 159–164
13. Ohuchi, E., Imai, K., Fujii, Y., Sato, H., Seiki, M., and Okada, Y. (1997) *J. Biol. Chem.* **272,** 2446–2451
14. Pei, D., and Weiss, S. J. (1996) *J. Biol. Chem.* **271,** 9135–9140
15. Holmbeck, K., Bianco, P., Caterina, J., Yamada, S., Kromer, M., Kuznetsov, S. A., Mankani, M., Robey, P. G., Poole, A. R., Pidoux, I., Ward, J. M., and Birkedal-Hansen, H. (1999) *Cell* **99,** 81–92
16. Hiraoka, N., Allen, E., Apel, I. J., Gyetko, M. R., and Weiss, S. J. (1998) *Cell* **95,** 365–377
17. Sato, H., Okada, Y., and Seiki, M. (1997) *Thromb. Haemostasis* **78,** 497–500
18. Kinoshita, T., Sato, H., Okada, A., Ohuchi, E., Imai, K., Okada, Y., and Seiki, M. (1998) *J. Biol. Chem.* **273,** 16098–16103
19. Butler, G. S., Butler, M. J., Atkinson, S. J., Will, H., Tamura, T., van Westrum, S. S., Crabbe, T., Clements, J., d'Ortho, M. P., and Murphy, G. (1998) *J. Biol. Chem.* **273,** 871–880
20. Zucker, S., Drews, M., Conner, C., Foda, H. D., DeClerck, Y. A., Langley, K. E., Bahou, W. F., Docherty, A. J., and Cao, J. (1998) *J. Biol. Chem.* **273,** 1216–1222
21. Cao, J., Rehemtulla, A., Bahou, W., and Zucker, S. (1996) *J. Biol. Chem.* **271,** 30174–30180
22. Cao, J., Drews, M., Lee, H. M., Conner, C., Bahou, W. F., and Zucker, S. (1998) *J. Biol. Chem.* **273,** 34745–34752
23. Imai, K., Ohuchi, E., Aoki, T., Nomura, H., Fujii, Y., Sato, H., Seiki, M., and Okada, Y. (1996) *Cancer Res.* **56,** 2707–2710
24. Lichte, A., Kolkenbrock, H., and Tschesche, H. (1996) *FEBS Lett.* **397,** 277–282
25. Lehti, K., Lohi, J., Valtanen, H., and Keski-Oja, J. (1998) *Biochem. J.* **334,** 345–353
26. Fridman, R., Fuerst, T. R., Bird, R. E., Hoyhtya, M., Oelkuct, M., Kraus, S., Komarek, D., Liotta, L. A., Berman, M. L., and Stetler-Stevenson, W. G. (1992) *J. Biol. Chem.* **267,** 15398–15405
27. Fridman, R., Bird, R. E., Hoyhtya, M., Oelkuct, M., Komarek, D., Liang, C. M., Berman, M. L., Liotta, L. A., Stetler-Stevenson, W. G., and Fuerst, T. R. (1993) *Biochem. J.* **289,** 411–6
28. Fuerst, T. R., Earl, P. L., and Moss, B. (1987) *Mol. Cell. Biol.* **7,** 2538–2544
29. Moss, B. (1992) *Bio/Technology* **20,** 345–362
30. Elroy-Stein, O., Fuerst, T. R., and Moss, B. (1989) *Proc. Natl. Acad. Sci. U. S. A.* **86,** 6126–6130
31. Olson, M. W., Gervasi, D. C., Mobashery, S., and Fridman, R. (1997) *J. Biol. Chem.* **272,** 29975–29983
32. Hoyhtya, M., Fridman, R., Komarek, D., Porter-Jordan, K., Stetler-Stevenson, W. G., Liotta, L. A., and Liang, C. M. (1994) *Int. J. Cancer* **56,** 500–505
33. Gervasi, D. C., Raz, A., Dehem, M., Yang, M., Kurkinen, M., and Fridman, R. (1996) *Biochem. Biophys. Res. Commun.* **228,** 530–538
34. Li, H., Bauzon, D. E., Xu, X., Tschesche, H., Cao, J., and Sang, Q. A. (1998) *Mol. Carcinog.* **22,** 84–94
35. Laemmli, U. K. (1970) *Nature* **227,** 680–685
36. Toth, M., Gervasi, D. C., and Fridman, R. (1997) *Cancer Res.* **57,** 3159–3167
37. Strongin, A. Y., Marmer, B. L., Grant, G. A., and Goldberg, G. I. (1993) *J. Biol. Chem.* **268,** 14033–14039
38. Knight, C. G., Willenbrock, F., and Murphy, G. (1992) *FEBS Lett.* **296,** 263–266
39. Knight, C. G. (1995) *Methods Enzymol.* **248,** 18–34
40. Ellerbroek, S. M., Fishman, D. A., Kearns, A. S., Bafetti, L. M., and Stack, M. S. (1999) *Cancer Res.* **59,** 1635–1641
41. Stanton, H., Gavrilovic, J., Atkinson, S. J., d'Ortho, M. P., Yamada, K. M., Zardi, L., and Murphy, G. (1998) *J. Cell Sci.* **111,** 2789–2798
42. Kurschat, P., Zigrino, P., Nischt, R., Breitkopf, K., Steurer, P., Klein, C. E., Krieg, T., and Mauch, C. (1999) *J. Biol. Chem.* **274,** 21056–21062
43. Will, H., Atkinson, S. J., Butler, G. S., Smith, B., and Murphy, G. (1996) *J. Biol. Chem.* **271,** 17119–17123
44. Steffensen, B., Bigg, H. F., and Overall, C. M. (1998) *J. Biol. Chem.* **273,**

20622–20628
45. Wallon, U. M., and Overall, C. M. (1997) *J. Biol. Chem.* **272,** 7473–7481
46. Brooks, P. C., Stromblad, S., Sanders, L. C., von Schalscha, T. L., Aimes, R. T., Stetler-Stevenson, W. G., Quigley, J. P., and Cheresh, D. A. (1996) *Cell* **85,** 683–693
47. Fridman, R., Toth, M., Pena, D., and Mobashery, S. (1995) *Cancer Res.* **55,** 2548–2555
48. Fernandez-Catalan, C., Bode, W., Huber, R., Turk, D., Calvete, J. J., Lichte, A., Tschesche, H., and Maskos, K. (1998) *EMBO J.* **17,** 5238–5248
49. Sato, H., Kinoshita, T., Takino, T., Nakayama, K., and Seiki, M. (1996) *FEBS Lett.* **393,** 101–104
50. Mallet, W. G., and Maxfield, F. R. (1999) *J. Cell Biol.* **146,** 345–359
51. Vey, M., Schafer, W., Berghofer, S., Klenk, H. D., and Garten, W. (1994) *J. Cell Biol.* **127,** 1829–1842

Biochemical and Biophysical Research Communications **281,** 126–130 (2001)
doi:10.1006/bbrc.2001.4323, available online at http://www.idealibrary.com on IDEAL®

Differential Roles of TIMP-4 and TIMP-2 in Pro-MMP-2 Activation by MT1-MMP

Sonia Hernandez-Barrantes,* Yoichiro Shimura,* Paul D. Soloway,†
QingXiang Amy Sang,‡ and Rafael Fridman*,[1]

**Department of Pathology, School of Medicine, Wayne State University, Detroit, Michigan 48201; †Department of Molecular and Cellular Biology, Roswell Park Cancer Institute, Buffalo, New York 14263; and ‡Department of Chemistry, Biochemistry Division, Florida State University, Tallahassee, Florida 32306*

Received January 9, 2001

The tissue inhibitors of metalloproteinases (TIMPs) are specific inhibitors of MMP enzymatic activity. However, TIMP-2 can promote the activation of pro-MMP-2 by MT1-MMP. This process is mediated by the formation of a complex between MT1-MMP, TIMP-2, and pro-MMP-2. Binding of TIMP-2 to active MT1-MMP also inhibits the autocatalytic turnover of MT1-MMP on the cell surface. Thus, under certain conditions, TIMP-2 is a positive regulator of MMP activity. TIMP-4, a close homologue of TIMP-2 also binds to pro-MMP-2 and can potentially participate in pro-MMP-2 activation. We coexpressed MT1-MMP with TIMP-4 and investigated its ability to support pro-MMP-2 activation. TIMP-4, unlike TIMP-2, does not promote pro-MMP-2 activation by MT1-MMP. However, TIMP-4 binds to MT1-MMP inhibiting its autocatalytic processing. When coexpressed with TIMP-2, TIMP-4 competitively reduced pro-MMP-2 activation by MT1-MMP. A balance between TIMP-2 and TIMP-4 may be a critical factor in determining the degradative potential of cells in normal and pathological conditions.

Key Words: **matrix metalloproteinases; TIMP; proteases; membrane proteins; cell surface.**

The activation of the zymogenic form of MMP-2 (pro-MMP-2) has been shown to be accomplished by the membrane-tethered MT1-MMP (MMP-14) (1, 2), which hydrolyses the Asn^{37}-Leu^{38} peptide bond in the prodomain of pro-MMP-2 (3). To facilitate the association of the prodomain of pro-MMP-2 with the active site of MT1-MMP, pro-MMP-2 must be positioned in close association with MT1-MMP. To achieve this, TIMP-2 acts as a molecular link between pro-MMP-2 and MT1-MMP (1). It has been shown that the NH_2-terminal region of TIMP-2 binds to the active site of an active MT1-MMP on the cell surface generating a pro-MMP-2 "receptor" (4). In turn, the COOH-terminal region of TIMP-2 binds to the COOH-terminal domain of pro-MMP-2, also known as the hemopexin-like domain (HLD) (1, 4–8). This trimeric MT1-MMP/TIMP-2/pro-MMP-2 complex permits the association of pro-MMP-2 to the cell surface, which eventually facilitates its activation by a neighboring TMP-2-free MT1-MMP. Under these conditions, TIMP-2 acts as a positive regulator of pro-MMP-2 activation (9). We have recently shown that in addition to its ability to form the pro-MMP-2 receptor, TIMP-2 can also regulate the nature of MT1-MMP forms present in the cells by its ability to inhibit MT1-MMP activity (6). This effect is due to the TIMP-2 inhibition of the autocatalytic turnover of MT1-MMP on the cell surface, which may represent a natural mechanism of clearance of active MT1-MMP from the cell surface once the enzyme has fulfilled its pericellular proteolytic function. As a consequence of the inhibition of autocatalytic degradation, *de novo* synthesis and membrane incorporation of new MT1-MMP molecules, TIMP-2 binding to active MT1-MMP results in accumulation of active MT1-MMP on the cell surface (6). These dual effects of TIMP-2 (ternary complex formation and inhibition of MT1-MMP autocatalytic turnover) contribute to the overall effects of MT1-MMP on the cell surface: activation of pro-MMP-2 and direct pericellular proteolysis (10, 11).

TIMP-2 belongs to a family of four TIMP inhibitors, which presently includes TIMP-1, TIMP-2, TIMP-3, and TIMP-4 (12). Studies on TIMP-MMP interactions have shown that TIMP-4, like TIMP-2 is also capable of forming a complex with pro-MMP-2, which is mediated by binding of the inhibitor to the HLD of the enzyme (13). Thus, functionally, TIMP-4 is similar to TIMP-2. In addition, sequence analyses revealed a 70% identity between TIMP-2 and TIMP-4 (12, 14). Based on these

[1] To whom correspondence should be addressed at Department of Pathology, Wayne State University, 540 E. Canfield Ave., Detroit, MI 48201. Fax: 313-577-8180. E-mail: rfridman@med.wayne.edu.

0006-291X/01 $35.00

observations, we asked whether TIMP-4, like TIMP-2, could also promote pro-MMP-2 activation by MT1-MMP. To answer this question, we expressed human TIMP-4 in a vaccinia expression system (15, 16) and tested its ability to promote pro-MMP-2 activation and inhibition of MT1-MMP autocatalysis in mammalian cells expressing MT1-MMP. Our studies demonstrate that unlike TIMP-2, TIMP-4 cannot promote MT1-MMP dependent pro-MMP-2 activation but can inhibit MT1-MMP autocatalytic degradation. Furthermore, if co-expressed with TIMP-2, TIMP-4 reduces the rate of pro-MMP-2 activation induced by TIMP-2.

MATERIALS AND METHODS

Cells. Nonmalignant monkey kidney epithelial BS-C-1 (CCL-26) cells were obtained from the American Type Culture Collection (ATCC, Rockville, MD) and cultured in Dulbecco's modified Eagle medium (DMEM) supplemented with 10% fetal bovine serum (FBS) and antibiotics. Immortalized homozygous *Timp2* (−/−) mutant mouse fibroblasts were isolated from *Timp2* deficient mice and immortalized by retroviral infection as described (7, 17, 18) and maintained in DMEM supplemented with 10% FBS and antibiotics. All tissue culture reagents were purchased from Gibco BRL (Grand Island, NY).

Vaccinia virus and construction of expression vectors. The generation of the vaccinia expression vector pTF7EMCV-1 (pTF7) containing the T7 RNA promoter and the production of vTF7-3, a recombinant vaccinia virus expressing bacteriophage T7 RNA polymerase, have been described by Fuerst *et al.* (16). The generation of the pTF7-T2 vector expressing human TIMP-2 (15) and pTF7-MT1 expressing human MT1-MMP (6) has been described. The human full-length TIMP-4 cDNA (14), a generous gift from Dr. Y. E. Shi (Albert Einstein College of Medicine, New Hyde Park, NY 11042), was amplified by the polymerase chain reaction (PCR) using the following oligonucleotide primers: 5′-CATTCCATGGCACCTGGGAGCCCT-3′ and 5′-CTTGGATCCCTAGGGCTGAACGATGTCAAC-3′ containing the NcoI and BamHI restriction sites, respectively. The amplified TIMP-4 fragment was isolated and cloned into pTF7 vector (16) to generate the pTF7-T4 plasmid. The DNA sequence of the TIMP-4 PCR fragment was verified by sequencing of both strands directly from the pTF7-T4 vector using an ABI377A DNA sequencer.

Expression of recombinant proteins by infection–transfection. Monkey kidney BS-C-1 or *Timp2* (−/−) mutant cells in 6-well plates were infected with 30 plaque-forming units (pfu)/cell of the vTF-3 virus in DMEM containing 2.5% FBS (15). Thirty minutes postinfection, the media were aspirated and the infected cells were cotransfected with a mixture of either pTF7-MT1 and pTF7-T4 plasmids (04 μg/ml each) or pTF7-MT1 and pTF7-T2 plasmids (04 μg/ml each) to coexpress MT1-MMP with each inhibitor using Effectene (Qiagen, Valencia, CA), as described by the manufacturer. In some experiments, MT1-MMP was coexpressed with both TIMP-4 and TIMP-2 by transfecting a mixture of the three plasmids (04 μg/ml each). As controls, the infected cells were transfected with pTF7-MT1, pTF7-T4, pTF7-T2 or the empty pFT7EMCV-1 expression vectors alone. An additional control included cells infected with vTF-3 virus but nontransfected. Four h post-transfection, the media were aspirated and replaced with 1 ml/well of OPTI-MEM (Gibco BRL).

Activation of pro-MMP-2. Eighteen hours following the infection/transfection procedure, the cells received 3 nM/well of purified recombinant pro-MMP-2, purified to homogeneity as previously described (15), followed by a 4-h incubation at 37°C. The media were collected and clarified by a brief centrifugation (13,000*g*, 15 min, 4°C) and the cells were solubilized in 100 μl/well of cold lysis buffer (25 mM Tris–HCl [pH 7.5], 1% IGEPAL CA-630, 100 mM NaCl, 10 μg/ml aprotinin, 1 μg/ml leupeptin, 2 mM benzamidine, and 1 mM PMSF) and centrifuged (13,000*g*) for 15 min at 4°C. Samples of the lysates (10 μl) were mixed with 4X Laemmli sample buffer (19) without reducing agents and without heating and subjected to gelatin zymography, as previously described (20).

Immunoprecipitation of TIMP-2 and TIMP-4. BS-C-1 cells Infected-transfected to express TIMP-2 or TIMP-4 with or without MT1-MMP, in 6-well plates, were metabolically labeled for 4 h at 37°C with 100 μCi/ml of ^{35}S-methionine in 1 ml/well of DMEM without methionine supplemented with 1% dialyzed FBS. The media were collected, clarified by a brief centrifugation and an aliquot incubated (16 h, 4°C) with either 5 μg of anti-TIMP-2 CA-101 monoclonal antibody or a rabbit polyclonal antibody to TIMP-4 (21) followed by the addition of 30 μl of Protein G-Sepharose beads for an additional 3-h incubation at 4°C. After recovering the beads by a brief centrifugation, the beads were washed (5 times) with cold 50 mM Tris–HCl pH 7.5 containing 150 mM NaCl, 0.1% NP-40, and 10% glycerol and resuspended in 15 μl Laemmli sample buffer with β-mercaptoethanol followed by boiling (5 min). The immunoprecipitates were resolved by 15% SDS–polyacrylamide gel electrophoresis (SDS–PAGE). Detection of radiolabeled proteins was performed by autoradiography.

Immunoblot analysis of MT1-MMP forms. Infected BS-C-1 cells in 6-well plates, as described above, were lysed in cold lysis buffer. The lysates were mixed with 4× Laemmli sample buffer with β-mercaptoethanol and then resolved by 10% SDS–PAGE followed by transfer to a nitrocellulose membrane as described (20). Detection of MT1-MMP and TIMP-4 were carried out using a polyclonal antibody to human MT1-MMP (pAb 437) (22) and a polyclonal antibody to human TIMP-4 (21), respectively. Detection of the antigen-antibody complex was performed using the SuperSignal Enhanced Chemiluminescence (ECL) system (Pierce, Rockford, IL), according to the manufacturer's instructions.

RESULTS AND DISCUSSION

Our previous studies demonstrated that co-expression of human MT1-MMP with TIMP-2 in a vaccinia expression system resulted in enhanced activation of pro-MMP-2 (6). Activation of pro-MMP-2 by MT1-MMP was TIMP-2-dependent since no activation was observed in cells devoid of TIMP-2 (*Timp2* mutant cells) (7). Furthermore, TIMP-2 presence induced the accumulation of the 57-kDa form of MT1-MMP, which represents the active enzyme starting at Y^{112}. Concomitantly with the accumulation of the 57-kDa form there was a reduction of the 44–40-kDa autocatalytic product of MT1-MMP in the cell lysates (7). To examine the effects of TIMP-4 on pro-MMP-2 activation, the full-length human TIMP-4 cDNA was cloned into the pTF7EMCV-1 vaccinia expression vector (16) and expressed in BS-C-1 cells with or without MT1-MMP using the infection-transfection procedure. For comparison, the cells were infected-transfected to co-express TIMP-2 and MT1-MMP. Analysis of TIMP-4 and TIMP-2 expression was monitored by immunoprecipitation of the inhibitors from the media of ^{35}S-labeled cells. As shown in Fig. 1, both TIMP-2 (Fig. 1, lane 2) and TIMP-4 (Fig. 1, lane 4) were detected in the media when expressed without MT1-MMP. In contrast, co-expression of the inhibitors with MT1-MMP

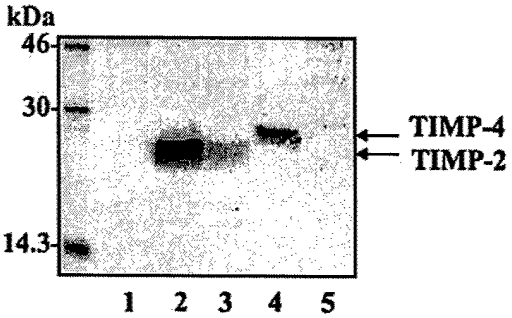

FIG. 1. Expression of TIMP-2 and TIMP-4 with and without MT1-MMP. BS-C-1 cells were infected–transfected to express TIMP-2 (lanes 2 and 3) or TIMP-4 (lanes 4 and 5) alone (lanes 2 and 4) or with MT1-MMP (lanes 3 and 5) as described under Materials and Methods. As control, cells were infected and then transfected with the empty vector. The next day, the media were collected and immunoprecipitated with antibodies to either TIMP-2 (lanes 2 and 3) or TIMP-4 (lanes 4 and 5) and Protein G-Sepharose beads. The medium of control-transfected cells (lane 1) was immunoprecipitated with both antibodies. The immunoprecipitates were resolved by reducing 15% SDS–PAGE followed by autoradiography. ^{14}C-labeled molecular weight standards were used as reference.

resulted in a significant reduction of TIMP-2 (Fig. 1, lane 3) and TIMP-4 (Fig. 1, lane 5) from the media. We have previously shown that co-expression of TIMP-2 with MT1-MMP results in the targeting of the inhibitor to the cell surface. This differential distribution is due to the binding of TIMP-2 to active MT1-MMP resulting in a specific downregulation of TIMP-2 protein from the media. Thus, the lack of detection of TIMP-4 in the supernatant of cells coexpressing MT1-MMP and TIMP-4 suggests that TIMP-4, like TIMP-2, associates with active MT1-MMP. Indeed, when coexpressed with MT1-MMP, TIMP-4 is found mostly in the cell lysate (shown in Fig. 3B, lane 3).

We next examined the ability of TIMP-4 to promote pro-MMP-2 activation by MT1-MMP. To this end, the BS-C-1 and the *Timp2* (−/−) mutant cells were infected-transfected to express MT1-MMP with or without TIMP-2 or TIMP-4. Then, the cells received exogenous pro-MMP-2. Activation was monitored by gelatin zymography of cell lysates. As shown in Fig. 2, BS-C-1 (Fig. 2A) or *Timp2* (−/−) mutant (Fig. 2B) cells coexpressing MT1-MMP and TIMP-2 (BS-C-1, Fig. 2A, lane 3; *Timp2* (−/−), Fig. 2B, lane 4) converted pro-MMP-2 (refer as P) into the active MMP-2 (refer as A) form of 62-kDa. In contrast, coexpression of MT1-MMP with TIMP-4 in either BS-C-1 (Fig. 2A, lane 4) or *Timp2* (−/−) mutant (Fig. 2B, lane 5) cells failed to promote pro-MMP-2 activation. BS-C-1 cells infected-transfected to express MT1-MMP alone (Fig. 2A, lane 2) exhibited a modest degree of active MMP-2 when compared to the activation observed when MT1-MMP was co-expressed with TIMP-2 (Fig. 2A, lane 3). This basal activation is due to the presence of some residual endogenous TIMP-2, which is present in the BS-C-1 cells, as reported previously (7). Indeed, in the *Timp2* (−/−) mutant cells, which are devoid of TIMP-2, no evidence of active MMP-2 was observed in cells expressing MT1-MMP alone (Fig. 2B, lane 3) consistent with the absolute requirement of TIMP-2 for the MT1-MMP-dependent activation of pro-MMP-2. As expected, no activation was observed in either cell type infected with the vTF7-3 virus and transfected with the empty vector (BS-C-1, Fig. 2A, lane 1; *Timp2* (−/−), Fig. 2B, lane 2). These studies establish the inability of TIMP-4 to promote pro-MMP-2 activation by MT1-MMP and demonstrate that this effect can only be mediated by TIMP-2 in spite of the ability of both inhibitors to form a non-covalent complex with pro-MMP-2 through its hemopexin-like domain (13, 15). The localization of TIMP-4 in the cell lysate when co-expressed with MT1-MMP suggested that TIMP-4 could bind to active MT1-MMP. Therefore, we wished to examine whether coexpression of TIMP-2 and TIMP-4 with MT1-MMP would affect the ability of TIMP-2 to enhance pro-MMP-2 activation. As shown in Fig. 2A, BS-C-1 cells coexpressing MT1-MMP, TIMP-2, and TIMP-4 (Fig. 2A, lane 5) exhibited a significant reduction in active MMP-2 when compared to the cells expressing MT1-MMP with TIMP-2 (Fig. 2A, lane 3). This result suggests that TIMP-4 competes for the binding of TIMP-2 to MT1-MMP and therefore prevents its ability to support pro-MMP-2 activation.

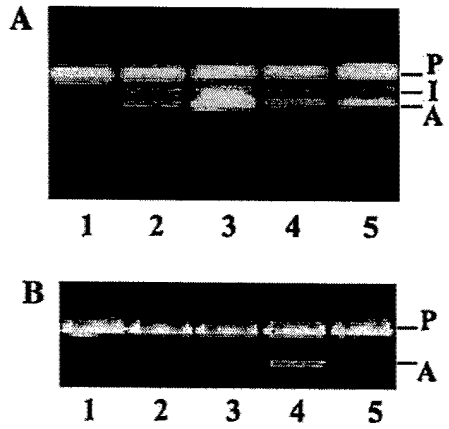

FIG. 2. Effect of TIMP-4 on pro-MMP-2 activation by MT1-MMP. (A) BS-C-1 cells were infected with 30 pfu/cell of vTF7-3 and then transfected with 0.4 μg/well each of plasmid DNA (lane 1, pTF7EMCV-1 empty vector; lane 2, pTF7-MT1; lane 3, pTF7-MT1 + pTF7-T2; lane 4, pTF7-MT1+ pTF7-T4; and lane 5, pTF7-MT1+ pTF7-T4 + pTF7-T2). Some cells were only infected with 30 pfu/cell of vTF7-3 (lane 1). At 18 h post-infection/transfection, the cells were incubated with 3 nM of purified recombinant pro-MMP-2 for an additional 4 h at 37°C followed by solubilization of the cells with lysis buffer. The lysates were then subjected to gelatin zymography. (B) *Timp2* (−/−) mutant cells were infected–transfected to express MT1-MMP alone (lane 3) or with either TIMP-2 (lane 4) or TIMP-4 (lane 5) as described in A. As control, some mutant cells were infected with vTF7-3 virus only or subsequently transfected with empty vector (lane 2). Activation of pro-MMP-2 was carried out as described in A. P, I, and A refer to pro-MMP-2 (72 kDa), intermediate form (64 kDa), and active MMP-2 (62 kDa).

Early studies showed a restricted pattern of expression of TIMP-4 in human and mouse tissues with preponderant expression in heart tissue (14, 23). However, recent studies indicate a broader tissue expression of TIMP-4 in normal tissues (24–26) and enhanced expression in pathological conditions (27–31). In various instances, the expression of TIMP-4 has been shown to overlap with that of TIMP-2 (27–29, 31). TIMP-4 has also been shown to inhibit tumor growth and metastasis of a human breast cancer cell line (32). However, its expression in human cancer tissues has not been examined in detail. Although the precise role of each TIMP in normal and pathological conditions remains to be further evaluated, the ability of TIMP-4 to inhibit the effect of TIMP-2 on pro-MMP-2 activation suggests that a balance of these inhibitors may alter the net activity of MMP-2 with TIMP-2, under certain conditions, promoting MMP-2- and MT1-MMP-dependent proteolysis and TIMP-4 acting as a general MMP inhibitor.

Presently, no information exists in regards to the molecular interactions of TIMP-4 with MT1-MMP. The crystal structures of TIMP-2 and TIMP-1 show that TIMP-2 has an insertion at Asp^{30}-Arg^{42} that extends the beta-sheets to interact with the catalytic domain of MT1-MMP. In addition, Tyr^{36} on TIMP-2 has hydrophobic interactions with the catalytic domain of MT1-MMP, fitting into a hydrophobic pocket above the active site groove near the S2/S3 site (5). These features, which are absent in TIMP-1, may partly explain the preferred binding of TIMP-2 to MT1-MMP (3, 5, 6). Energy-minimized computer modeling of the TIMP-4 structure based on the x-ray crystal structure of TIMP-2 (5) shows that TIMP-4 (12, 14), as opposed to TIMP-1, possesses a similar insertion at Val^{29}-Met^{41} that could potentially enhance interactions with the catalytic domain of MT1-MMP (Drs. Mobashery and Kotra, Dept. of Chemistry, Wayne State University, Personal communication) and inhibit MT1-MMP activity. We have previously shown that TIMP-2 induces accumulation of the 57-kDa active form of MT1-MMP (6). This effect is a direct consequence of the inhibitory action of TIMP-2 on MT1-MMP activity, which inhibits the autocatalytic turnover of active MT1-MMP into the inactive forms of 44–40 kDa. The 44-kDa form possesses an N-terminus starting at G^{285} and its formation involves the deletion of the entire catalytic domain of MT1-MMP (6). Accumulation of active MT1-MMP and reduction of the 44-kDa form are also observed with synthetic MMP inhibitors consistent with the autocatalytic nature of this process (6). Thus, both TIMP-2 and synthetic MMP inhibitors regulate the nature of the MT1-MMP forms present in the cells. Here, we examined the lysates of BS-C-1 cells expressing MT1-MMP alone or with TIMP-4 for the profile of MT1-MMP forms by immunoblot analysis. As shown in Fig. 3, in the absence of TIMP-4, MT1-MMP is detected in its 60-, 57-, and 44–40-kDa forms (Fig. 3, lane 2) as previously reported (6). The 60-kDa protein represents pro-MT1-MMP starting at S^{24} (6). The 62-, 55-, and 37–35 kDa bands are nonspecific, as they are detected in infected cells transfected with empty vector (Fig. 3, lane 1). In the presence of TIMP-4 (Fig. 3, lane 3), there is a significant increase in the 57-kDa species of MT1-MMP and a reduction in the 44-40-kDa forms. Figure 3B shows the presence of TIMP-4 in the same lysates as detected with a specific anti-TIMP-4 antibody (lane 3) (21). Similar results were obtained with the *Timp2* (−/−) mutant cells (data not shown). From these results we conclude that, like TIMP-2, TIMP-4 inhibits the autocatalytic turnover of MT1-MMP and thus, TIMP-4 is likely to form a complex with the active form of MT1-MMP. This is further supported by the lack of detection of TIMP-4 in the supernatant of cells co-expressing MT1-MMP with the inhibitor as discussed above. Although not directly proven here, these results suggest that the lack of pro-MMP-2 activation in the presence of TIMP-4 is due to the inability of this inhibitor to generate a ternary complex with MT1-MMP and pro-MMP-2. Thus, while TIMP-4 binds to active MT1-MMP, the TIMP-4/MT1-MMP complex cannot act as a receptor for pro-MMP-2 and therefore activation does not ensue. The structural constrains that impede the formation of the ternary complex awaits elucidation of the crystal structure of the TIMP-4/MT1-MMP complex. In conclusion, the results of this study demonstrate a differential role for members of the TIMP family in the inhibition of MT1-MMP activity and in MT1-MMP-dependent pro-MMP-2 activation.

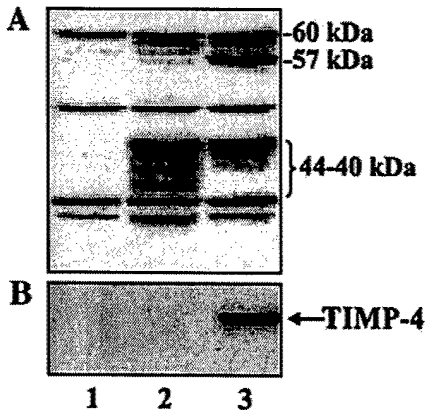

FIG. 3. Profile of MT1-MMP forms in the presence of TIMP-4. (A) BS-C-1 cells were infected–transfected to express MT1-MMP alone (lane 2) or with TIMP-4 (lane 3) as described in the legend to Fig. 2A. As control, some cells were infected–transfected with empty vector (lane 1). The cells lysates were resolved by reducing 10% SDS–PAGE followed by immunoblot analysis with anti-MT1-MMP antibodies and detection by ECL. (B) The same blot was reprobed with anti-TIMP-4 antibodies and developed by ECL.

AKNOWLEDGMENTS

Supported by National Institutes of Health (NIH) Grant CA-61986, Department of Defense (DOD) Grant DAMD17-99-1-9440 (both to R.F.), and NIH Grant CA-78646 (to Q-X.S.). S. H-B. was supported by a DOD Predoctoral Fellowship DAMD17-99-1-9441.

REFERENCES

1. Strongin, A. Y., Collier, I., Bannikov, G., Marmer, B. L., Grant, G. A., and Goldberg, G. I. (1995) *J. Biol. Chem.* **270,** 5331–5338.
2. Sato, H., Takino, T., Okada, Y., Cao, J., Shinagawa, A., Yamamoto, E., and Seiki, M. (1994) *Nature* **370,** 61–65.
3. Will, H., Atkinson, S. J., Butler, G. S., Smith, B., and Murphy, G. (1996) *J. Biol. Chem.* **271,** 17119–17123.
4. Butler, G. S., Butler, M. J., Atkinson, S. J., Will, H., Tamura, T., van Westrum, S. S., Crabbe, T., Clements, J., d'Ortho, M. P., and Murphy, G. (1998) *J. Biol. Chem.* **273,** 871–880.
5. Fernandez-Catalan, C., Bode, W., Huber, R., Turk, D., Calvete, J. J., Lichte, A., Tschesche, H., and Maskos, K. (1998) *EMBO J.* **17,** 5238–5248.
6. Hernandez-Barrantes, S., Toth, M., Bernardo, M. M., Yurkova, M., Gervasi, D. C., Raz, Y., Sang, Q. A., and Fridman, R. (2000) *J. Biol. Chem.* **275,** 12080–12089.
7. Toth, M., Bernardo, M. M., Gervasi, D. C., Soloway, P. D., Wang, Z., Bigg, H. F., Overall, C. M., DeClerck, Y. A., Tschesche, H., Cher, M. L., Brown, S., Mobashery, S., and Fridman, R. (2000) *J. Biol. Chem.* **275,** 41415–41423.
8. Zucker, S., Drews, M., Conner, C., Foda, H. D., DeClerck, Y. A., Langley, K. E., Bahou, W. F., Docherty, A. J., and Cao, J. (1998) *J. Biol. Chem.* **273,** 1216–1222.
9. Jo, Y., Yeon, J., Kim, H. J., and Lee, S. T. (2000) *Biochem. J.* **345** (Part 3), 511–519.
10. Hotary, K., Allen, E., Punturieri, A., Yana, I., and Weiss, S. J. (2000) *J. Cell. Biol.* **149,** 1309–1323.
11. Caterina, J. J., Yamada, S., Caterina, N. C., Longenecker, G., Holmback, K., Shi, J., Yermovsky, A. E., Engler, J. A., and Birkedal-Hansen, H. (2000) *J. Biol. Chem.* **275,** 26416–26422.
12. Brew, K., Dinakarpandian, D., and Nagase, H. (2000) *Biochim. Biophys. Acta* **1477,** 267–283.
13. Bigg, H. F., Shi, Y. E., Liu, Y. E., Steffensen, B., and Overall, C. M. (1997) *J. Biol. Chem.* **272,** 15496–154500.
14. Greene, J., Wang, M., Liu, Y. E., Raymond, L. A., Rosen, C., and Shi, Y. E. (1996) *J. Biol. Chem.* **271,** 30375–30380.
15. Fridman, R., Fuerst, T. R., Bird, R. E., Hoyhtya, M., Oelkuct, M., Kraus, S., Komarek, D., Liotta, L. A., Berman, M. L., and Stetler-Stevenson, W. G. (1992) *J. Biol. Chem.* **267,** 15398–15405.
16. Fuerst, T. R., Earl, P. L., and Moss, B. (1987) *Mol. Cell. Biol.* **7,** 2538–2544.
17. Soloway, P. D., Alexander, C. M., Werb, Z., and Jaenisch, R. (1996) *Oncogene* **13,** 2307–2314.
18. Wang, Z., Juttermann, R., and Soloway, P. D. (2000) *J. Biol. Chem.* **275,** 26411–26415.
19. Laemmli, U. K. (1970) *Nature* **227,** 680–685.
20. Toth, M., Gervasi, D. C., and Fridman, R. (1997) *Cancer Res.* **57,** 3159–3167.
21. Li, H., Bauzon, D. E., Xu, X., Tschesche, H., Cao, J., and Sang, Q. A. (1998) *Mol. Carcinog.* **22,** 84–94.
22. Gervasi, D. C., Raz, A., Dehem, M., Yang, M., Kurkinen, M., and Fridman, R. (1996) *Biochem. Biophys. Res. Commun.* **228,** 530–538.
23. Leco, K. J., Apte, S. S., Taniguchi, G. T., Hawkes, S. P., Khokha, R., Schultz, G. A., and Edwards, D. R. (1997) *FEBS Lett.* **401,** 213–217.
24. Wu, I., and Moses, M. A. (1998) *Matrix Biol.* **16,** 339–342.
25. Riley, S. C., Leask, R., Denison, F. C., Wisely, K., Calder, A. A., and Howe, D. C. (1999) *J. Endocrinol.* **162,** 351–359.
26. Fata, J. E., Leco, K. J., Moorehead, R. A., Martin, D. C., and Khokha, R. (1999) *Dev. Biol.* **211,** 238–254.
27. Dollery, C. M., McEwan, J. R., Wang, M., Sang, Q. A., Liu, Y. E., and Shi, Y. E. (1999) *Circ. Res.* **84,** 498–504.
28. Michael, M., Babic, B., Khokha, R., Tsao, M., Ho, J., Pintilie, M., Leco, K., Chamberlain, D., and Shepherd, F. A. (1999) *J. Clin. Oncol.* **17,** 1802–1808.
29. Reno, C., Boykiw, R., Martinez, M. L., and Hart, D. A. (1998) *Biochem. Biophys. Res. Commun.* **252,** 757–763.
30. Thomas, P., Khokha, R., Shepherd, F. A., Feld, R., and Tsao, M. S. (2000) *J. Pathol.* **190,** 150–156.
31. Selman, M., Ruiz, V., Cabrera, S., Segura, L., Ramirez, R., Barrios, R., and Pardo, A. (2000) *Am. J. Physiol. Lung Cell Mol. Physiol.* **279,** L562–L574.
32. Wang, M., Liu, Y. E., Greene, J., Sheng, S., Fuchs, A., Rosen, E. M., and Shi, Y. E. (1997) *Oncogene* **14,** 2767–2774.

THE JOURNAL OF BIOLOGICAL CHEMISTRY

Vol. 277, No. 29, Issue of July 19, pp. 26340–26350, 2002
Printed in U.S.A.

Complex Pattern of Membrane Type 1 Matrix Metalloproteinase Shedding

REGULATION BY AUTOCATALYTIC CELL SURFACE INACTIVATION OF ACTIVE ENZYME*

Received for publication, January 22, 2002, and in revised form, April 15, 2002
Published, JBC Papers in Press, May 9, 2002, DOI 10.1074/jbc.M200655200

Marta Toth‡, Sonia Hernandez-Barrantes‡§, Pamela Osenkowski‡, M. Margarida Bernardo‡, David C. Gervasi‡, Yoichiro Shimura‡, Oussama Meroueh¶, Lakshmi P. Kotra¶, Beatriz G. Gálvez‖, Alicia G. Arroyo‖, Shahriar Mobashery¶, and Rafael Fridman‡**

From the Departments of ‡Pathology and ¶Chemistry, Wayne State University, Detroit, Michigan 48201 and the ‖Departamento de Inmunologia, Hospital de la Princesa, 28006 Madrid, Spain

Membrane type 1 matrix metalloproteinase (MT1-MMP) is a type I transmembrane MMP shown to play a critical role in normal development and in malignant processes. Emerging evidence indicates that MT1-MMP is regulated by a process of ectodomain shedding. Active MT1-MMP undergoes autocatalytic processing on the cell surface, leading to the formation of an inactive 44-kDa fragment and release of the entire catalytic domain. Analysis of the released MT1-MMP forms in various cell types revealed a complex pattern of shedding involving two major fragments of 50 and 18 kDa and two minor species of 56 and 31–35 kDa. Protease inhibitor studies and a catalytically inactive MT1-MMP mutant revealed both autocatalytic (18 kDa) and non-autocatalytic (56, 50, and 31–35 kDa) shedding mechanisms. Purification and sequencing of the 18-kDa fragment indicated that it extends from Tyr^{112} to Ala^{255}. Structural and sequencing data indicate that shedding of the 18-kDa fragment is initiated at the Gly^{284}-Gly^{285} site, followed by cleavage between the conserved Ala^{255} and Ile^{256} residues near the conserved methionine turn, a structural feature of the catalytic domain of all MMPs. Consistently, a recombinant 18-kDa fragment had no catalytic activity and did not bind TIMP-2. Thus, autocatalytic shedding evolved as a specific mechanism to terminate MT1-MMP activity on the cell surface by disrupting enzyme integrity at a vital structural site. In contrast, functional data suggest that the non-autocatalytic shedding generates soluble active MT1-MMP species capable of binding TIMP-2. These studies suggest that ectodomain shedding regulates the pericellular and extracellular activities of MT1-MMP through a delicate balance of active and inactive enzyme-soluble fragments.

Release of the extracellular portion of type I transmembrane proteins, referred to as ectodomain shedding, has been established as a major regulatory mechanism to control the activity of a variety of membrane-bound proteins on the cell surface (1). Recent evidence suggests that ectodomain shedding is also characteristic of the membrane type matrix metalloproteinases (MT-MMPs),[1] a subfamily of membrane-anchored MMPs by means of a transmembrane domain or a glycosylphosphatidylinositol anchor (2, 3). The MT-MMPs are major mediators of proteolytic events on the cell surface, including turnover of extracellular matrix components (4, 5), cleavage of various surface adhesion receptors (6–8), and initiation of zymogen activation cascades (9, 10). Uncontrolled MT-MMP activity contributes to abnormal development (11) and is a key determinant in cancer metastasis and tumor angiogenesis (12–14). To control the extent of pericellular activity, the MT-MMPs are inhibited by the tissue inhibitors of metalloproteinases (TIMPs), a family of natural protein MMP inhibitors. In addition, MT-MMPs have a unique regulatory mechanism in which the active enzyme undergoes a series of processing steps, either autocatalytic (15–17) or mediated by other proteases (18), that regulate the activity and nature of the enzyme species at the cell surface and at the pericellular space. Previous studies have shown that active MT1-MMP is autocatalytically processed on the cell surface to an inactive membrane-tethered ~44-kDa species lacking the entire catalytic domain (17). This processing is inhibited by TIMP-2, TIMP-4, and synthetic MMP inhibitors consistent with being an intermolecular autocatalytic event (19, 20). Inhibition of MT1-MMP processing induces accumulation of the active enzyme on the cell surface, and, as a consequence, net MT1-MMP-dependent proteolysis is enhanced. Indeed, we have shown that, under certain conditions, inhibition of MT1-MMP autocatalysis by synthetic MMP inhibitors enhances pro-MMP-2 activation by MT1-MMP in the presence of TIMP-2 (20, 21). Thus, although the presence of inhibitors will stabilize MT1-MMP on the cell surface, the absence or reduced levels of inhibitors will facilitate autocatalysis. As a membrane-anchored protein, the autocatalytic processing of active MT1-MMP on the cell surface raises questions as to the fate of the ectodomain and its functional consequences. Accumulating evidence suggests that catalytic domain shedding may represent a general characteristic of several members of the MT-MMP family, and both autocatalytic and non-autocatalytic mechanisms of shedding have been described, *e.g.* autocatalysis was implicated in the shedding of

* This work was supported in part by National Institutes of Health Grant CA-61986 and by United States Army Breast Cancer Program Grant DAMD17-99-1-9440 (to R. F.). The costs of publication of this article were defrayed in part by the payment of page charges. This article must therefore be hereby marked "*advertisement*" in accordance with 18 U.S.C. Section 1734 solely to indicate this fact.

§ Supported by Predoctoral Fellowship DAMD17-99-1-9441 from the United States Army Breast Cancer Program. The costs of publication of this article were defrayed in part by the payment of page charges. This article must therefore be hereby marked "*advertisement*" in accordance with 18 U.S.C. Section 1734 solely to indicate this fact.

** To whom all correspondence should be addressed: Dept. of Pathology, Wayne State University, 540 E. Canfield Ave., Detroit, MI 48201. E-mail: rfridman@med.wayne.edu.

[1] The abbreviations used are: MT-MMP, membrane type matrix metalloproteinase; MMP, matrix metalloproteinase; TIMP, tissue inhibitor of metalloproteinase; mAb, monoclonal antibody; pAb, polyclonal antibody; ConA, concanavalin A; TPA, 12-*O*-tetradecanoylphorbol-13-acetate.

MT1-MMP in cells transfected to overexpress MT1-MMP (22). Other studies reported shedding of MT1-MMP from a breast carcinoma cell line after treatment with concanavalin A (ConA) (23–25), which was not inhibited by TIMP-2 (23); therefore, autocatalysis could not be involved. MT5-MMP sheds its catalytic domain in a process that appears to be mediated by a pro-convertase that removes the ectodomain intracellularly (26). Pre-mRNA splicing was reported to be involved in the generation of a soluble form of MT3-MMP, which retained catalytic activity and sensitivity to TIMP-2 inhibition (27). Thus, although different mechanisms of shedding may exist, collectively, these data suggest a unique property of MT-MMPs: the ability to generate soluble fragments by a process of ectodomain shedding, which may possess important functional consequences for pericellular proteolysis in normal and malignant processes. Here we have identified the major soluble forms of MT1-MMP and characterized the major autocatalytic fragment. We demonstrated that the autocatalytic shedding mechanism of MT1-MMP is likely to have evolved to terminate MT1-MMP-dependent proteolysis by hydrolyzing the enzyme at specific and vital sites.

EXPERIMENTAL PROCEDURES

Cell Culture—The characteristics and culture conditions of nonmalignant monkey kidney epithelial BS-C-1 (CCL-26) (28), human fibrosarcoma HT-1080 (CCL-121) (29), human fibroblasts HFL1 (CCL-153) (29), and human breast carcinoma MDA-MB-231 (HTB-26) (30) cells have been previously described. Human glioblastoma U-87 MG (HTB-14) cells, obtained from the American Tissue Culture Collection (ATCC), and immortalized homozygous *Timp2* (−/−) mutant mouse fibroblasts, a gift from Dr. P. Soloway (Roswell Park Cancer Institute, Buffalo, NY) (20, 31), were maintained in Dulbecco's modified Eagle's medium (DMEM) supplemented with 10% fetal bovine serum and antibiotics. The *Timp2* (−/−) mutant cells were stably transfected to express full-length human MT1-MMP using an MT1-MMP expression vector (P_6R-MT1-MMP) with hygromycin resistance (a gift from Dr. G. Goldberg, Washington University, St. Louis, MO). A stable hygromycin-resistant clone designated *Timp2* (−/−)-MT1 was selected for further studies.

Recombinant Vaccinia Viruses—The production of the recombinant vaccinia virus (vTF7–3) expressing bacteriophage T7 RNA polymerase has been described (32). Recombinant vaccinia viruses expressing pro-MMP-2 (vT7-GELA), MT1-MMP (vT7-MT1), TIMP-2 (vSC59-T2), or TIMP-1 (vT7-T1) were obtained by homologous recombination as previously described (17, 28, 33).

Recombinant Proteins, Synthetic MMP Inhibitors, and Antibodies—Human recombinant pro-MMP-2, TIMP-2, and TIMP-1 were expressed in HeLa cells and purified to homogeneity, as previously described (34). Human TIMP-4 was a generous gift from Dr. C. Overall (University of British Columbia, Vancouver, Canada). A recombinant catalytic domain of human MT1-MMP (Tyr^{112} to Gly^{288}) designated MT1-MMP_{cat} was purchased from Calbiochem. Marimastat (BB-2516) was obtained from British Biotech (Annapolis, MD) (35). SB-3CT was produced and characterized as described (36). The anti-TIMP-2 monoclonal antibody (mAb) CA-101 (33), the rabbit polyclonal antibody (pAb) 437 to the hemopexin-like domain of MT1-MMP (17), and the rabbit pAb to human TIMP-1 have been previously described (37, 38). The rabbit pAb 160 to the catalytic domain of MT1-MMP (25) was a generous gift from Dr. A. Sang (Florida State University, Tallahassee, FL). The mAb LEM-2/15 to the catalytic domain of human MT1-MMP has been described (39).

Cell Treatments and Metabolic Labeling—HT1080, MDA-MB-231, U-87 and HFL1 cells were grown to 80% confluence in 150-mm tissue culture dishes and then incubated (16 h, 37 °C) with serum-free DMEM (15 ml/dish) supplemented with or without 100 nM 12-*O*-tetradecanoylphorbol-13-acetate (TPA) or 10 μg/ml concanavalin A (ConA) (Sigma). In some experiments, these cell lines and the *Timp2* (−/−)-MT1 cells were metabolically labeled (6–16 h, 37 °C) with 70–100 μCi/ml [^{35}S]methionine (PerkinElmer Life Sciences) in starving medium (DMEM without methionine supplemented with 25 mM HEPES).

Cell Surface Biotinylation—HT1080 cells in six-well plates were untreated or treated with 100 nM TPA or 10 μg/ml ConA in 1 ml of serum-free medium overnight. The cells were rinsed with cold phosphate-buffered saline containing 0.1 mM $CaCl_2$ and 1 mM $MgCl_2$ and then biotinylated with 0.5 mg/ml sulfo-NHS-biotin as described (38). The cells were lysed with 0.5 ml/well harvest buffer (0.5% SDS, 60 mM Tris/HCl, pH 7.5, 2 mM EDTA) and boiled. The lysates were supplemented with 2.5% Triton X-100 (final concentration) followed by addition of either pAb 437 or pAb 160/Protein A-agarose beads. After a 12-h incubation period (4 °C), the beads were washed three times with harvest buffer supplemented with 2.5% Triton X-100 (final concentration) followed by one wash with collagenase buffer (50 mM Tris/HCl, pH 7.5, 150 mM NaCl, 5 mM $CaCl_2$, and 0.02% Brij-35). The immunoprecipitates were eluted with Laemmli SDS sample buffer (40), boiled, and resolved by reducing 8–16% SDS-PAGE, followed by transfer to a nitrocellulose membrane. The biotinylated MT1-MMP forms were detected with streptavidin-horseradish peroxidase and ECL.

Expression of MT1-MMP and Treatment with MMP Inhibitors—To express full-length human MT1-MMP, confluent cultures of BS-C-1 or *Timp2* (−/−) mutant cells in six-well plates were co-infected with 5–10 plaque-forming units/cell each of vTF7–3 and vT7-MT1 viruses for 45 min in infection medium (DMEM + 2.5% fetal bovine serum and antibiotics) at 37 °C. As a control, the cells were infected only with the vTF7–3 virus. After infection, the cultures were incubated (12 h, 37 °C) with serum-free DMEM supplemented with various protease inhibitors: TIMP-2, TIMP-4, and TIMP-1 (0–100 nM); marimastat (0–500 nM); SB-3CT (0–100 nM); aprotinin (20 and 40 μg/ml); leupeptin (40 μg/ml); or E64 (10 μM) overnight, as described (20). TPA-treated HT1080 cells, as described above, received 100 μg/ml aprotinin or 100 nM human recombinant TIMP-2. The serum-free conditioned media were collected and processed for immunoblot analysis, as described below.

Cloning, Expression, and Isolation of Recombinant MT1-MMP Mutants—A catalytically inactive mutant of MT1-MMP was generated by replacing Glu^{240} with Ala (E240A-MT1) using the QuikChange™ site-directed mutagenesis kit (Stratagene, La Jolla, CA). A cytosolic domain (CD) deletion mutant (ΔCD-MT1) was constructed by introducing a termination codon at Arg^{563} by polymerase chain reaction (PCR) using specific primers and wild-type MT1-MMP cDNA as the template. The amplified E240A-MT1 and ΔCD-MT1 cDNA fragments were cloned into the pTF7EMCV-1 vaccinia expression vector using appropriate restriction sites to generate the respective expression vectors pTF7-E240A-MT1 and pTF7-ΔCD-MT1, as described (28, 33). The sequence of the inserts was verified by DNA sequencing. Expression of the MT1-MMP mutants was carried out in BS-C-1 cells by the infection/transfection procedure (28, 32, 33). Briefly, BS-C-1 cells were grown in 100-mm culture dishes to 80% confluence and infected with 5 plaque-forming units/cell vTF7–3 virus in infection medium for 45 min, as described (32). The cells were washed with phosphate-buffered saline and then transfected with 2 μg/dish pTF7-MT1 (wild type MT1-MMP), pTF7-E240A-MT1, or pTF7-ΔCD-MT1 DNA plasmids using Effectene transfection reagent (Qiagen, Valencia, CA), as described by the manufacturer. Control cells were infected but received no plasmid DNA. Four h after transfection, the cells were metabolically labeled (12 h, 37 °C) with 100 μCi/ml [^{35}S]methionine. The media were collected, clarified by centrifugation, and concentrated to ~0.5 ml followed by immunoprecipitation, as described below.

To express the 21-kDa (Tyr^{112}–Gly^{284}) and 18-kDa (Tyr^{112}–Ala^{255}) fragments of MT1-MMP, we utilized high fidelity PCR to amplify the respective cDNA fragments, which were cloned into the *Nde*I and *Hin*dIII restriction sites of the pET-24a(+) expression vector (Novagen, Madison, WI). The recombinant plasmid vectors were introduced into recipient *Escherichia coli* BL21(DE3) by transformation. For protein expression, 5 ml of the bacterial cultures were induced overnight at 37 °C with 0.4 mM isopropyl-β-D-galactopyranoside. Cells were pelleted by centrifugation, resuspended in 0.5 ml of collagenase buffer, and sonicated. Inclusion bodies were collected by centrifugation and dissolved in collagenase buffer containing 8 M urea. The solubilized proteins were diluted 10-fold in collagenase buffer supplemented with 50% glycerol and dialyzed overnight against collagenase buffer with 10% glycerol. The MT1-MMP fragments were resolved by 15% SDS-PAGE and stained with Coomassie Blue. The same samples were also analyzed for enzymatic activity and ability to bind TIMP-2 as described below.

Immunoaffinity Purification and Microsequencing of the 18-kDa MT1-MMP Fragment—BS-C-1 cells in 150-mm tissue culture dishes were infected to express MT1-MMP as described (17). Three h after infection, the cells were rinsed with serum-free media and incubated overnight with 15 ml/dish serum-free DMEM. The media (~300 ml) were collected, clarified by centrifugation, and concentrated ~15–20-fold with Centricon Plus-80. The concentrated medium was incubated (12 h, 4 °C) with pAb 160/Protein A-agarose beads to immunoprecipitate the MT1-MMP forms. The beads were washed twice with serum-free DMEM and twice with HNTG buffer (50 mM Tris/HCl, pH 7.5,

150 mM NaCl, 0.1% Nonidet P-40, and 10% glycerol). The immunoprecipitated proteins were eluted with reducing sample buffer, boiled and subjected to 15% SDS-PAGE, transferred to a polyvinylidene difluoride membrane, and stained with Coomassie Blue R-250. As reference, an aliquot of the eluate was also subjected to immunoblot analysis using pAb 160. The Coomassie Blue-stained 18-kDa protein was cut out from the polyvinylidene difluoride membrane and was submitted for N-terminal microsequencing by Edman-based chemistry to ProSeq (Boxford, MA). The amino acid sequence of the 18-kDa protein was also determined by mass spectrometry. To this end, the 18-kDa form bound to pAb 160/Protein A-agarose beads was eluted with 100 mM glycine/HCl, pH 2.5, and the collected fractions were neutralized with 1.88 M Tris, pH 8.8. An aliquot of each fraction was subjected to immunoblot analysis using pAb 160 to identify the 18-kDa protein. The fractions with the 18-kDa fragment were concentrated and subjected to 4–20% SDS-PAGE followed by Coomassie Blue R-250 staining. The protein was cut out from the gel and sent to the Harvard Microchemistry Facility for sequence analysis by microcapillary reverse-phase high performance liquid chromatography nano-electrospray tandem mass spectrometry on a Finnigan LCQ DECA quadrupole ion trap mass spectrometer.

Computational Modeling—A full computational model (minus the hinge region) for the ectodomain of pro-MT1-MMP was developed for the studies of the various aspects of the biochemistry of this enzyme. The primary sequence of MT1-MMP was obtained from Swiss-Prot data bank (code MM14_HUMAN). An initial model of MT1-MMP was generated by homology modeling with the aid of COMPOSER software, implemented in the SYBYL package version 6.7, and it was further refined with energy minimization procedures. The catalytic and propeptide domains were constructed based on the structure of stromelysin-1 (Protein Data Bank identification code 1slm) (41) following similar procedures that were used for construction of the hemopexin-like domain (42). Individual domains of MT1-MMP were thus constructed using homology modeling and three-dimensional structure alignment, except for the catalytic domain, which was based on the published x-ray structure of the catalytic domain of MT1-MMP (Protein Data Bank identification code 1bqq) (43). The hinge region of MT1-MMP was not modeled because of the lack of any homologous protein that could serve as a three-dimensional template. Energy minimization of the complete MT1-MMP complex was carried out using the SANDER module of the AMBER 5.0 suite of programs (44). The force field of Cornell *et al.* (45) was used to model the enzyme. The parameters for bonds, angles, and van der Waals interactions involving zinc atoms were taken from Massova *et al.* (46). The enzyme was immersed in a 97 × 96 × 98-Å^3 box of TIP3P-water (47). Water molecules present in the x-ray crystallographic structure were retained in the model. A 10-Å cutoff was applied to the model, and the nonbonded list was updated every 50 cycles. A total of 20,000 energy minimization cycles were carried out, which consisted of 300 steepest descent steps, followed by conjugate gradient minimization.

Enzyme Kinetic and Inhibition Studies—All enzymatic assays were carried out using the fluorescence substrate MOCAcPLGLA$_2$pr(Dnp)A-RNH$_2$ (Peptides International, Louisville, KY) in a buffer consisting of 50 mM HEPES, pH 7.5, 150 mM NaCl, 5 mM $CaCl_2$, 0.01% Brij-35, and 1% Me_2SO (buffer R). Substrate hydrolysis was monitored with a Photon Technology International spectrofluorometer at excitation and emission wavelengths of 328 and 393 nm, respectively. The synthetic peptide MOCAcPLG (Peptides International) was used to calibrate the assays as described by Knight (48). Concentrations of MT1-MMP$_{cat}$ (Tyr^{112}–Gly^{288}) and that of the recombinant 21-kDa (Tyr^{112}–Gly^{284}) fragment were determined by titration with TIMP-2. The TIMP-2 concentration was determined using a molar extinction coefficient of 39,600 M^{-1} cm^{-1} (49). Concentration of the 18-kDa (Tyr^{112}–Ala^{255}) fragment was determined by the BCA protein assay (Pierce) relative to a calibration curve established with the recombinant 21-kDa (Tyr^{112}–Gly^{284}) fragment as a standard. The kinetic parameters k_{cat} and K_m for the reaction of the recombinant 18-kDa (Tyr^{112}–Ala^{255}) and 21-kDa (Tyr^{112}–Gly^{284}) MT1-MMP species with the fluorogenic substrate were determined by computer fitting the substrate concentration dependence of the initial rates of substrate hydrolysis to the Michaelis-Menten equation using the program Scientist (MicroMath, Salt Lake City, UT). The fluorogenic substrate concentration was varied between 0.1 and 11 μM, where the extent of trivial quenching of the substrate is insignificant. Inhibition studies were carried out as previously described (20). The determination of k_{off} was attempted from the enzyme activity recovered after dilution of a pre-formed enzyme-inhibitor complex. The dissociation of the MT1-MMP·TIMP-2 complex, however, was too slow for the direct analysis of the k_{off} parameter for TIMP-2. The k_{off} value was estimated based on a 10-fold difference observed between the slopes of the linear portions of the dissociation curves for the complexes of MT1-MMP$_{cat}$ with a C-terminal deletion TIMP-2 mutant (ΔCTD-TIMP-2) (steady state rate) and wild type TIMP-2, as previously described (20).

MT1-MMP-TIMP-2 Interactions—Binding of soluble MT1-MMP forms to TIMP-2 was examined using various approaches. (i) Serum-free ^{35}S-labeled media (1 ml) from BS-C-1 cells expressing or not MT1-MMP were incubated (4 h, 4 °C) with or without 100 ng of either recombinant TIMP-2 or TIMP-1. The samples that received TIMP-2 or TIMP-1 were immunoprecipitated with anti-TIMP-2 or anti-TIMP-1 antibodies and Protein G-agarose beads. The samples without TIMP addition were immunoprecipitated with anti-MT1-MMP antibodies and Protein A-agarose beads. The immunoprecipitates were resolved by reducing 15% SDS-PAGE followed by autoradiography. (ii) Conditioned medium of BS-C-1 cells infected to express MT1-MMP in the presence of 1 μM marimastat, to induce the appearance of the 31–35-kDa species, was subjected to TIMP-2-affinity binding using immobilized TIMP-2 on an Affi-Gel 10 matrix, prepared as previously described (17). Briefly, the medium was concentrated (~80-fold), and ~0.4 ml of the concentrated medium (0.3 μM final marimastat concentration) was incubated (12 h, 4 °C) with Affi-Gel 10-TIMP-2 matrix by continuous rotation. After a brief centrifugation, the supernatant containing the unbound proteins was collected. The bound proteins were eluted with reducing Laemmli sample buffer (40). The bound and unbound fractions were resolved by reducing 15% SDS-PAGE followed by immunoblot analysis. (iii) Purified recombinant 18- and 21-kDa MT1-MMP fragments were incubated (1 h, 4 °C) with TIMP-2 (1:1 molar ratio) in 50 μl of collagenase buffer followed by immunoprecipitation with anti-TIMP-2 or anti-MT1-MMP antibodies. The complexes were detected by immunoblot analysis.

Immunoprecipitation—For immunoprecipitation of soluble MT1-MMP forms, serum-free media from ^{35}S-labeled cells expressing recombinant or natural MT1-MMP were immunoprecipitated with pAb 160/Protein A-agarose beads under nondenaturing conditions as described (15). In some experiments, the ^{35}S-labeled media were concentrated (10-fold) before immunoprecipitation. To immunoprecipitate denatured samples, the concentrated media were supplemented with 10× harvest buffer and boiled. The samples then received 2.5% Triton X-100 (final concentration) followed by addition of either pAb 437 or pAb 160 and Protein A-agarose beads as previously described (17). MT1-MMP·TIMP-2 complexes in ^{35}S-labeled medium samples or in mixtures of recombinant MT1-MMP fragments and TIMP-2 were co-immunoprecipitated with mAb 101 to TIMP-2 under nondenaturing conditions as previously described (33). The immunoprecipitates were resolved by reducing 15% SDS-PAGE, followed by autoradiography or by immunoblot analysis.

Gelatin Zymography and Immunoblot Analysis—Gelatin zymography was performed using 10% or 15% Tris-glycine SDS-polyacrylamide gels containing 0.1% gelatin as described (38). For immunoblot analysis, the serum-free conditioned media were collected, clarified by centrifugation, and concentrated (~80-fold) on a Centricon Plus-20 concentrator (Fisher, Itasca, IL). An aliquot was resolved by reducing 15% SDS-PAGE followed by transfer to nitrocellulose membrane. The membranes were incubated with the appropriate antibodies as described (38). The immunocomplexes were detected by ECL according to the manufacturer's instructions (Pierce).

Pro-MMP-2 Activation—Purified human pro-MMP-2 (25 nM) in collagenase buffer was incubated (22 h, 37 °C) with either 5 nM MT1-MMP$_{cat}$ (Calbiochem) or recombinant 18- and 21-kDa MT1-MMP fragments or concentrated serum-free conditioned media from BS-C-1 cell expressing MT1-MMP or from BS-C-1 cells infected only with the T7 RNA polymerase-expressing virus (vTF7–3). As a positive control, pro-MMP-2 was activated with 1 mM *p*-aminophenylmercuric acetate for 1 h at 37 °C. Pro-MMP-2 activation was monitored by gelatin zymography

RESULTS

Membrane-bound and Soluble Forms of MT1-MMP—We have previously shown that active MT1-MMP (57 kDa) is autocatalytically processed to a major membrane-bound 44-kDa species starting at Gly^{285} (17). This processing should release the entire catalytic domain of MT1-MMP. We therefore examined the surface and extracellular distribution of MT1-MMP in various cell lines known to express natural MT1-MMP and in cells engineered to express recombinant MT1-MMP as a model system. In cells expressing natural MT1-MMP, these studies

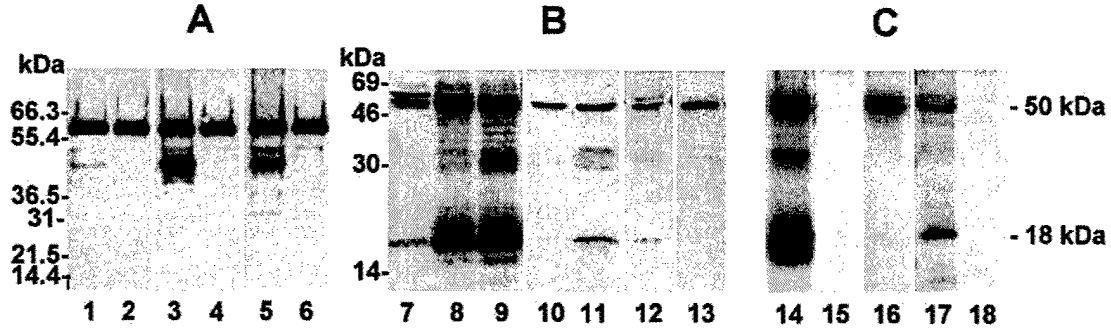

FIG. 1. **Membrane-bound and soluble MT1-MMP forms.** *A*, biotinylation of membrane-bound MT1-MMP forms. HT1080 cells were untreated (*lanes 1* and *2*) or treated with either 100 nM TPA (*lanes 3* and *4*) or 10 μg/ml ConA (*lanes 5* and *6*) in serum-free media overnight. The cells were then surface-biotinylated, as described (38). The biotinylated MT1-MMP forms were immunoprecipitated with pAb 437 (*lanes 1*, *3*, and *5*) or with pAb 160 (*lanes 2*, *4*, and *6*). The immunoprecipitates were resolved by reducing 8–16% SDS-PAGE, transferred to a nitrocellulose membrane, and detected with streptavidin-horseradish peroxidase and ECL. *B*, immunoblot analysis of soluble MT1-MMP forms. HT1080 (*lanes 7–9*), HFL1 (*lanes 10* and *11*), U-87 (*lane 12*), and MDA-MB-231 (*lane 13*) cells were untreated (*lanes 7* and *10*) or treated with either 100 nM TPA (*lane 8*) or 10 μg/ml ConA (*lanes 9*, *11*, *12*, and *13*) in serum-free media overnight. The concentrated (~80-fold) conditioned media were analyzed by immunoblot analysis using the anti-MT1-MMP mAb LEM-2/15. *C*, immunoprecipitation of soluble MT1-MMP forms. HT1080 (*lanes 14* and *15*), MDA-MB-231 (*lane 16*) and *Timp2* (−/−)-MT1 (*lanes 17* and *18*) cells were metabolically labeled with [^{35}S]methionine as described under "Experimental Procedures." HT1080 and MDA-MB-231 cells were treated with 100 nM TPA or 10 μg/ml ConA, respectively, in serum-free media during metabolic labeling. The ^{35}S-labeled media were immunoprecipitated with pAb 160/Protein A-agarose beads (*lanes 14*, *16*, and *17*) or with Protein A-agarose beads without antibody (*lanes 15* and *18*). The immunoprecipitates were resolved by reducing 15% SDS-PAGE followed by autoradiography.

were carried out either without stimulation or after stimulation with TPA or ConA, two agents known to induce MT1-MMP expression (10, 16, 29, 50). Surface biotinylation followed by immunoprecipitation with pAb 160 to the catalytic domain or pAb 437 to the hemopexin-like domain demonstrated that untreated HT1080 cells display the 57-kDa species of MT1-MMP as the major enzyme form on the cell surface (Fig. 1*A*, *lanes 1* and *2*). Treatment with either TPA (Fig. 1*A*, *lanes 3* and *4*) or ConA (Fig. 1*A*, *lanes 5* and *6*) induced the appearance of a 44-kDa species on the cell surface, which was detected only with the pAb 437 (Fig. 1*A*, *lanes 3* and *5*), indicating that this species represents a membrane-inserted form lacking the catalytic domain, in agreement with our previous studies using a vaccinia expression system (17). Thus, both TPA and ConA promote the processing of natural MT1-MMP (57 kDa) into the inactive 44-kDa form.

We next examined the serum-free conditioned media of various cell lines (untreated or treated with TPA or ConA) and *Timp-2* (−/−) mouse fibroblasts stable transfected to express recombinant MT1-MMP for soluble MT1-MMP forms by immunoblot analysis (Fig. 1*B*) and immunoprecipitation (Fig. 1*C*). As shown in Fig. 1*B*, the medium of untreated HT1080 cells contains three proteins of 56, 50, and 18 kDa, which were recognized by a mAb to the catalytic domain of MT1-MMP (Fig. 1*B*, *lane 7*). TPA (Fig. 1*B*, *lane 8*) and ConA (Fig. 1*B*, *lane 9*) treatment of HT1080 cells enhanced the levels of these forms in the media and resulted in the appearance of an additional soluble MT1-MMP form of ~31–35 kDa, which was particularly evident with ConA (Fig. 1*B*, *lane 9*). Media of untreated HFL1 fibroblasts (Fig. 1*B*, *lane 10*) and U-87 glioblastoma cells (data not shown) showed presence of the 50-kDa species. Media of ConA-treated HFL1 (Fig. 1*B*, *lane 11*) and U-87 (Fig. 1*B*, *lane 12*) cells contained the 50- and 18-kDa species and very low levels of the ~31–35-kDa species. Media of ConA-treated MDA-MB-231 contained mostly the 50-kDa form, as determined by immunoblot analysis (Fig. 1*B*, *lane 13*) or immunoprecipitation (Fig. 1*C*, *lane 16*). With the exception of the 18- and the 31–35-kDa species, the 56- and 50-kDa species were recognized by pAb 437 to the hemopexin-like domain, indicating that they comprise most of the ectodomain (data not shown).

Metabolic labeling of TPA-treated HT1080 cells followed by immunoprecipitation with pAb 160 yielded the 56-, 50-, 31–35-, and 18-kDa species (Fig. 1*C*, *lane 14*), whereas the same procedure in *Timp-2* (−/−) cells expressing MT1-MMP yielded mostly the 50- and 18-kDa species (Fig. 1*C*, *lane 17*). No signal was observed in samples precipitated with Protein A-agarose beads without antibody (Fig. 1*C*, *lanes 15* and *18*). Considering that the 18-kDa species contains only one methionine residue (based on sequencing data, as shown below), the results of the immunoprecipitation of the ^{35}S-labeled media indicate that the 18-kDa species, compared with the other forms, exhibits a relatively higher specific activity and hence represents the major soluble form of MT1-MMP.

The concentrated serum-free media of untreated HT1080 cells and BS-C-1 cells expressing MT1-MMP were subjected to ultracentrifugation (100,000 × *g* for 1 h at 4 °C) to assess the distribution of the released MT1-MMP species. Under these conditions, membrane fragments and their associated proteins and large protein aggregates go to the pellet, whereas membrane-free soluble species distribute mostly in the supernatant (51, 52). Immunoblot analysis showed that the 18-, 31–35-, and 50-kDa species were detected in the supernatant, whereas the 56-kDa species remained in the pellet (data not shown). These results suggest that, with the exception of the 56-kDa species, the other MT1-MMP species are true soluble forms.

Complex Regulation of MT1-MMP Shedding—We next investigated the effects of various protease inhibitors on the profile of MT1-MMP forms present in the media. To this end, we used TPA-treated HT1080 cells (Fig. 2*A*), which express natural MT1-MMP and the *Timp2* (−/−) cells (Fig. 2*C*) expressing recombinant MT1-MMP. In addition, we used BS-C-1 cells infected with vaccinia virus expressing MT1-MMP, as we have previously reported (17, 20). The profile of soluble MT1-MMP species found in the vaccinia expression system (shown in Fig. 2*B*) was the same as that observed in cells expressing natural MT1-MMP (Fig. 1) and hence is not a consequence of overexpression of recombinant enzyme or cell lysis. Thus, this experimental system recapitulates the natural pattern of MT1-MMP shedding. The protease inhibitor studies showed that presence of the 18-kDa species in the media was specifically inhibited by TIMP-2, marimastat, and TIMP-4 in all cells tested (Fig. 2, *A–C*). TIMP-1, an extremely poor MT1-MMP inhibitor (53) (Fig. 2*B*, *lane 7*), and SB-3CT, a mechanism-based synthetic inhibitor specific for the gelatinases (36) (Fig.

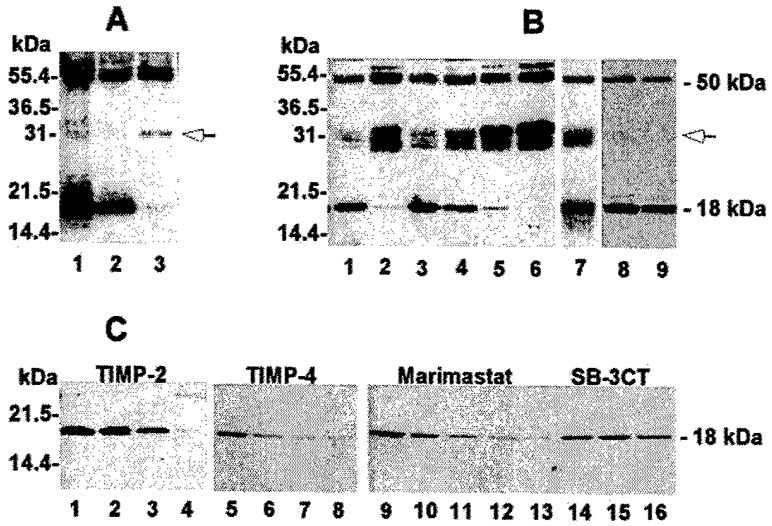

FIG. 2. **Effect of protease inhibitors in MT1-MMP shedding.** *A*, HT1080 cells were treated with 100 nM TPA overnight in serum-free media in the absence (*lane 1*) or presence of 100 μg/ml aprotinin (*lane 2*) or 100 nM human recombinant TIMP-2 (*lane 3*). The conditioned media were collected, concentrated (~80-fold), and subjected to reducing 15% SDS-PAGE followed by immunoblot analysis using the anti-MT1-MMP mAb (LEM-2/15). *B* and *C*, BS-C-1 (*B*) or *Timp-2* (−/−) (*C*) mutant cells were co-infected with vaccinia viruses to express MT1-MMP as described under "Experimental Procedures." After infection, the media were aspirated and replaced with serum-free DMEM supplemented without or with various concentrations of protease inhibitors for overnight incubation. The conditioned media were collected and subjected to reducing 15% SDS-PAGE followed by immunoblot analysis using pAb 160. Inhibitor doses in *B* were as follows: none (*lane 1*); TIMP-2, 20 nM (*lane 2*); marimastat, 10^{-6}, 10^{-4}, 10^{-2}, and 1 μM (*lanes 3, 4, 5,* and *6*, respectively); TIMP-1, 100 nM (*lane 7*); and aprotinin, 20 and 40 μg/ml (*lanes 8* and *9*, respectively). Inhibitor doses in *C* were as follows: TIMP-2, 0, 1, 10, and 100 nM (*lanes 1, 2, 3,* and *4*, respectively); TIMP-4, 0, 1, 10, and 100 nM (*lanes 5, 6, 7,* and *8*, respectively); marimastat, 0, 4, 20, 100, and 500 nM (*lanes 9, 10, 11, 12,* and *13*, respectively); and SB-3CT, 4, 20, and 100 nM (*lanes 14, 15,* and *16*, respectively). *Open arrows* show the 31–35-kDa fragment.

2*C*, *lanes 14–16*), had no effect. Aprotinin (Fig. 2, *A* (*lane 2*) and *B* (*lanes 8* and *9*)) and leupeptin (40 μg/ml; data not shown), two serine protease inhibitors, and E64 (10 μM), an aspartic protease inhibitor (data not shown), had no effect on the shedding of the 18-kDa species. None of the inhibitors tested had a significant effect on the levels of the 50-kDa form and in fact, the levels of this species were somewhat increased in the presence of TIMP-2 and marimastat in BS-C-1 cells (Fig. 2*B*, *lanes 2* and *6*, respectively) but not in HT1080 cells (Fig. 2*A*, *lane 3*). Interestingly, we also found that, both in HT1080 cells (Fig. 2A, *lane 3*) and in BS-C-1 cells expressing MT1-MMP (Fig. 2B, *lanes 2–6*), the ~31–35-kDa species accumulated in the presence of TIMP-2 and marimastat but not in the presence of aprotinin (Fig. 2, *A* (*lane 2*) and *B* (*lanes 8* and *9*)).

The inhibitor profile studies suggested that shedding of the 18-kDa species is an autocatalytic event, whereas shedding of the 50-kDa species is not. To further investigate this process, we generated a catalytically inactive mutant of MT1-MMP by replacing Glu^{240} with Ala (E240A-MT1). We also examined the role of the cytosolic domain of MT1-MMP in shedding. To this end, we constructed a truncated MT1-MMP lacking the cytosolic domain (ΔCD-MT1) by introducing a stop codon at Arg^{563}. Wild type MT1-MMP and the E240A-MT1 and ΔCD-MT1 mutants were expressed in BS-C-1 cells using the infection-transfection procedure followed by metabolic labeling as described under "Experimental Procedures." The ^{35}S-labeled conditioned media were immunoprecipitated with pAb 160. As shown in Fig. 3, wild type MT1-MMP shed the 50-, 31–35-, and 18-kDa species (Fig. 3, *lane 1*). In contrast, the E240A-MT1 catalytic mutant shed the 50-kDa species and a ~28-kDa form but not the 18-kDa fragment (Fig. 3, *lane 2*) consistent with the autocatalytic shedding of the latter species. The ΔCD-MT1 mutant showed a shedding pattern similar to that observed with the wild type enzyme (Fig. 3, *lane 3*).

Structure and Characterization of the 18-kDa MT1-MMP Soluble Form—The relatively higher amounts of the 18-kDa fragment allowed its purification and characterization. N-terminal sequencing by Edman degradation revealed that the 18-kDa species displays Tyr^{112} in the N terminus, in agreement with the N terminus displayed by membrane-tethered active MT1-MMP (57 kDa) (9, 17). Mass spectrometry analysis of tryptic digests was performed to determine the C terminus of the 18-kDa fragment. As shown in the table of Fig. 4*A* (*inset*), a total of 32 peptides were isolated and their sequence determined. Three peptides demonstrated a C terminus ending at Ala^{255}, indicating that the 18-kDa form extends from Tyr^{112} to Ala^{255} and therefore comprises most of the catalytic domain. Indeed, SDS-PAGE analysis demonstrated an ~3-kDa difference between the shed 18-kDa fragment (Fig. 4*B*, *lane 2*) and a commercially available recombinant catalytic domain of MT1-MMP ($MT1\text{-}MMP_{cat}$), which is known to extend from Tyr^{112} to Gly^{288} (Fig. 4*B*, *lane 1*).

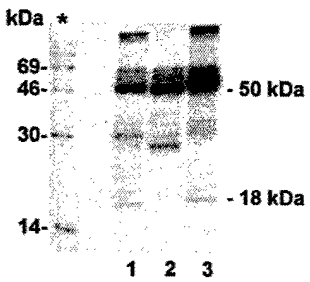

FIG. 3. **Shedding in MT1-MMP mutants.** Wild type human MT1-MMP (*lane 1*), E240A-MT1 (*lane 2*), and ΔCD-MT1 (*lane 3*) MT1-MMP mutants were expressed in BS-C-1 cells by infection/transfection as described under "Experimental Procedures" followed by metabolic labeling (12 h, 37 °C) with [^{35}S]methionine. The ^{35}S-labeled medium was subjected to immunoprecipitation with pAb 160/Protein A-agarose beads, and the immunoprecipitates were resolved by reducing 15% SDS-PAGE followed by autoradiography. The *asterisk* indicates the lane with ^{14}C-labeled molecular size standards.

Considering that the 44-kDa membrane-tethered species of MT1-MMP starts at Gly^{285} (17), shedding of the 18-kDa fragment would require two cleavage events: one between Ala^{255}

A

Number of Peptides and Sequences	AA# in MT1-MMP
2 YAIQGLR	112-118
1 WQHNEITFCIQNYTPK	119-134
2 VGEYATYEAIR	135-145
2 VGEYATYEAIRK	135-146
2 VWESATPLR	150-158
2 ESATPLR	152-158
3 EVPYAYIR	161-168
1 PYAYIR	163-168
2 QADIMIF	174-180
4 AYFPGPNIGGDTHFDSAEPWTVR	202-224
1 PGPNIGGDTHFDSAEPWTVR	205-224
4 IGGDTHFDSAEPWTVR	209-224
1 AYFPGPN	202-208
2 NEDLNGNDIFLVAVHELGH	225-243
1 VHELGHALGLEHSSDPSA	238-255
2 HALGLEHSSDPSA	244-255

B

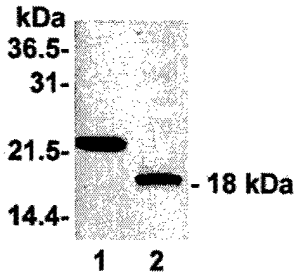

FIG. 4. **Characterization of the 18-kDa MT1-MMP soluble fragment.** *A*, summary of the tandem mass spectrometry peptide sequences of the 18-kDa form. The last two peptides in the *highlighted box* comprise the C-terminal region of the 18-kDa fragment. *AA*, amino acid. *B*, immunoblot analysis of 20 ng of recombinant MT1-MMP$_{cat}$ (Tyr^{112}–Gly^{288}) (*lane 1*) and concentrated serum-free medium of *Timp-2* (−/−) mutant cells infected to express MT1-MMP. The antigens were detected with pAb 160 and ECL.

and Ile^{256} and another between Gly^{284} and Gly^{285}. To determine the relative location of these sites in the catalytic domain of MT1-MMP, we used an energy-minimized computational model of the ectodomain of human pro-MT1-MMP that was recently constructed in our laboratory.[2] The only missing piece of structural information in this model pertained to the hinge between the catalytic and the hemopexin-like domains. The spatial *location of the hemopexin-like domain in the computational model (data not shown) was based on that seen in the x-ray structure of MMP-2 (54). From this model, Fig. 5A* shows only a view of the catalytic domain extending from Tyr^{112} to Ser^{287}. In the event that the hinge actually would not dislocate the hemopexin-like domain in MT1-MMP, the Ala^{255}-Ile^{256} bond is sheltered by the hemopexin-like domain, leaving the cleavage site Gly^{284}-Gly^{285} as the only likely candidate for the first hydrolytic cleavage event. However, even if the hemopexin-like domain of MT1-MMP is dislocated away from the catalytic domain, leaving the surface regions shown in Fig. 5*B* fully exposed to the milieu, still the cleavage site Gly^{284}-Gly^{285} is more readily accessible than is Ala^{255}-Ile^{256} because of the nature of the secondary structures in the protein. Therefore, shedding of the 18-kDa fragment is likely to be initiated at the Gly^{284}-Gly^{285} peptide bond, followed by a second cleavage at the Ala^{255}-Ile^{256} site. Fig. 5*C* depicts a diagram of active MT1-MMP (Tyr^{112}–Val^{582}), showing the two cleavages at the Gly^{284}-Gly^{285} and Ala^{255}-Ile^{256} sites leading to the formation of the inactive 44-kDa species, which has been isolated and characterized from plasma membranes (17), and the soluble 18-kDa species. To shed the 18-kDa species, this process would have also generated a ~21-kDa intermediate fragment (Fig. 5*C*, *dashed bracket*) extending from Tyr^{112} to Gly^{284}. However, a soluble fragment of ~21 kDa, the putative precursor of the 18-kDa species, was not detected. Additionally, hydrolysis at the Ala^{255}-Ile^{256} peptide bond predicted impaired catalytic activity of the 18-kDa species because of the proximity of this site to the conserved methionine residue (Met^{257}) of the so-called methionine turn (55) and to the consensus sequence of the catalytic zinc ion binding site (Fig. 5*C*).

To gain insight into the biochemical properties of the 18-kDa (Tyr^{112}–Ala^{255}) fragment and the putative 21-kDa (Tyr^{112}–Gly^{284}) intermediate species, these proteins were expressed in bacteria and purified to homogeneity for further analyses. Fig. 6*A* shows the purity of the recombinant 18-kDa (Tyr^{112}–Ala^{255}) (*lane 1*) and 21-kDa (Tyr^{112}–Gly^{284}) (*lane 2*) proteins isolated. Activity assays demonstrated that, whereas the 21-kDa (Tyr^{112}–Gly^{284}) fragment exhibited gelatinolytic (Fig. 6*B*, *lane 4*) and pro-MMP-2-activating activities (Fig. 6*C*, *lane 6*), the 18-kDa (Tyr^{112}–Ala^{255}) fragment was catalytically inactive (Fig. 6, *B* (*lane 3*) and *C* (*lane 5*)). To obtain quantitative data, the recombinant fragments were examined for their ability to hydrolyze a fluorogenic peptide substrate as a function of time. MT1-MMP$_{cat}$ was used as a positive control. As summarized in Table I, k_{cat} and K_m values of ~1 s^{-1} and 10 μM, respectively, were obtained yielding k_{cat}/K_m values of 10^5 M^{-1} s^{-1}, which reflects the high reactivity of MT1-MMP$_{cat}$ and the 21-kDa (Tyr^{112}–Gly^{284}) enzymes toward the synthetic peptide substrate used. Moreover, indistinguishable values were obtained for these two MT1-MMP species. In contrast, no enzyme concentration dependence of the rate of substrate hydrolysis was detected with the 18-kDa (Tyr^{112}–Ala^{255}) fragment with concentrations up to 235 nM. In fact, the hydrolysis rate of the substrate in the presence of the enzyme was essentially indistinguishable from the background hydrolysis detected in buffer only. A comparable concentration of the 21-kDa (Tyr^{112}–Gly^{284}) species (54 nM) yielded an increase in fluorescence that rapidly exceeded the detection limit of the instrument used. Together, these studies indicate that autocatalytic processing of MT1-MMP at the Ala^{255}-Ile^{256} site obliterates catalytic competence resulting in an inactive soluble form of 18 kDa.

Although the 18-kDa species of MT1-MMP is inactive, the other soluble species may maintain enzymatic activity. Unfortunately, the paucity of these enzyme species in the media precluded purification and characterization. Thus, to investigate the activity of the soluble MT1-MMP species, we used conditioned medium of BS-C-1 cells infected to express MT1-MMP and examined its ability to promote pro-MMP-2 activation after addition of exogenous recombinant pro-MMP-2. This cell expression system was chosen because it is devoid of MMP-2 (33) and because it releases the 50- and 18-kDa form of MT1-MMP into the media (Fig. 2*B*, *lane 1*). As a control, we used conditioned media of BS-C-1 cells infected only with the T7 RNA polymerase-expressing vaccinia vTF7–3 virus (33). As shown in Fig. 7, the conditioned media derived from the MT1-MMP-expressing cells promoted the generation of the intermediate form of MMP-2 (Fig. 7, *lane 6*), consistent with the two-step model of surface activation of pro-MMP-2 by MT1-MMP, as previously proposed (53, 56). In contrast, no processing of pro-MMP-2 was observed with the control media (Fig. 7, *lane 4*), demonstrating the specificity of the reaction. Because the 18-kDa species is inactive, these studies suggest that MT1-MMP fragments other than the 18-kDa form, such as the 50-kDa species, are likely to be the enzyme species responsible in the media for the processing of pro-MMP-2.

Interactions with TIMP-2—We have previously shown that, on the cell surface, TIMP-2 binds to the active 57-kDa form of MT1-MMP but not the 44-kDa inactive species (17), indicating that binding is mostly mediated by the catalytic domain. Here

[2] O. Meroueh, L. P. Kotra, R. Fridman, and S. Mobashery, unpublished data.

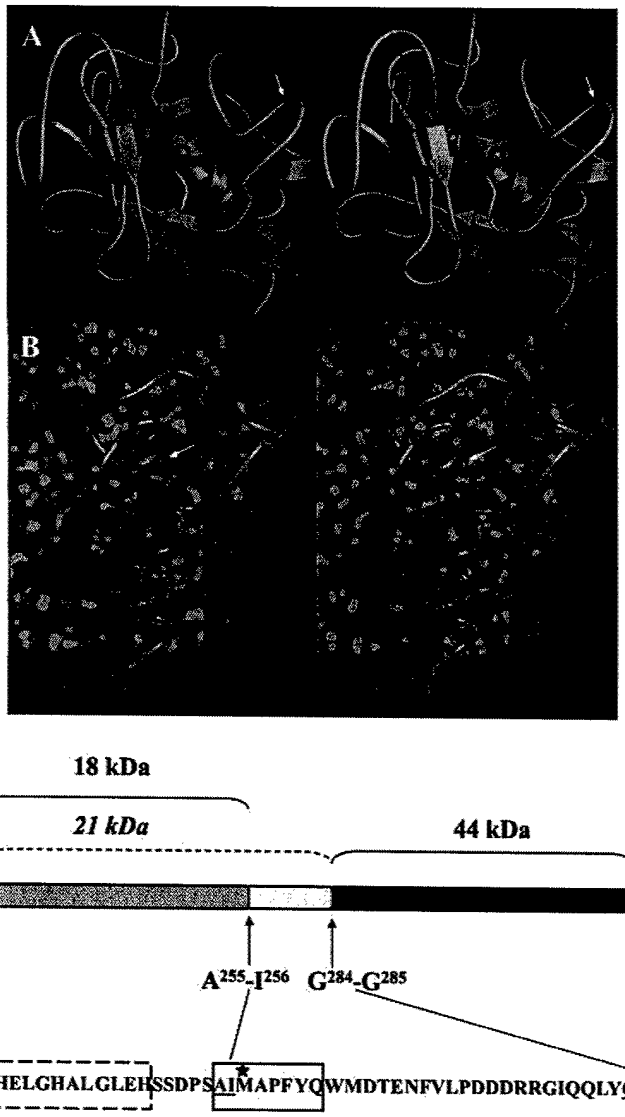

FIG. 5. **Computational model of MT1-MMP.** *A*, stereo view of the energy-minimized computational model of the MT1-MMP region spanning residues Tyr^{112} and Ser^{287}. *White* and *red arrows* are pointing to the Ala^{255}-Ile^{256} and Gly^{284}-Gly^{285} cleavage sites, respectively. *B*, a close-up view depicting the cleavage sites with *white* and *red arrows* corresponding to same cleavage sites described in *A*. Residues from the catalytic domain downstream of the Ala^{255}-Ile^{256} cleavage site are rendered in *white tube* representation, with the side chains shown. A Connolly water-accessible surface is constructed around the remaining residues. Residues at the cleavage sites are rendered in *yellow capped-sticks* representation. *B*, the Gly^{284}-Gly^{285} cleavage site is more readily accessible than that of Ala^{255}-Ile^{256}. *C*, diagram showing the location of the cleavage sites within active MT1-MMP (Tyr^{112}–Val^{582}) that lead to the formation of the membrane-inserted 44-kDa species (*black*) and the shedding of the 18-kDa species (*gray*). The *italics* and *dashed bracket* depict the putative 21-kDa intermediate species (*light gray*) predicted to precede the 18-kDa species. However, a 21-kDa species was not detected. Also shown is the sequence of amino acids around the cleavage sites including the conserved catalytic zinc-binding region (*dashed line rectangle*) and the conserved residues among transmembrane MT-MMPs (MT1-, MT2-, MT3-, and MT5-MMP) (*solid line rectangle*) containing the Ala^{255}-Ile^{256} site and the conserved methionine residue (marked by a *star*) comprising the methionine turn. The *underlines* indicate the Ala^{255}-Ile^{256} and Gly^{284}-Gly^{285} cleavage sites. The hinge region of MT1-MMP starts downstream of Gly^{285}.

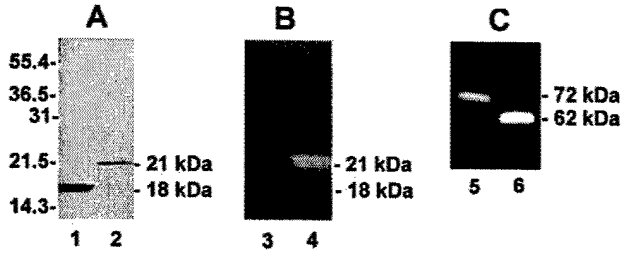

FIG. 6. **Activity of the recombinant 21- and 18-kDa MT1-MMP forms.** *A* and *B*, the purified recombinant 18-kDa (Tyr^{112}–Ala^{255}) (*lanes 1* and *3*) and 21-kDa (Tyr^{112}–Gly^{284}) (*lanes 2* and *4*) were subjected to reducing 15% SDS-PAGE followed by Coomassie Blue staining (*A*) and a 15% SDS-PAGE gelatin zymogram (*B*). *C*, pro-MMP-2 was incubated (12 h, 37 °C) with either the 18-kDa (Tyr^{112}–Ala^{255}) form (*lane 5*) or with the 21-kDa (Tyr^{112}–Gly^{284}) form (*lane 6*). An aliquot of the reaction was subjected to gelatin zymography. The 72-kDa form represents pro-MMP-2, and the 62-kDa form represents the fully active MMP-2.

TABLE I

Kinetic parameters for the reaction of MT1-MMP fragments with the fluorogenic substrate MOCAcPLGLA$_2$pr(Dnp)ARNH$_2$

The fluorescence of reaction mixtures containing 0.2 nM enzyme and increasing concentrations of the fluorogenic substrate (0.1–11 μM) in buffer R was monitored at excitation and emission wavelengths of 328 and 393 nM, respectively. The kinetic parameters were determined by nonlinear least squares analysis of the substrate concentration dependence of initial hydrolysis rates as described under "Experimental Procedures."

Enzyme	k_{cat}	K_m	k_{cat}/K_m
	s^{-1}	μM	$M^{-1}\ s^{-1}$
MT1-MMP$_{cat}$ (Tyr^{112}–Gly^{288})	1.2 ± 0.3	10 ± 3	(1.25 ± 0.05) × 10^5
21-kDa (Tyr^{112}–Gly^{284})	3.3 ± 0.2	9 ± 1	(3.49 ± 0.05) × 10^5
18-kDa (Tyr^{112}–Ala^{255})	ND[a]	ND	ND

[a] ND, not detectable proteolytic activity of the enzyme toward the fluorogenic substrate was observed at concentrations up to 235 nM.

we examined the ability of the soluble MT1-MMP forms to bind TIMP-2. To this end, media of ^{35}S-labeled BS-C-1 cells infected to express MT1-MMP were incubated with or without exogenous recombinant TIMP-2 or TIMP-1 followed by immunoprecipitation. As shown in Fig. 8*A*, MT1-MMP-expressing BS-C-1 cells shed the 50- and 18-kDa species of MT1-MMP, as determined after immunoprecipitation with pAb 160 (Fig. 8*A*, *lane 1*). No signal was detected without antibody (Fig. 8*A*, *lane 2*). After addition of exogenous TIMP-2 and immunoprecipitation with mAb 101, only the 50-kDa species of MT1-MMP and some endogenously produced ^{35}S-TIMP-2 were detected in the coprecipitate (Fig. 8*A*, *lane 3*). Indeed, BS-C-1 cells produce very low levels of endogenous TIMP-2 (20). No signal was detected in samples that received exogenous TIMP-1 and anti-TIMP-1 pAb (Fig. 8*A*, *lane 4*). Accordingly, the 50-kDa species could not

FIG. 7. **Pro-MMP-2 activation by soluble MT1-MMP.** Recombinant pro-MMP-2 (25 nM) was incubated (37 °C) with either 5 nM MT1-MMP_{cat} (*lanes 1* and *2*) or with concentrated serum-free media from control infected BS-C-1 cells (*lanes 3* and *4*) or with concentrated media from BS-C1 cells expressing MT1-MMP (*lanes 5* and *6*). Samples were incubated for 0 min (*lanes 1*, *3*, and *5*) and 22 h (*lanes 2*, *4*, and *6*). Aliquots from the samples were subjected to gelatin zymography. *Lane 7* shows APMA-activated pro-MMP-2 (62 kDa) as a positive control.

be detected with pAb 160 after TIMP-2 addition because of epitope occupancy in the enzyme-inhibitor complex as this pAb is directed to the catalytic domain (data not shown). These results indicate that TIMP-2, but not TIMP-1, binds to the soluble 50-kDa species via the catalytic domain, in agreement with the known TIMP-binding profile of MT1-MMP (53). In contrast, the soluble 18-kDa fragment cannot form a stable complex with TIMP-2.

A TIMP-2 affinity binding procedure was carried out to assess whether the 31–35-kDa species could bind TIMP-2. To this end, we used conditioned medium from BS-C-1 cells that were infected to express MT1-MMP in the presence of 1 μM marimastat, which induces the appearance of these species, as shown in Fig. 2*B*. The media were subjected to TIMP-2 affinity binding using immobilized TIMP-2, and the bound and unbound fractions were analyzed by immunoblot analysis as described under "Experimental Procedures." As shown in Fig. 8*B*, the 31–35- and the 50-kDa species were detected in the bound fraction (Fig. 8*B*, *lane 3*), albeit a significant amount of these species remained in the unbound fraction (Fig. 8*B*, *lane 2*) when compared with the load (Fig. 8*B*, *lane 1*), suggesting that they exhibit a relatively low affinity for TIMP-2, under the experimental conditions. In contrast, the 18-kDa species did not bind to the TIMP-2 affinity matrix, in agreement with the immunoprecipitation data. Although these studies are not quantitative, the poor binding of the soluble MT1-MMP species to the immobilized TIMP-2 is unlikely to be the result of the presence of marimastat because the affinity matrix is saturated with TIMP-2 and the final concentration of marimastat was less than 0.3 μM.

We next examined the ability of the recombinant MT1-MMP fragments to bind TIMP-2 by co-immunoprecipitation. These studies demonstrated that only the 21-kDa (Tyr^{112}–Gly^{284}) species was able to form a stable complex with the inhibitor (Fig. 8*C*, *lane 3*). Thus, loss of the 29 amino acids between Ala^{255} and Gly^{284} during the formation of the 18-kDa fragment strongly compromised TIMP-2 interactions. Consistently, inhibition studies demonstrated that TIMP-2 was an effective slow-binding inhibitor of the 21-kDa (Tyr^{112}–Gly^{284}) species when compared with MT1-MMP_{cat} (Table II). Fitting the data to a slow-binding inhibition model yielded k_{on} and k_{off} values of 10^6 M^{-1} s^{-1} and 2×10^{-4} s^{-1}, respectively, resulting in sub-nanomolar K_i values.

DISCUSSION

The stability of active MT1-MMP on the cell surface is a complex process involving a balance between autocatalytic processing (17) and enzyme internalization (57, 58). Both processes can regulate the amount of active enzyme available for pericellular proteolysis and appear to be regulated in part by the presence of TIMPs. The major pathway of active MT1-MMP processing on the cell surface is an autocatalytic event that generates a 44-kDa membrane-anchored fragment starting at Gly^{285} and thus lacks the entire catalytic domain (17). This process may switch the proteolytic machinery from the cell surface to the pericellular space if the released fragments are competent enzymes or may obliterate proteolysis on all fronts, if the soluble fragments are inactive and/or in a complex with TIMPs. To define the fate of the catalytic domain after processing, we set out to investigate the nature and properties of the MT1-MMP soluble fragments produced in various cellular systems. Here we have shown that media of cells expressing natural or recombinant MT1-MMP contain a complex profile of

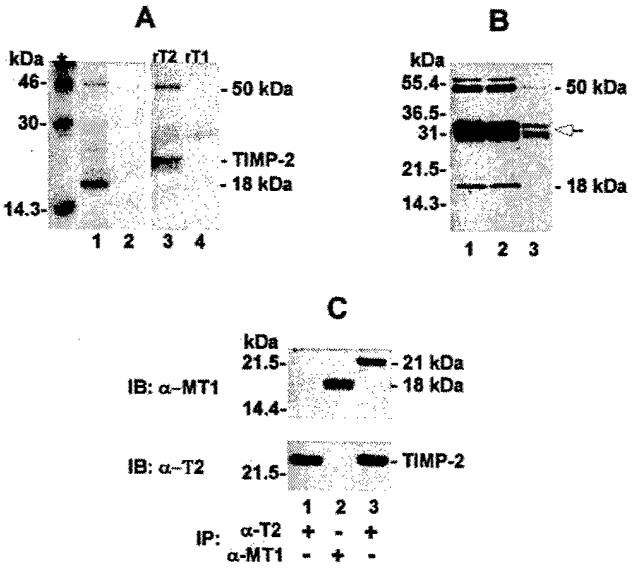

FIG. 8. **Interactions with TIMP-2.** *A*, ^{35}S-labeled-medium of BS-C-1 cells infected to express MT1-MMP was subjected to immunoprecipitation with pAb 160 and Protein A-agarose beads (*lane 1*) or Protein A-agarose beads alone (*lane 2*). An aliquot (1 ml) of the conditioned ^{35}S-labeled medium received 100 ng of unlabeled recombinant TIMP-2 (*rT2*, *lane 3*) or TIMP-1 (*rT1*, *lane 4*) followed by immunoprecipitation with anti-TIMP-2 (mAb 101) or anti-TIMP-1 pAb, respectively, and Protein G-agarose beads. The immunoprecipitates were resolved by reducing 15% SDS-PAGE followed by autoradiography. The *asterisk* indicates the lane with ^{14}C-labeled molecular size standards. *B*, BS-C-1 cells were co-infected with vaccinia viruses to express MT1-MMP. After infection the cells were incubated overnight in serum-free DMEM supplemented with 1 μM marimastat to induce appearance of the 31–35-kDa species. The conditioned media were collected, concentrated (~80-fold), and subjected to TIMP-2 affinity binding as described under "Experimental Procedures." The unbound and bound MT1-MMP forms were resolved by reducing 15% SDS-PAGE followed by immunoblot analysis using the mAb LEM-2/15. *Lane 1*, sample before affinity binding; *lane 2*, unbound fraction; *lane 3*, bound fraction. *C*, the recombinant 18-kDa (Tyr^{112}–Ala^{255}) (*lanes 1* and *2*) and 21-kDa (Tyr^{112}–Gly^{284}) (*lane 3*) MT1-MMP fragments were incubated (1 h) with TIMP-2 (1:1 molar ratio) in 50 μl of collagenase buffer. The samples were subjected to immunoprecipitation with pAb 160 to MT1-MMP (*lane 2*) or mAb 101 to TIMP-2 (*lanes 1* and *3*). The immunoprecipitates were resolved by 15% SDS-PAGE followed by immunoblot (*IB*) analysis with the same antibodies.

TABLE II
Kinetic parameters for inhibition of the 21-kDa MT1-MMP fragment by TIMP-2

The enzyme (0.2–0.8 nM) was added to a solution of $MOCAcPLGLA_2pr(Dnp)ARNH_2$ (10 μM) and increasing concentrations of TIMP-2 in buffer R. Substrate hydrolysis was monitored for 20 min. The kinetic parameters were evaluated as described under "Experimental Procedures."

Enzyme	k_{on}	k_{off}	K_i
	M^{-1} s^{-1}	s^{-1}	nM
MT1-MMP_{cat} (Tyr^{112}–Gly^{288})	$(3.54 \pm 0.56) \times 10^6$	2×10^{-4} [a]	0.06
21-kDa (Tyr^{112}–Gly^{284})	$(3.81 \pm 0.23) \times 10^6$	2×10^{-4} [a]	0.05

[a] Estimated value based on a 10-fold difference between the slopes of the linear portions of the dissociation curves for the complexes of MT1-MMP_{cat} with ΔCTD-TIMP-2 (steady state rate) and wild type TIMP-2.

MT1-MMP species including two major species of 50- and 18 kDa and a series of minor fragments of 56, and 31–35 kDa, which are differentially regulated by TPA, ConA, and MMP inhibitors. With the exception of the 56-kDa species, which was retained in the pellet after ultracentrifugation and thus, may be associated with membrane fragments (52), all other MT1-MMP species were soluble and thus, represent true shedding. Shedding of the 50- and 18-kDa species occurred without external stimulation, indicating that they represent a normal process of MT1-MMP turnover under basal conditions. However, exposure of cells to either TPA or ConA, two nonphysiological agents known to induce MT1-MMP expression and pro-MMP-2 activation (29, 50, 59), resulted in increased levels of all the soluble forms in the media. Based on the protease inhibitor profile, both autocatalytic and non-autocatalytic processes are involved in MT1-MMP shedding. High affinity natural (TIMP-2 and TIMP-4, but not TIMP-1) and synthetic MMP inhibitors, known to stabilize active MT1-MMP on the cell surface by inhibiting the processing of MT1-MMP to the 44-kDa form (17, 19–21), inhibited shedding of the 18-kDa species. Additionally, the E240A-MT1 catalytic mutant enzyme, which cannot be processed to the 44-kDa species (22, 60), failed to shed this fragment. Thus, shedding of the 18-kDa species is the product of the autocatalytic processing of active MT1-MMP (57 kDa) on the cell surface, which yields a major inactive membrane-tethered species of 44 kDa (17). Consistently, TPA and ConA treatments, which promote MT1-MMP expression and processing on the cell surface, stimulate shedding of the 18-kDa fragment. The ability of cells to elicit autocatalytic shedding depends on the expression level of MT1-MMP on the cell surface and the levels and availability of TIMPs. High levels of TIMP-2 and/or presence of other TIMP-2-binding MMPs will alter the autocatalytic pathway by modifying TIMP-2 availability as shown in MDA-MB-231 cells, which, as opposed to HT1080 cells, do not produce MMP-2; therefore, the autocatalytic shedding (release of the 18-kDa species) is restricted.

A battery of protease inhibitors including metalloprotease, serine, and aspartic protease inhibitors failed to reduce the levels of the 50- and 31–35-kDa species. Additionally, these species were observed in the media of cells expressing the E240A-MT1 catalytic mutant. Thus, production of these soluble MT1-MMP fragments is a non-autocatalytic event. Interestingly, TPA and ConA, which promote autocatalytic processing, enhanced the levels of these species, suggesting an additional level of regulation by these agents (50). The identity of the protease(s) responsible for the non-autocatalytic shedding of MT1-MMP remains to be determined. Our evidence and previous evidence (23, 24) suggest that, in the case of the 50-kDa species, the protease(s) must cleave within the juxtamembrane (stem) region of MT1-MMP causing the release of the entire ectodomain. Consistently, the soluble 50-kDa species was able to form a complex with TIMP-2, in agreement with early studies (24). Whether cleavage at the stem region takes place at the cell surface or intracellularly, as shown with MT5-MMP (18), remains to be determined. However, it is unlikely that a furin-like enzyme is involved in this process because, in contrast to MT5-MMP, a specific furin-recognition motif was not found in the ectodomain of MT1-MMP (18). Based on the pattern of MT1-MMP forms present on the cell surface (the 57- and 44-kDa species) and the high levels of the 18-kDa species, as determined by the immunoprecipitation experiments, the non-autocatalytic pathway is likely to comprise a minor aspect of the shedding process. However, this process may produce functional enzyme fragments, such as the 50-kDa species (24), which would promote pro-MMP-2 processing, as demonstrated here with the conditioned media of BS-C-1 cells expressing MT1-MMP, and as shown previously in gelatin zymography assays (24). Thus, soluble ectodomain fragments with catalytic activity may extend MT1-MMP-dependent proteolysis beyond the cell surface environment by promoting the hydrolysis of a variety of substrates including extracellular matrix components (4). In addition, these fragments by binding TIMP-2 may deprive the membrane-tethered enzyme of inhibitor regulation.

An interesting observation of this study was the appearance of a 31–35-kDa soluble species that was induced either by ConA treatment or high levels of TIMP-2 or marimastat. The appearance of the 31–35-kDa species in the presence of TIMP-2 or marimastat correlated with a decrease in the levels of the 18-kDa species, suggesting the possibility that the formation of these species may be related. For example, it is possible that, in addition to the autocatalytic shedding, there is a non-MMP-dependent shedding mechanism that releases the 31–35-kDa fragment, which in turn is processed to the 18-kDa species via a metalloprotease-dependent process, as suggested by the accumulation of the 31–35-kDa species in the presence of TIMP-2 or marimastat. Alternatively, TIMP-2 binding to the 31–35-kDa species may prevent a non-metalloprotease from accessing the Ala^{255}-Ile^{256} site, thus resulting in accumulation. Indeed, the 31–35-kDa species binds TIMP-2, albeit with an apparent low affinity. Another possibility is that the accumulation of the 31–35-kDa species in the presence of TIMP-2 or marimastat represents shedding of MT1-MMP catalytic domain-inhibitor complexes. Stabilization of the membrane-anchored enzyme by formation of enzyme-inhibitor complexes (17) may induce conformational changes, which may predispose the enzyme to a non-metalloprotease-mediated ectodomain shedding. However, the lack of a readily detectable counterpart to the 31–35-kDa species on the plasma membrane suggests the possibility that this fragment(s) is not a shedding product of the membrane-bound enzyme but a result of the turnover of the larger MT1-MMP soluble species, like the 50-kDa species, via a TIMP-2-insensitive process. Structural data and studies in cellular systems with defined proteolytic backgrounds will help to distinguish between these possibilities. Although the potential contribution of the 31–35-kDa species to the formation of the 18-kDa species cannot be disregarded, this is likely to be minimal when compared with the formation of the 18-kDa species generated by the autocatalytic processing of MT1-MMP on the cell surface. Taken together, these observations further underscore the complexity of the MT1-MMP shedding process and the unexpected consequences that TIMP-2 and synthetic MMP inhibitors may have on the regulation of MT1-MMP on the cell surface, as we have previously documented (20, 21).

Previous studies reported that the cytosolic domain of MT1-MMP plays a role in the stabilization of MT1-MMP on the cell surface by altering the rate of enzyme internalization (58) and is also involved in enzyme homodimerization (60), a process thought to favor autocatalytic turnover (61). Here we have shown that the pattern of MT1-MMP shedding was essentially unaltered in enzymes lacking the cytosolic domain. This finding suggests that homotypic physical interactions mediated by the cytosolic domain (60) are not essential for MT1-MMP autocatalytic and non-autocatalytic shedding.

The autocatalytic pathway of MT1-MMP shedding concludes with the release of an 18-kDa fragment that extends from Tyr^{112} to Ala^{255}, 29 amino acid residues upstream of the Gly^{285} displayed at the N terminus of the membrane-tethered 44-kDa species (17). Therefore, shedding of the 18-kDa fragment would require cleavage at both the Ala^{255}-Ile^{256} and the Gly^{284}-Gly^{285} peptide bonds. The computational model of MT1-MMP shows that the Ala^{255}-Ile^{256} peptide bond near the methionine turn is sheltered and thus is less accessible to proteolysis. This sug-

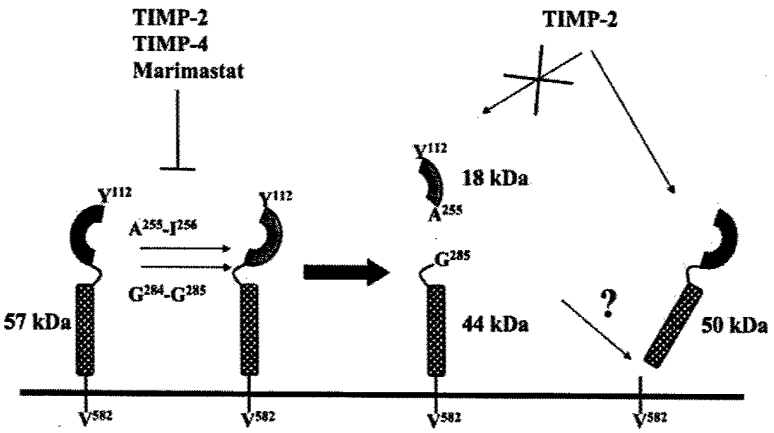

FIG. 9. **Schematic representation of the autocatalytic and non-autocatalytic shedding of MT1-MMP.** A membrane-inserted active MT1-MMP (57 kDa) undergoes intermolecular processing by a sequential cleavage at the Gly^{284}-Gly^{285} site at the beginning of the hinge region and at the Ala^{255}-Ile^{256} site within the catalytic domain. These events result in the shedding of a soluble 18-kDa species comprising Tyr^{112}–Ala^{255} and yield a residual membrane-tethered species of 44 kDa comprising Gly^{285}–Val^{582}, both of which are inactive enzyme fragments and incapable of binding TIMP-2. The autocatalytic shedding is inhibited by the natural MT1-MMP inhibitors, TIMP-2 and TIMP-4, and high affinity synthetic MMP inhibitors like marimastat. Consequently, these inhibitors stabilize active MT1-MMP on the cell surface (16, 17, 19, 21, 62). In the non-autocatalytic shedding of MT1-MMP (on *right side* of figure), a yet unknown protease releases the ectodomain (~50 kDa, no structural information yet), which possess catalytic activity (24). This species can bind TIMP-2. Not shown here is the minor ~31–35-kDa soluble fragment, which may be related to these pathways of shedding. *Single-letter* amino acid codes are used.

gests that cleavage at the Gly^{284}-Gly^{285} peptide bond, which is on the surface, is likely to precede that at the Ala^{255}-Ile^{256} site. However, at present, it is unclear whether cleavage at the Gly^{284}-Gly^{285} site predisposes for hydrolysis at the second Ala^{255}-Ile^{256} site. Data from the recombinant 21-kDa fragment, which contains the Ala^{255}-Ile^{256} site but ends at Gly^{284}, clearly indicates that disruption of the Gly^{284}-Gly^{285} site does not disturb the integrity and functionality of the Ala^{255}-Ile^{256} peptide bond. Indeed, we have shown that the 21-kDa fragment is stable and catalytically competent. Furthermore, the 21-kDa fragment was not hydrolyzed at the Ala^{255}-Ile^{256} site when was incubated alone or with HT1080 cells or their conditioned media (data not shown). We posit that the sequence of events leading to the cleavage of the Ala^{255}-Ile^{256} peptide bond after cleavage at the Gly^{284}-Gly^{285} site occur only within membrane-tethered active MT1-MMP molecules. Conceivably, cleavage at the Gly^{284}-Gly^{285} site within a membrane-anchored enzyme destabilizes the structure yielding the Ala^{255}-Ile^{256} peptide bond susceptible for subsequent hydrolysis. The inhibitor profile suggests that cleavage at the Gly^{284}-Gly^{285} site is an autocatalytic event because high affinity MT1-MMP protease inhibitors like TIMP-2 and TIMP-4 (19, 53, 62) prevented formation of the 44-kDa species starting at Gly^{285} (17). Additionally, a catalytic mutant of MT1-MMP was not processed to the 44-kDa species, as previously reported (22, 60). In regard to the Ala^{255}-Ile^{256} site, the data suggest that cleavage at that site is most likely to be also autocatalytic because TIMP-1 does not prevent shedding of the 18-kDa species. In addition, if it were mediated by another metalloprotease or a serine protease, the presence of TIMP-1, marimastat, or serine protease inhibitors should have resulted in the appearance of the 21-kDa fragment extending from Tyr^{112} to Gly^{284}, which was not detected. According to the N terminus of the membrane-bound 44-kDa species (Gly^{285}) and the C-terminal end of the soluble 18-kDa fragment (Ala^{255}), shedding of the catalytic domain should proceed via an intermediate species of ~21 kDa. However, such a species could not be detected on the cell surface or in the media of cells expressing recombinant or natural MT1-MMP. A plausible explanation for the absence of a soluble 21-kDa fragment during the shedding of the 18-kDa species is that the cleavages at the Ala^{255}-Ile^{256} and Gly^{284}-Gly^{285} sites occur rapidly and sequentially and thus would preclude accumulation of a 21-kDa intermediate form and thus ends with the 18-kDa fragment as the final product. Attempts to induce accumulation of the intermediate 21-kDa species by generating A255V or A255I substitutions at the Ala^{255}-Ile^{256} cleavage site were unsuccessful as these mutants failed to undergo activation and processing, demonstrating the importance of this site for catalytic competence.[3]

The 18-kDa fragment ends just one residue upstream of the conserved Met^{257} known to be part of the methionine turn, a structural feature characteristic of all members of the MMP family and of the super family of metzincins (55). Topologically, the methionine turn is positioned near the three histidines that coordinate with the catalytic zinc ion and is on the opposite side of these residues with respect to the active site cavity. Thus, the methionine turn is thought to be critical for catalysis, based on its close proximity to the coordination site for the catalytic zinc ion. Furthermore, the side chain of Ile^{256}, upstream of Met^{257}, forms a portion of the S1′ pocket of this enzyme. The loss of the 29-amino acid fragment during the formation of the 18-kDa MT1-MMP species would by necessity truncate the S1′ pocket; hence, it has the ability to potentially impair or alter substrate binding properties. Furthermore, the proximity of the surface loop that bears the methionine residue to the TIMP-2 binding region (43) indicates that a disorder in this location would likely impair TIMP-2 binding. Our results with the 18-kDa fragment support this notion and provide experimental documentation of the importance of the methionine turn for MMP-mediated catalysis and TIMP binding. It is worth noting that, as far as we know, the proteolytic inactivation at the methionine turn as it occurs during MT1-MMP processing has not been reported for other members of the MMP family including soluble MMPs, despite the conserved nature of this motif. This suggests the possibility that MT1-MMP specifically developed a self-controlling mechanism to allow the enzyme to function principally as a membrane-anchored protease, and any perturbation in its cellular localization would result in specific enzyme inactivation. This may explain why a transmembrane-deleted soluble MT1-MMP expressed in HT1080 cells was processed at the Ala^{255}-Ile^{256} site,

[3] P. Osenkowski and R. Fridman, manuscript in preparation.

possibly by the endogenous MT1-MMP (15). Together, these data reveal the importance of the Ala^{255}-Ile^{256} site for the maintenance of catalytic competence in MT1-MMP. Sequence alignment of the transmembrane MT-MMPs (MT1-, MT2-, MT3-, and MT5-MMP) (26) reveals a complete homology around the A-I peptide bond and the residues near the methionine turn (depicted in Fig. 5*C*). Presently, the shedding mechanisms of the MT-MMP family members have not been completely elucidated. It would be interesting to determine whether cleavage at the conserved Ala-Ile peptide bond represents a common and specific mechanism designed to terminate MT-MMP-dependent catalysis and TIMP interactions at the cell surface.

In summary, we have identified the major soluble forms of MT1-MMP and demonstrated the complexity of MT1-MMP shedding and its regulation by natural and synthetic MMP inhibitors. Fig. 9 depicts the autocatalytic processing of MT1-MMP on the cell surface leading to the release of the inactive 18-kDa species and the non-autocatalytic shedding leading to the release of the entire ectodomain by a yet unknown protease. Inhibitors of MT1-MMP block autocatalytic shedding and thus stabilize the active enzyme on the cell surface (17). The autocatalytic shedding terminates MT1-MMP-dependent pericellular proteolysis, independently of endogenous inhibitors, by specific hydrolysis at vital conserved sites (methionine turn). On the other hand, the non-autocatalytic shedding, as represented by the 50-kDa species (24) and possibly the 31–35-kDa species (not shown in Fig. 9), may still contribute to pericellular proteolysis and partly compensate for the removal of enzyme from the cell surface by shifting the proteolytic machinery to a new front, possibly with different substrates and functional consequences. Finally, the shed ectodomain of MT1-MMP may bind TIMPs (24) and hence alter the enzyme-inhibitor balance at the cell surface and/or may play new unexpected roles (3).

REFERENCES

1. Kiessling, L. L., and Gordon, E. J. (1998) *Chem. Biol.* **5,** R49–R62
2. Seiki, M. (1999) *APMIS* **107,** 137–143
3. Hernandez-Barrantes, S., Bernardo, M. M., Toth, M., and Fridman, R. (2002) *Semin. Cancer Biol.* **12,** 131–138
4. d'Ortho, M. P., Will, H., Atkinson, S., Butler, G., Messent, A., Gavrilovic, J., Smith, B., Timpl, R., Zardi, L., and Murphy, G. (1997) *Eur. J. Biochem.* **250,** 751–757
5. Ohuchi, E., Imai, K., Fujii, Y., Sato, H., Seiki, M., and Okada, Y. (1997) *J. Biol. Chem.* **272,** 2446–2451
6. Belkin, A. M., Akimov, S. S., Zaritskaya, L. S., Ratnikov, B. I., Deryugina, E. I., and Strongin, A. Y. (2001) *J. Biol. Chem.* **276,** 18415–18422
7. Deryugina, E. I., Ratnikov, B. I., Postnova, T. I., Rozanov, D. V., and Strongin, A. Y. (2002) *J. Biol. Chem.* **277,** 9749–9756
8. Kajita, M., Itoh, Y., Chiba, T., Mori, H., Okada, A., Kinoh, H., and Seiki, M. (2001) *J. Cell Biol.* **153,** 893–904
9. Strongin, A. Y., Collier, I., Bannikov, G., Marmer, B. L., Grant, G. A., and Goldberg, G. I. (1995) *J. Biol. Chem.* **270,** 5331–5338
10. Sato, H., Takino, T., Okada, Y., Cao, J., Shinagawa, A., Yamamoto, E., and Seiki, M. (1994) *Nature* **370,** 61–65
11. Holmbeck, K., Bianco, P., Caterina, J., Yamada, S., Kromer, M., Kuznetsov, S. A., Mankani, M., Robey, P. G., Poole, A. R., Pidoux, I., Ward, J. M., and Birkedal-Hansen, H. (1999) *Cell* **99,** 81–92
12. Hotary, K., Allen, E., Punturieri, A., Yana, I., and Weiss, S. J. (2000) *J. Cell Biol.* **149,** 1309–1323
13. Sato, H., Okada, Y., and Seiki, M. (1997) *Thromb. Haemostasis* **78,** 497–500
14. Tsunezuka, Y., Kinoh, H., Takino, T., Watanabe, Y., Okada, Y., Shinagawa, A., Sato, H., and Seiki, M. (1996) *Cancer Res.* **56,** 5678–5683
15. Lehti, K., Lohi, J., Valtanen, H., and Keski-Oja, J. (1998) *Biochem. J.* **334,** 345–353
16. Stanton, H., Gavrilovic, J., Atkinson, S. J., d'Ortho, M. P., Yamada, K. M., Zardi, L., and Murphy, G. (1998) *J. Cell Sci.* **111,** 2789–2798
17. Hernandez-Barrantes, S., Toth, M., Bernardo, M. M., Yurkova, M., Gervasi, D. C., Raz, Y., Sang, Q. A., and Fridman, R. (2000) *J. Biol. Chem.* **275,** 12080–12089
18. Wang, X., and Pei, D. (2001) *J. Biol. Chem.* **276,** 35953–35960
19. Hernandez-Barrantes, S., Shimura, Y., Soloway, P. D., Sang, Q. A., and Fridman, R. (2001) *Biochem. Biophys. Res. Commun.* **281,** 126–130
20. Toth, M., Bernardo, M. M., Gervasi, D. C., Soloway, P. D., Wang, Z., Bigg, H. F., Overall, C. M., DeClerck, Y. A., Tschesche, H., Cher, M. L., Brown, S., Mobashery, S., and Fridman, R. (2000) *J. Biol. Chem.* **275,** 41415–41423
21. Bernardo, M. M., Brown, S., Li, Z. H., Fridman, R., and Mobashery, S. (2002) *J. Biol. Chem.* **277,** 11201–11207
22. Lehti, K., Valtanen, H., Wickstrom, S., Lohi, J., and Keski-Oja, J. (2000) *J. Biol. Chem.* **275,** 15006–15013
23. Harayama, T., Ohuchi, E., Aoki, T., Sato, H., Seiki, M., and Okada, Y. (1999) *Jpn. J. Cancer Res.* **90,** 942–950
24. Imai, K., Ohuchi, E., Aoki, T., Nomura, H., Fujii, Y., Sato, H., Seiki, M., and Okada, Y. (1996) *Cancer Res.* **56,** 2707–2710
25. Li, H., Bauzon, D. E., Xu, X., Tschesche, H., Cao, J., and Sang, Q. A. (1998) *Mol. Carcinog.* **22,** 84–94
26. Pei, D. (1999) *J. Biol. Chem.* **274,** 8925–8932
27. Matsumoto, S., Katoh, M., Saito, S., Watanabe, T., and Masuho, Y. (1997) *Biochim. Biophys. Acta* **1354,** 159–170
28. Fridman, R., Bird, R. E., Hoyhtya, M., Oelkuct, M., Komarek, D., Liang, C. M., Berman, M. L., Liotta, L. A., Stetler-Stevenson, W. G., and Fuerst, T. R. (1993) *Biochem. J.* **289,** 411–416
29. Gervasi, D. C., Raz, A., Dehem, M., Yang, M., Kurkinen, M., and Fridman, R. (1996) *Biochem. Biophys. Res. Commun.* **228,** 530–538
30. Toth, M., Sado, Y., Ninomiya, Y., and Fridman, R. (1999) *J. Cell. Physiol.* **180,** 131–139
31. Wang, Z., Juttermann, R., and Soloway, P. D. (2000) *J. Biol. Chem.* **275,** 26411–26415
32. Fuerst, T. R., Earl, P. L., and Moss, B. (1987) *Mol. Cell. Biol.* **7,** 2538–2544
33. Fridman, R., Fuerst, T. R., Bird, R. E., Hoyhtya, M., Oelkuct, M., Kraus, S., Komarek, D., Liotta, L. A., Berman, M. L., and Stetler-Stevenson, W. G. (1992) *J. Biol. Chem.* **267,** 15398–15405
34. Olson, M. W., Gervasi, D. C., Mobashery, S., and Fridman, R. (1997) *J. Biol. Chem.* **272,** 29975–29983
35. Brown, P. D. (1997) *Med. Oncol.* **14,** 1–10
36. Brown, S., Bernardo, M. M., Zhi-Hong, L., Kotra, L. P., Tanaka, Y., Fridman, R., and Mobashery, S. (2000) *J. Am. Chem. Soc.* **122,** 6799–6800
37. Olson, M. W., Toth, M., Gervasi, D. C., Sado, Y., Ninomiya, Y., and Fridman, R. (1998) *J. Biol. Chem.* **273,** 10672–10681
38. Toth, M., Gervasi, D. C., and Fridman, R. (1997) *Cancer Res.* **57,** 3159–3167
39. Galvez, B. G., Matias-Roman, S., Albar, J. P., Sanchez-Madrid, F., and Arroyo, A. G. (2001) *J. Biol. Chem.* **276,** 37491–37500
40. Laemmli, U. K. (1970) *Nature* **227,** 680–685
41. Becker, J. W., Marcy, A. I., Rokosz, L. L., Axel, M. G., Burbaum, J. J., Fitzgerald, P. M., Cameron, P. M., Esser, C. K., Hagmann, W. K., Hermes, J. D., and Springer, J. D. (1995) *Protein Sci.* **4,** 1966–1976
42. Massova, I., Kotra, L. P., Fridman, R., and Mobashery, S. (1998) *FASEB J.* **12,** 1075–1095
43. Fernandez-Catalan, C., Bode, W., Huber, R., Turk, D., Calvete, J. J., Lichte, A., Tschesche, H., and Maskos, K. (1998) *EMBO J.* **17,** 5238–5248
44. Case, D. A., Pearlman, D. A., Caldwell, J. W., Cheatham, T. E., III, Ross, W. S., Simmerling, C. L., Darden, T. A., Merz, K. M., Stanton, R. V., Cheng, A. L., Vincent, J. J., Crowley, M., Ferguson, D. M., Radmer, R. J., Seibel, G. L., Singh, U. C., Weiner, P. K., and Kollman, P. A. (1997) *AMBER 5.0 Computer Program*, University of California, San Francisco, CA
45. Cornell, W. D., Cieplak, P., Bayly, C. I., Gould, I. R., Merz, K. M., Ferguson, D. M., Spellmeyer, D. C., Fox, T., Caldwell, J. W., and Kollman, P. A. (1995) *J. Am. Chem. Soc.* **117,** 5179–5197
46. Massova, I., Fridman, R., and Mobashery, S. (1997) *J. Mol. Model.* **3,** 17–30
47. Jorgensen, W. L., Chandraseklar, J., Maduar, J. D., Impey, R. W., and Klein, M. L. (1983) *J. Chem. Phys.* **79,** 926–935
48. Knight, C. G. (1995) *Methods Enzymol.* **248,** 18–34
49. Murphy, G., and Willenbrock, F. (1995) *Methods Enzymol.* **248,** 496–510
50. Yu, M., Sato, H., Seiki, M., and Thompson, E. W. (1995) *Cancer Res.* **55,** 3272–3277
51. Dolo, V., Ginestra, A., Cassara, D., Violini, S., Lucania, G., Torrisi, M. R., Nagase, H., Canevari, S., Pavan, A., and Vittorelli, M. L. (1998) *Cancer Res.* **58,** 4468–4474
52. Taraboletti, G., D'Ascenzo, S., Borsotti, P., Giavazzi, R., Pavan, A., and Dolo, V. (2002) *Am. J. Pathol.* **160,** 673–680
53. Will, H., Atkinson, S. J., Butler, G. S., Smith, B., and Murphy, G. (1996) *J. Biol. Chem.* **271,** 17119–17123
54. Morgunova, E., Tuuttila, A., Bergmann, U., Isupov, M., Lindqvist, Y., Schneider, G., and Tryggvason, K. (1999) *Science* **284,** 1667–1670
55. Bode, W., Gomis-Ruth, F. X., and Stockler, W. (1993) *FEBS Lett.* **331,** 134–140
56. Butler, G. S., Will, H., Atkinson, S. J., and Murphy, G. (1997) *Eur. J. Biochem.* **244,** 653–657
57. Maquoi, E., Frankenne, F., Baramova, E., Munaut, C., Sounni, N. E., Remacle, A., Noel, A., Murphy, G., and Foidart, J. M. (2000) *J. Biol. Chem.* **275,** 11368–11378
58. Jiang, A., Lehti, K., Wang, X., Weiss, S. J., Keski-Oja, J., and Pei, D. (2001) *Proc. Natl. Acad. Sci. U. S. A.* **98,** 13693–13698
59. Foda, H. D., George, S., Conner, C., Drews, M., Tompkins, D. C., and Zucker, S. (1996) *Lab. Invest.* **74,** 538–545
60. Rozanov, D. V., Deryugina, E. I., Ratnikov, B. I., Monosov, E. Z., Marchenko, G. N., Quigley, J. P., and Strongin, A. Y. (2001) *J. Biol. Chem.* **276,** 25705–25714
61. Lehti, K., Lohi, J., Juntunen, M. M., Pei, D., and Keski-Oja, J. (2002) *J. Biol. Chem.* **277,** 8440–8448
62. Bigg, H. F., Morrison, C. J., Butler, G. S., Bogoyevitch, M. A., Wang, Z., Soloway, P. D., and Overall, C. M. (2001) *Cancer Res.* **61,** 3610–3618

seminars in **CANCER BIOLOGY**, Vol. 12, 2002: pp. 131–138
doi:10.1006/scbi.2001.0421, available online at http://www.idealibrary.com on IDEAL®

Regulation of membrane type-matrix metalloproteinases

*Sonia Hernandez-Barrantes, Margarida Bernardo, Marta Toth and Rafael Fridman**

Pericellular proteolysis is a hallmark of tumor cell metastasis. The membrane type (MT)-matrix metalloproteinases (MMPs) constitute a distinctive group of membrane-bound MMPs that are central mediators of surface proteolytic events that regulate tumor cell motility, metastasis and angiogenesis. As membrane-tethered proteases, the MT-MMPs exhibit unique regulatory mechanisms and interactions with metalloproteinase inhibitors and other relevant molecules. This review will focus on new emerging information on the mechanisms that regulate MT-MMP processing, activity and inhibition, and their significance for enzyme function in the tumor microenvironment.

Key words: matrix metalloproteinases / proteases / tumor invasion / stroma

Introduction

Tumor progression to the malignant phenotype is greatly dependent on the permissive action of the microenvironment. From angiogenesis to inflammation to metastasis, the interactions of tumor cells with their microenvironment provide many of the essential factors that will impact the fate of the tumor cells. One critical factor regulated by the tumor microenvironment is the production of specific proteolytic enzymes and protease inhibitors capable of altering the immediate pericellular milieu. The matrix metalloproteinases (MMPs) represent a large family of proteolytic enzymes regulated by tumor–stromal interactions that play key roles in cancer progression, promoting proliferation, angiogenesis and tumor metastasis.[1] The versatile and ubiquitous expression of MMPs in many tumor tissues exemplifies the evolutionary advantage that these enzymes confer on the neoplastic process. The MMPs' contribution to the malignant process derives from their ability to promote the degradation of a variety of biologically relevant molecules that are not limited to extracellular matrix (ECM) components but includes a growing family of MMP substrates, among them cytokines, growth factor receptors, and cell–cell and cell–matrix adhesion molecules.[2] In tumor tissues, MMP production is a contribution of both tumor and stromal cells.[3] However, MMP action must occur at the immediate pericellular space to effectively influence cellular activities. To achieve their full potential in pericellular proteolysis, the members of the MMP family evolved into secreted and membrane-tethered multidomain enzymes by incorporating distinct domains that facilitate binding to ECM components and surface molecules in the case of soluble MMPs and unique domains that anchor the enzyme to the cell surface, in the case of the MT-MMPs. New emerging data show that the MT-MMPs are major modifiers of the pericellular environment and key regulators of tumor cell behavior. This review will focus on the unique mechanisms that regulate MT-MMP function and inhibition and their significance for tumor proteolysis.

MT-MMPs and cancer

The MT-MMPs are a relatively new subfamily of membrane-anchored MMPs, which as of today includes six members: MT1-,[4,5] MT2-,[6] MT3-,[7] MT4-,[8] MT5-,[9,10] and MT6-MMP[11] (Table 1). These enzymes are highly expressed in almost all types of human cancers[12–20] and their expression has been associated with malignant parameters.[13,21–25] Consistent with their high expression in tumors, experimental *in vitro* and *in vivo* studies demon-

*From the Department of Pathology, Wayne State University, Detroit MI 48201, USA. *Corresponding author. Department of Pathology, Wayne State University, 540 E. Canfield Ave., Detroit, MI 48201, USA.*
E-mail: rfridman@med.wayne.edu

1044–579X/02/$ – see front matter

strated the importance of MT-MMPs in promoting cell migration,[26–28] invasion,[29–32] experimental metastasis[33] and angiogenesis.[34,35] The role of MT-MMPs in invasion is tightly linked to the integrity of the membrane anchoring domains and the cytoplasmic tail. In the case of MT1-MMP, deletion of the transmembrane domain (TMD)[30,31,34,36] or deletions of and mutations at the cytoplasmic tail[31,37] impair *in vitro* cell invasion. MT1-MMP regulation of cell migration is not related exclusively to its catalytic activity against ECM components. Recent evidence indicates that MT1-MMP cleaves the hyaluronate receptor CD44 and, as a consequence, cells become migratory.[28] Furthermore, cleavage by MT1-MMP of tissue transglutaminase, an integrin-binding adhesion co-receptor, inhibits migration on fibronectin but enhances migration on collagen.[27] Together, these data suggest that the MT-MMPs by means of their specific cell surface localization and substrate profile allow cells to modify the necessary molecular machinery that controls the migratory and invasive phenotype.

An overview of the MT-MMP family

Structurally, the MT-MMPs possess the five basic characteristic domains of most MMPs, namely, (i) a signal sequence, (ii) a prodomain that maintains latency, (iii) a zinc-containing catalytic domain, (iv) a hinge region and (v) a C-terminal domain also known as the hemopexin-like domain (HLD).[38,39] However, the hallmark of the MT-MMPs is the presence of plasma membrane anchoring domains (Table 1). These domains, which extend from the HLD, consist of a sequence of ~30-amino acid stem region that is followed by a ~20-amino acid extension rich in hydrophobic residues which either (i) transverses the plasma membrane (known as the transmembrane domain (TMD)) and is followed by a cytoplasmic tail (~20 amino acids long) as in MT1-, MT2-, MT3-, and MT5-MMP[9] or (ii) forms a glycosylphosphatidylinositol (GPI) anchor as in MT4- and MT6-MMP.[40,41]

The prodomain of MT-MMPs contains a ~10-amino acid insert ending with a stretch of conserved basic residues (RXKR). This motif constitutes a cleavage site for enzymes of the pro-protein convertase family of serine proteases such as furin and is thought to play a role in pro-MT-MMP activation.[4,9,42] However, the proteases responsible for activation have not been clearly defined and both convertase[42–44] and non-convertase-dependent mechanisms[37] for activation have been described. Moreover, the need of prodomain cleavage for MT1-MMP activity has been questioned.[45] Recent functional and sequence analysis studies suggested the possibility of existence of a second set of basic motifs in pro-MT1-MMP that could serve as an alternate convertase-recognition site.[44]

Like all MMPs, the MT-MMPs are inhibited by the tissue inhibitors of metalloproteinases (TIMPs) family which includes four members (TIMP-1, TIMP-2, TIMP-3 and TIMP-4). However, unlike soluble MMPs, the MT-MMPs exhibit significant differences in affinities for the various TIMPs (Table 1). For example, MT1-,[46] MT2-,[47] MT3-[48] and MT5-MMP[10] are practically not inhibited by TIMP-1 but are efficiently inhibited by TIMP-2 and TIMP-3. MT1-MMP is also inhibited by TIMP-4.[49] Although exhibiting a higher affinity for TIMP-2, MT2-,[47] MT4-[50] and MT6-MMP[51] are inhibited by TIMP-1.

The MT-MMPs, with the exception of MT4-MMP, are classical ECM-degrading endopeptidases, and as such they exhibit a broad spectrum of substrate specificity degrading one or more ECM components (Table 1). It is noteworthy that MT1-MMP hydrolyzes native collagen I into 3/4–1/4 fragments in a typical collagenase fashion.[52,53] This activity has been suggested to be a major cause for the severe phenotype exhibited by MT1-MMP-deficient mice.[35,54] MT1-, MT4-, and MT6-MMP can also hydrolyze fibrinogen and fibrin.[34,50,51] Perhaps the most interesting aspect of the MT-MMP substrate profile is the emerging family of non-ECM proteins that is susceptible to their action. As shown in Table 1, proteins as diverse as pro-tumor necrosis factor-α,[50] CD44,[28] α1-proteinase inhibitor, α2-macroglobulin,[48] myelin inhibitory protein[55] and tissue transglutaminase[27] were all shown to be targets of MT-MMP activity. This underlies the broad functional relevance of MT-MMPs as modulators of cellular behavior.

MT-MMPs as zymogen activators

The major physiological activators of pro-MMP-2 (gelatinase A) are members of the MT-MMP family, and in the case of MT1-MMP this process involves the action of TIMP-2. The complex of TIMP-2 with active MT1-MMP evolved as a novel surface 'receptor' for pro-MMP-2[5,56,57] [shown in Figure 1(c)]. The TIMP-2/MT1-MMP complex leaves the C-terminal portion of TIMP-2 available for the binding of the HLD of

Table 1. Major properties of MT-MMPs

	Subgroup	Substrates ECM	Non-ECM	Representative tumor expression	Inhibitor	Soluble/ shed form
MT1-MMP (MMP-14)	TMD	Col I, II, III, Gel, Fb Fn, Ln-1, Ln-5, Ng Te, Vn, Agg, DS, Per	Pro-MMP-2 Pro-MMP-13 tTG, CD44, MIP α1-PI, α2M	Breast, Cervical, Gastric, Glioblastoma, Colorectal, Prostate, Hepatocellular, Esophageal Squamous Cell	T2, T3, T4	Yes
MT2-MMP (MMP-15)	TMD	Gel, Fn, Ln-1, Ng, Te Agg, Per	Pro-MMP-2 tTG	Gliomas, Renal Cell, Bladder, Larynx, Pancreas	T1, T2, T3	NI
MT3-MMP (MMP-16)	TMD	Col III, Gel, Fn, Ln-1 Vn, Agg	Pro-MMP-2 tTG, α1-PI, α2M	Breast, Renal Cell	T2, T3	Yes
MT4-MMP (MMP-17)	GPI	Gel, Fb, Fg	Pro-TNFα	Breast	T1, T2, T3	Yes
MT5-MMP (MMP-24)	TMD	Gel, Fn, CS, DS	Pro-MMP-2	Brain	T2	Yes
MT6-MMP (MMP-25)	GPI	Col IV, Gel, Fb, Fg Fn, CS, DS	Pro-MMP-2 α1-PI	Brain	T1, T2, T3	NI

Abreviations: **Agg**, Aggrecan; **CD44**, Hyaluronan Receptor; **Col**, Collagen; **CS**, Chondroitin Sulfate; **DS**, Dermatan Sulfate; **Fb**, Fibrin; **Fg**, Fibrinogen; **Fn**, Fibronectin; **Gel**, Gelatin; **GPI**, Glycosylphosphatidyl-Inositol; **Ln**, Laminin; **MIP**, Myelin-Inhibitory Protein; **NI**, No Information; **Ng**, Nidogen; **Per**, Perlecan; **T**, Tissue Inhibitor of Metalloproteinases; **Te**, Tenascin; **TMD**, Transmembrane Domain; **TNF**, Transforming Growth Factor; **tTG**, Surface Tissue Transglutaminase; **Vn**, Vitronectin; **α1-PI**, α1-Proteinase Inhibitor; **α2M**, α2 Macroglobulin.

pro-MMP-2. The MT1-MMP/TIMP-2/pro-MMP-2 complex, referred to as the 'ternary complex', facilitates the first cleavage of the pro-MMP-2 prodomain by a neighboring TIMP-2-free active MT1-MMP [Figure 1(c)]. Full activation of pro-MMP-2 is achieved by a second cleavage event in which the intermediate MMP-2 species is autocatalytically processed to the fully active enzyme.[58] This process occurs only at low TIMP-2 concentrations relative to MT1-MMP[59] to permit availability of enough inhibitor-free MT1-MMP to initiate pro-MMP-2 activation. On the other hand, high levels of TIMP-2 inhibit activation by blocking all free MT1-MMP molecules. The ternary complex model of pro-MMP-2 activation is restricted to TIMP-2 since TIMP-3 and TIMP-4, in spite of being able to bind to the HLD of pro-MMP-2,[49,60] do not support pro-MMP-2 activation.[49,60,61] In fact, TIMP-4 prevents activation by displacing TIMP-2 from the HLD of pro-MMP-2.[49] Thus, TIMP-4 can counteract the stimulatory effect of TIMP-2 in pro-MMP-2 activation[61] [Figure 1(c)]. These findings suggest a new paradigm in the regulation of proteolysis in cancer tissues in which a balance between TIMP-2 and TIMP-4 may determine the net activity of MMP-2 generated by MT1-MMP.

Regarding other MT-MMPs, which can also activate pro-MMP-2 (Table 1), it is still unknown whether these enzymes also use TIMP-2 for the activation process. However, although the ternary complex model of pro-MMP-2 activation is kinetically highly efficient, TIMP-2 independent mechanisms of pro-MMP-2 activation by MT-MMPs may exist, which may include the involvement of the $\alpha v\beta 3$ integrin[26,62] and members of the tight junction family of proteins such as claudin.[63]

MT1-MMP also promotes the activation of pro-collagenase-3 (MMP-13),[64] a collagenolytic MMP that was identified in the stroma of breast carcinomas.[65] The activation of pro-collagenase-3 can be directly mediated by MT1-MMP or indirectly via MMP-2.[64] The linkage of the collagenolytic activity of MT1-MMP and collagenase-3 with the gelatinolytic activity of MMP-2 illustrates an evolutionary triumph of a proteolytic system designed to promote coordinated collagen degradation in the pericellular space. These three enzymes are expressed in tumor stroma and therefore may act in concert to facilitate tumor cell invasion.

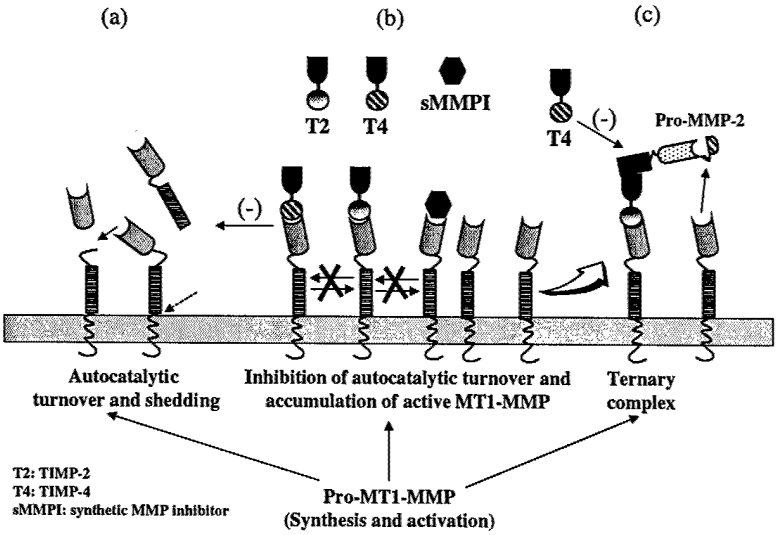

Figure 1. Role of TIMPs and synthetic MMPIs in MT1-MMP processing and function. (a) In the absence of inhibitors, autocatalytic processing of active MT1-MMP results in shedding of the ectodomain and generation of an inactive membrane-tethered form. (b) TIMP-2, TIMP-4, and synthetic MMPIs bind active MT1-MMP inhibiting autocatalytic turnover. As a consequence, active MT1-MMP accumulates on the cell surface as cells continue to synthesize and activate pro-MT1-MMP. (c) The accumulation of active MT1-MMP contributes to ternary complex formation enhancing pro-MMP-2 activation by a TIMP-2-free MT1-MMP. TIMP-4 cannot form a ternary complex and inhibits the effect of TIMP-2 on pro-MMP-2 activation.

Processing of active MT-MMPs. A new paradigm in protease regulation

The MT-MMPs developed a unique mechanism of regulation in which the active enzyme undergoes a series of processing events, either autocatalytic[66–68] or mediated by other proteases[9,69,70] that control the activity and nature of enzyme species at the cell surface and at the pericellular space. Most of the information on enzyme processing has been gathered with MT1-MMP, and thus the forthcoming schemes relate mostly to this enzyme. The processing of active MT1-MMP (57 kDa) is mostly an autocatalytic intermolecular event that results in the generation of an inactive membrane-tethered form of 44 kDa and in the shedding of the catalytic domain[31,67,68] [Figure 1(a)]. The shedding may also include release of the entire extracellular extension of MT1-MMP comprising both the catalytic domain and the HLD.[70] While this process would terminate activity on the plasma membrane independently of exogenous inhibitors, the shed catalytic domain may contribute to pericellular proteolysis. This process may compensate for the removal of enzyme from the cell surface by shifting the proteolytic machinery to a new front, possibly with different substrates and functional consequences. The shed ectodomains of MT-MMPs may also bind exogenous TIMPs and hence alter the enzyme–inhibitor balance at the cell surface.

In the case of MT1-MMP, the interaction of the active enzyme with either TIMP-2, TIMP-4 or synthetic MMP inhibitors (MMPIs) inhibits processing. As a result of this inhibition and continuous synthesis and activation of pro-MT1-MMP, the cells accumulate the 57 kDa active MT1-MMP species on the cell surface[67,68] [Figure 1(b)], which can generate additional pro-MMP-2 'receptors' by binding TIMP-2, thereby facilitating activation [Figure 1(c), right open arrow]. Thus, the inhibition of MT1-MMP processing generates a pool of active enzyme on the cell surface that supports ternary complex formation. Indeed, synthetic MMPIs, which inhibit MT1-MMP processing but cannot form a pro-MMP-2 'receptor', can further enhance the activation of pro-MMP-2 by MT1-MMP in the presence of TIMP-2 [Figure 1(b) and 1(c)].[71] Interestingly, TIMP-4, as opposed to the synthetic MMPIs, is unable to work synergistically with TIMP-2 in pro-MMP-2 activation in spite of its ability to inhibit MT1-MMP processing [Figure 1(b)],[71] possibly due to the high-affinity binding of the MT1/TIMP-4 complex,[49] which may not be displaced by TIMP-2.

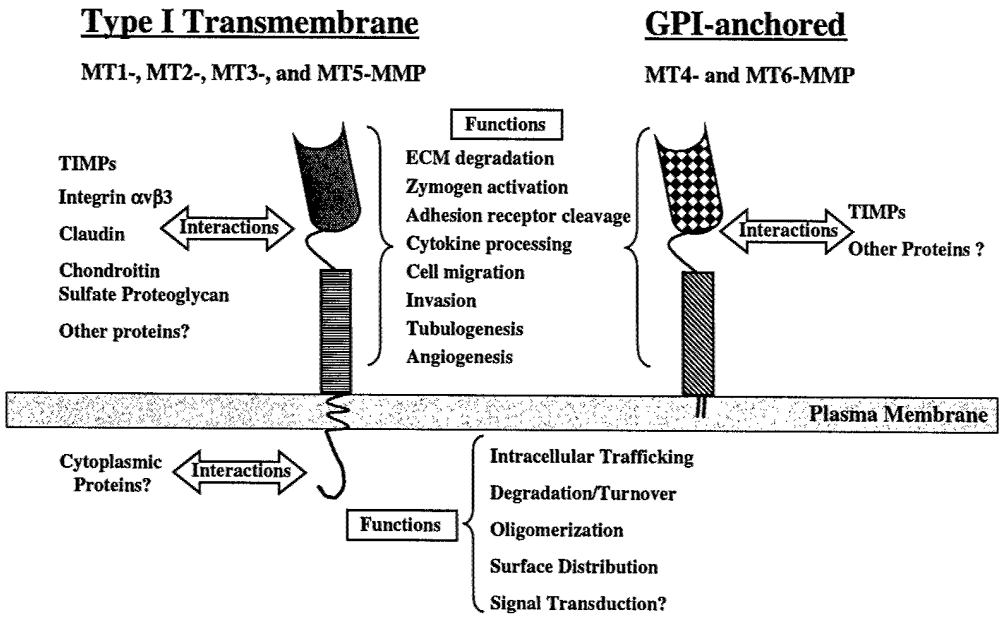

Figure 2. Multiple functions and interactions of MT-MMPs. The MT-MMPs, sub-classified as Type I transmembrane- and GPI-anchored MMPs, interact with a variety of molecules through their ectodomains. Several functions for the ectodomains were reported, as indicated. The cytoplasmic tails of the MT-MMPs with a TMD play roles in several processes and possess the potential to interact with cytoplasmic proteins.

The inhibition of autocatalytic processing may also positively influence the overall activity of MT1-MMP against a variety of pericellular substrates by stabilizing the enzyme on the cell surface. In tumor tissues, the effects of MT1-MMP stabilization in pro-MMP-2 activation and possibly in ECM degradation may contribute to the overall process of tumor cell invasion. Thus, under certain conditions, the inhibition of processing of MT1-MMP and possibly of other MT-MMPs as well, by natural or synthetic MMPIs, may produce undesirable consequences. In this regard, it is noteworthy that certain invasive tumors express high levels of stromal TIMP-2, which were found to be associated with malignant parameters.[72–76] The stromal production of TIMP-2 may represent a mechanism to counteract MMP-mediated proteolytic activity. However, given the role of TIMP-2 in MT1-MMP function, the production of TIMP-2 under certain conditions may stimulate MT1-MMP activity. Likewise, the inadequate inhibition of MT1-MMP by synthetic MMPIs may produce undesirable side effects due to the enhancement of cell surface activity as a consequence of enzyme stabilization. This complex regulation of MT1-MMP activity emphasizes the importance of understanding the molecular mechanisms and consequences of enzyme inhibition, which clinically pose new challenges for the design of novel MMP inhibitors.

Multiple functions and interactions of MT-MMPs

The MT-MMPs are emerging as major regulators of cell surface proteolysis. New interactions of MT-MMP domains with a distinctive array of cellular proteins that influence cellular behavior are being described. These interactions include associations with TIMPs, cytoplasmic and cytoskeletal proteins and cell–cell and cell–matrix receptors. Functionally, the MT-MMPs mediate pericellular proteolysis through direct ECM modification and indirectly through initiation of zymogen activation cascades and specific hydrolysis of key surface molecules (Figure 2). We can predict that the versatility of the MT-MMP molecules, some spanning from the intracellular to the extracellular milieu, will continue to supply an array of unexpected and exciting discoveries, perhaps equivalent only to that encountered with surface signaling molecules. Ultimately, the

complexity of the molecular interactions and the processes regulating MT-MMP action will have to be considered for the design of new anti-MMP therapies to be effective. Hopefully, the discovery of new MT-MMP functions and interacting molecules will also bring novel targets for intervention, which may have an impact in cancer therapy.

References

1. MacDougall JR, Matrisian LM (1995) Contributions of tumor and stromal matrix metalloproteinases to tumor progression, invasion and metastasis. Cancer Metastasis Rev 14:351–362
2. Werb Z (1997) ECM and cell surface proteolysis: regulating cellular ecology. Cell 91:439–442
3. Crawford HC, Matrisian LM (1994) Tumor and stromal expression of matrix metalloproteinases and their role in tumor progression. Invasion Metastasis 14:234–245
4. Sato H, Takino T, Okada Y, Cao J, Shinagawa A, Yamamoto E, Seiki M (1994) A matrix metalloproteinase expressed on the surface of invasive tumour cells. Nature 370:61–65
5. Strongin AY, Collier I, Bannikov G, Marmer BL, Grant GA, Goldberg GI (1995) Mechanism of cell surface activation of 72-kDa type IV collagenase. Isolation of the activated form of the membrane metalloprotease. J Biol Chem 270:5331–5338
6. Takino T, Sato H, Shinagawa A, Seiki M (1995) Identification of the second membrane-type matrix metalloproteinase (MT-MMP-2) gene from a human placenta cDNA library. MT-MMPs form a unique membrane-type subclass in the MMP family. J Biol Chem 270:23013–23020
7. Will H, Hinzmann B (1995) cDNA sequence and mRNA tissue distribution of a novel human matrix metalloproteinase with a potential transmembrane segment. Eur J Biochem 231:602–608
8. Puente XS, Pendas AM, Llano E, Velasco G, Lopez-Otin C (1996) Molecular cloning of a novel membrane-type matrix metalloproteinase from a human breast carcinoma. Cancer Res 56:944–949
9. Pei D (1999) Identification and characterization of the fifth membrane-type matrix metalloproteinase MT5-MMP. J Biol Chem 274:8925–8932
10. Llano E, Pendas AM, Freije JP, Nakano A, Knauper V, Murphy G, Lopez-Otin C (1999) Identification and characterization of human MT5-MMP, A new membrane-bound activator of progelatinase A overexpressed in brain tumors. Cancer Res 59:2570–2576
11. Velasco G, Cal S, Merlos-Suarez A, Ferrando AA, Alvarez S, Nakano A, Arribas J, Lopez-Otin C (2000) Human MT6-matrix metalloproteinase: identification, progelatinase A activation, and expression in brain tumors. Cancer Res 60:877–882
12. Okada A, Bellocq JP, Rouyer N, Chenard MP, Rio MC, Chambon P, Basset P (1995) Membrane-type matrix metalloproteinase (MT-MMP) gene is expressed in stromal cells of human colon, breast, and head and neck carcinomas. Proc Natl Acad Sci USA 92:2730–2734
13. Nakada M, Kita D, Futami K, Yamashita J, Fujimoto N, Sato H, Okada Y (2001) Roles of membrane type 1 matrix metalloproteinase and tissue inhibitor of metalloproteinases 2 in invasion and dissemination of human malignant glioma. J Neurosurg 94:464–473
14. Yamamoto M *et al.* (1996) Differential expression of membrane-type matrix metalloproteinase and its correlation with gelatinase A activation in human malignant brain tumors *in vivo* and *in vitro*. Cancer Res 56:384–392
15. Ueno H, Nakamura H, Inoue M, Imai K, Noguchi M, Sato H, Seiki M, Okada Y (1997) Expression and tissue localization of membrane-types 1, 2, and 3 matrix metalloproteinases in human invasive breast carcinomas. Cancer Res 57:2055–2060
16. Ellenrieder V *et al.* (2000) Role of MT-MMPs and MMP-2 in pancreatic cancer progression. Int J Cancer 85:14–20
17. Nomura H, Sato H, Seiki M, Mai M, Okada Y (1995) Expression of membrane-type matrix metalloproteinase in human gastric carcinomas. Cancer Res 55:3263–3266
18. Ohashi K, Nemoto T, Nakamura K, Nemori R (2000) Increased expression of matrix metalloproteinase 7 and 9 and membrane type 1-matrix metalloproteinase in esophageal squamous cell carcinomas. Cancer 88: 2201–2209
19. Upadhyay J, Shekarriz B, Nemeth JA, Dong Z, Cummings GD, Fridman R, Sakr W, Grignon DJ, Cher ML (1999) Membrane type 1-matrix metalloproteinase (MT1-MMP) and MMP-2 immunolocalization in human prostate: change in cellular localization associated with high-grade prostatic intraepithelial neoplasia. Clin Cancer Res 5:4105–4110
20. Sakakibara M *et al.* (1999) Membrane-type matrix metalloproteinase-1 expression and activation of gelatinase A as prognostic markers in advanced pediatric neuroblastoma. Cancer 85:231–239
21. Gilles C, Polette M, Piette J, Munaut C, Thompson EW, Birembaut P, Foidart JM (1996) High level of MT-MMP expression is associated with invasiveness of cervical cancer cells. Int J Cancer 65:209–213
22. Bando E *et al.* (1998) Immunohistochemical study of MT-MMP tissue status in gastric carcinoma and correlation with survival analyzed by univariate and multivariate analysis. Oncol Rep 5:1483–1488
23. Sardinha TC, Nogueras JJ, Xiong H, Weiss EG, Wexner SD, Abramson S (2000) Membrane-type 1 matrix metalloproteinase mRNA expression in colorectal cancer. Dis Colon Rectum 43:389–395
24. Shimada T, Nakamura H, Yamashita K, Kawata R, Murakami Y, Fujimoto N, Sato H, Seiki M, Okada Y (2000) Enhanced production and activation of progelatinase A mediated by membrane-type 1 matrix metalloproteinase in human oral squamous cell carcinomas: implications for lymph node metastasis. Clin Exp Metastasis 18:179–188
25. Mimori K, Ueno H, Shirasaka C, Mori M (2001) Clinical significance of MT1-MMP mRNA expression in breast cancer. Oncol Rep 8:401–403
26. Deryugina EI, Bourdon MA, Jungwirth K, Smith JW, Strongin AY (2000) Functional activation of integrin alpha V beta 3 in tumor cells expressing membrane-type 1 matrix metalloproteinase. Int J Cancer 86:15–23
27. Belkin AM, Akimov SS, Zaritskaya LS, Ratnikov BI, Deryugina EI, Strongin AY (2001) Matrix-dependent proteolysis of surface transglutaminase by membrane-type metalloproteinase regulates cancer cell adhesion and locomotion. J Biol Chem 276:18415–18422
28. Kajita M, Itoh Y, Chiba T, Mori H, Okada A, Kinoh H, Seiki M (2001) Membrane-type 1 matrix metalloproteinase cleaves cd44 and promotes cell migration. J Cell Biol 153:893–904
29. Rosenthal EL, Hotary K, Bradford C, Weiss SJ (1999) Role of membrane type 1-matrix metalloproteinase and gelatinase A in head and neck squamous cell carcinoma invasion in vitro. Otolaryngol Head Neck Surg 121:337–343

30. Hotary K, Allen E, Punturieri A, Yana I, Weiss SJ (2000) Regulation of cell invasion and morphogenesis in a three-dimensional type I collagen matrix by membrane-type matrix metalloproteinases 1, 2, and 3. J Cell Biol 149:1309–1323
31. Lehti K, Valtanen H, Wickstrom S, Lohi J, Keski-Oja J (2000) Regulation of membrane-type-1 matrix metalloproteinase activity by its cytoplasmic domain. J Biol Chem 275: 15006–15013
32. Kang T, Yi J, Yang W, Wang X, Jiang A, Pei D (2000) Functional characterization of MT3-MMP in transfected MDCK cells: progelatinase A activation and tubulogenesis in 3-D collagen lattice. Faseb J 14:2559–2568
33. Tsunezuka Y, Kinoh H, Takino T, Watanabe Y, Okada Y, Shinagawa A, Sato H, Seiki M (1996) Expression of membrane-type matrix metalloproteinase 1 (MT1-MMP) in tumor cells enhances pulmonary metastasis in an experimental metastasis assay. Cancer Res 56:5678–5683
34. Hiraoka N, Allen E, Apel IJ, Gyetko MR, Weiss SJ (1998) Matrix metalloproteinases regulate neovascularization by acting as pericellular fibrinolysins. Cell 95:365–377
35. Zhou Z, Apte SS, Soininen R, Cao R, Baaklini GY, Rauser RW, Wang J, Cao Y, Tryggvason K (2000) Impaired endochondral ossification and angiogenesis in mice deficient in membrane-type matrix metalloproteinase I. Proc Natl Acad Sci USA 97:4052–4057
36. Nakahara H, Howard L, Thompson EW, Sato H, Seiki M, Yeh Y, Chen WT (1997) Transmembrane/cytoplasmic domain-mediated membrane type 1-matrix metalloprotease docking to invadopodia is required for cell invasion. Proc Natl Acad Sci USA 94:7959–7964
37. Rozanov DV, Deryugina EI, Ratnikov BI, Monosov EZ, Marchenko GN, Quigley JP, Strongin AY (2001) Mutation analysis of membrane type-1 matrix metalloproteinase (MT1-MMP). The role of the cytoplasmic tail Cys-574, the active site Glu-240 and furin cleavage motifs in oligomerization, processing and self-proteolysis of MT1-MMP expressed in breast carcinoma cells. J Biol Chem 276:25705–25714
38. Massova I, Kotra LP, Fridman R, Mobashery S (1998) Matrix metalloproteinases: structures, evolution, and diversification. Faseb J 12:1075–1095
39. Bode W, Fernandez-Catalan C, Tschesche H, Grams F, Nagase H, Maskos K (1999) Structural properties of matrix metalloproteinases. Cell Mol Life Sci 55:639–652
40. Itoh Y, Kajita M, Kinoh H, Mori H, Okada A, Seiki M (1999) Membrane type 4 matrix metalloproteinase (MT4-MMP, MMP-17) is a glycosylphosphatidylinositol-anchored proteinase. J Biol Chem 274:34260–34266
41. Kojima S, Itoh Y, Matsumoto S, Masuho Y, Seiki M (2000) Membrane-type 6 matrix metalloproteinase (MT6-MMP, MMP-25) is the second glycosyl-phosphatidyl inositol (GPI)-anchored MMP. FEBS Lett 480:142–146
42. Pei D, Weiss SJ (1996) Transmembrane-deletion mutants of the membrane-type matrix metalloproteinase-1 process progelatinase A and express intrinsic matrix-degrading activity. J Biol Chem 271:9135–9140
43. Sato H, Kinoshita T, Takino T, Nakayama K, Seiki M (1996) Activation of a recombinant membrane type 1-matrix metalloproteinase (MT1-MMP) by furin and its interaction with tissue inhibitor of metalloproteinases (TIMP)-2. FEBS Lett 393:101–104
44. Yana I, Weiss SJ (2000) Regulation of membrane type-1 matrix metalloproteinase activation by proprotein convertases. Mol Biol Cell 11:2387–2401
45. Cao J, Rehemtulla A, Bahou W, Zucker S (1996) Membrane type matrix metalloproteinase 1 activates pro-gelatinase A without furin cleavage of the N-terminal domain. J Biol Chem 271:30174–30180
46. Will H, Atkinson SJ, Butler GS, Smith B, Murphy G (1996) The soluble catalytic domain of membrane type 1 matrix metalloproteinase cleaves the propeptide of progelatinase A and initiates autoproteolytic activation. Regulation by TIMP-2 and TIMP-3. J Biol Chem 271:17119–17123
47. Butler GS, Will H, Atkinson SJ, Murphy G (1997) Membrane-type-2 matrix metalloproteinase can initiate the processing of progelatinase A and is regulated by the tissue inhibitors of metalloproteinases. Eur J Biochem 244:653–657
48. Shimada T, Nakamura H, Ohuchi E, Fujii Y, Murakami Y, Sato H, Seiki M, Okada Y (1999) Characterization of a truncated recombinant form of human membrane type 3 matrix metalloproteinase. Eur J Biochem 262:907–914
49. Bigg HF, Morrison CJ, Butler GS, Bogoyevitch MA, Wang Z, Soloway PD, Overall CM (2001) Tissue inhibitor of metalloproteinases-4 inhibits but does not support the activation of gelatinase A via efficient inhibition of membrane type 1-matrix metalloproteinase. Cancer Res 61:3610–3618
50. English WR, Puente XS, Freije JM, Knauper V, Amour A, Merryweather A, Lopez-Otin C, Murphy G (2000) Membrane type 4 matrix metalloproteinase (MMP17) has tumor necrosis factor-alpha convertase activity but does not activate pro-MMP2. J Biol Chem 275:14046–14055
51. English WR, Velasco G, Stracke JO, Knauper V, Murphy G (2001) Catalytic activities of membrane-type 6 matrix metalloproteinase (MMP25). FEBS Lett 491:137–142
52. d'Ortho MP *et al.* (1997) Membrane-type matrix metalloproteinases 1 and 2 exhibit broad-spectrum proteolytic capacities comparable to many matrix metalloproteinases. Eur J Biochem 250:751–757
53. Ohuchi E, Imai K, Fujii Y, Sato H, Seiki M, Okada Y (1997) Membrane type 1 matrix metalloproteinase digests interstitial collagens and other extracellular matrix macromolecules. J Biol Chem 272:2446–2451
54. Holmbeck K *et al.* (1999) MT1-MMP-deficient mice develop dwarfism, osteopenia, arthritis, and connective tissue disease due to inadequate collagen turnover. Cell 99:81–92
55. Belien AT, Paganetti PA, Schwab ME (1999) Membrane-type 1 matrix metalloprotease (MT1-MMP) enables invasive migration of glioma cells in central nervous system white matter. J Cell Biol 144:373–384
56. Zucker S, Drews M, Conner C, Foda HD, DeClerck YA, Langley KE, Bahou WF, Docherty AJ, Cao J (1998) Tissue inhibitor of metalloproteinase-2 (TIMP-2) binds to the catalytic domain of the cell surface receptor, membrane type 1-matrix metalloproteinase 1 (MT1-MMP). J Biol Chem 273:1216–1222
57. Butler GS *et al.* (1998) The TIMP2 membrane type 1 metalloproteinase 'receptor' regulates the concentration and efficient activation of progelatinase A. A kinetic study. J Biol Chem 273:871–880
58. Atkinson SJ, Crabbe T, Cowell S, Ward RV, Butler MJ, Sato H, Seiki M, Reynolds JJ, Murphy G (1995) Intermolecular autolytic cleavage can contribute to the activation of progelatinase A by cell membranes. J Biol Chem 270: 30479–30485
59. Jo Y, Yeon J, Kim HJ, Lee ST (2000) Analysis of tissue inhibitor of metalloproteinases-2 effect on pro-matrix metalloproteinase-2 activation by membrane-type 1 matrix metalloproteinase using baculovirus/insect-cell expression system. Biochem J 345 Pt 3:511–519
60. Butler GS, Apte SS, Willenbrock F, Murphy G (1999) Human tissue inhibitor of metalloproteinases 3 interacts with both the

N- and C-terminal domains of gelatinases A and B. Regulation by polyanions. J Biol Chem 274:10846–10851
61. Hernandez-Barrantes S, Shimura Y, Soloway PD, Sang QA, Fridman R (2001) Differential roles of TIMP-4 and TIMP-2 in pro-MMP-2 activation by MT1- MMP. Biochem Biophys Res Commun 281:126–130
62. Brooks PC, Stromblad S, Sanders LC, von Schalscha TL, Aimes RT, Stetler-Stevenson WG, Quigley JP, Cheresh DA (1996) Localization of matrix metalloproteinase MMP-2 to the surface of invasive cells by interaction with integrin alpha v beta 3. Cell 85:683–693
63. Miyamori H, Takino T, Kobayashi Y, Tokai H, Itoh Y, Seiki M, Sato H (2001) Claudin promotes activation of Pro-MMP-2 mediated by membrane-type matrix metalloproteinases. J Biol Chem, May 29 [epub ahead of print]
64. Knauper V, Will H, Lopez-Otin C, Smith B, Atkinson SJ, Stanton H, Hembry RM, Murphy G (1996) Cellular mechanisms for human procollagenase-3 (MMP-13) activation. Evidence that MT1-MMP (MMP-14) and gelatinase A (MMP-2) are able to generate active enzyme. J Biol Chem 271:17124–17131
65. Freije JM, Diez-Itza I, Balbin M, Sanchez LM, Blasco R, Tolivia J, Lopez-Otin C (1994) Molecular cloning and expression of collagenase-3, a novel human matrix metalloproteinase produced by breast carcinomas. J Biol Chem 269: 16766–16773
66. Lehti K, Lohi J, Valtanen H, Keski-Oja J (1998) Proteolytic processing of membrane-type-1 matrix metalloproteinase is associated with gelatinase A activation at the cell surface. Biochem J 334:345–353
67. Stanton H, Gavrilovic J, Atkinson SJ, d'Ortho MP, Yamada KM, Zardi L, Murphy G (1998) The activation of ProMMP-2 (gelatinase A) by HT1080 fibrosarcoma cells is promoted by culture on a fibronectin substrate and is concomitant with an increase in processing of MT1-MMP (MMP-14) to a 45 kDa form. J Cell Sci 111:2789–2798
68. Hernandez-Barrantes S, Toth M, Bernardo MM, Yurkova M, Gervasi DC, Raz Y, Sang QA, Fridman R (2000) Binding of active (57 kDa) membrane type 1-matrix metalloproteinase (MT1-MMP) to tissue inhibitor of metalloproteinase (TIMP)-2 regulates MT1-MMP processing and pro-MMP-2 activation. J Biol Chem 275:12080–12089
69. Shofuda K, Yasumitsu H, Nishihashi A, Miki K, Miyazaki K (1997) Expression of three membrane-type matrix metalloproteinases (MT-MMPs) in rat vascular smooth muscle cells and characterization of MT3-MMPs with and without transmembrane domain. J Biol Chem 272:9749–9754
70. Harayama T, Ohuchi E, Aoki T, Sato H, Seiki M, Okada Y (1999) Shedding of membrane type 1 matrix metalloproteinase in a human breast carcinoma cell line. Jpn J Cancer Res 90:942–950
71. Toth M *et al.* (2000) Tissue inhibitor of metalloproteinase (TIMP)-2 acts synergistically with synthetic matrix metalloproteinase (MMP) inhibitors but not with TIMP-4 to enhance the (Membrane type 1)-MMP-dependent activation of pro- MMP-2. J Biol Chem 275:41415–41423
72. Davidson B, Goldberg I, Gotlieb WH, Kopolovic J, Ben-Baruch G, Nesland JM, Berner A, Bryne M, Reich R (1999) High levels of MMP-2, MMP-9, MT1-MMP and TIMP-2 mRNA correlate with poor survival in ovarian carcinoma. Clin Exp Metastasis 17:799–808
73. Maeta H, Ohgi S, Terada T (2001) Protein expression of matrix metalloproteinases 2 and 9 and tissue inhibitors of metalloproteinase 1 and 2 in papillary thyroid carcinomas. Virchows Arch 438:121–128
74. Remacle A, McCarthy K, Noel A, Maguire T, McDermott E, O'Higgins N, Foidart JM, Duffy MJ (2000) High levels of TIMP-2 correlate with adverse prognosis in breast cancer. Int J Cancer 89:118–121
75. Visscher DW, Hoyhtya M, Ottosen SK, Liang CM, Sarkar FH, Crissman JD, Fridman R (1994) Enhanced expression of tissue inhibitor of metalloproteinase-2 (TIMP-2) in the stroma of breast carcinomas correlates with tumor recurrence. Int J Cancer 59:339–344
76. Yoshizaki T, Maruyama Y, Sato H, Furukawa M (2001) Expression of tissue inhibitor of matrix metalloproteinase-2 correlates with activation of matrix metalloproteinase-2 and predicts poor prognosis in tongue squamous cell carcinoma. Int J Cancer 95:44–50